The Dissertation Committee for Kristin Renee Fathe Certifies that this is the approved version of the following dissertation:

Dietary and Genetic Influences on Neural Tube Defects

Committee:

Richard Finnell, Supervisor

Dean Appling

Seongmin Lee

John Wallingford

Yan Jessie Zhang

Dietary and Genetic Influences on Neural Tube Defects

by

Kristin Renee Fathe, B.S.

Dissertation

Presented to the Faculty of the Graduate School of

The University of Texas at Austin

in Partial Fulfillment

of the Requirements

for the Degree of

Doctor of Philosophy

The University of Texas at Austin

August 2014

Dedication

For my Matt and my parents.

Acknowledgements

I would like to first thank Dr. Richard Finnell for his years of mentorship. Rick: thank you for taking me into your lab, always supporting me academically, and for your continued words of encouragement. I will always appreciate your years of help and patience while I learned and grew scientifically and personally. I would like to thank all of my committee members, Drs. Appling, Lee, Wallingford, and Zhang, for all of the time that you have spent providing input and support to my project. I would also like to thank Drs. Maria Person and Yue Li for their help with the mass spectrometry facilities and confocal microscopy facilities respectively.

I am especially appreciative to the Finnell lab members, past and present. Thank you Dr. Yunping Lei, for always being there to talk to me about science (or not) and always being there to help teach and inspire me in our projects. You are an excellent scientist and second mentor, and I wish you only the best. I would also like to thank Drs. Robert Cabrera and Bogdan Woldarczyk for providing help, mentorship, and entertainment. I am additionally thankful for Ms. Vickie Grier, Ms. Krystal Ogle, and Dr. Linda Lin, not only for their help, but for their close personal friendships. Vickie, thank you for knowing everything and always solving my problems, even if the solution was just happy hour.

Finally, I would like to thank my family. Mom and Dad, thank you both for more than you can know. Thank you for always believing in me and for all of the support. Mom, I don't think I could have done this without you. You have spent endless hours on the phone listening to me be frustrated, stressed, and terrified. I love you both and always will be happy to know that I have the best parents. I would also like to thank Matt. Matt, for every hour my mom has listened to me, you

have listened to five more. Thank you for all of the unconditional love, hugs, the walks, the comforting and calming me down, and your endless patience when I "ran to lab for just a few minutes." You mean the world to me, and I could not have done this nearly as well without you by my side. Begona and Nicola, thanks for being my "grad school friends," and for always being willing to talk or get free Nike stuff. Sarita, thanks for always complaining with me and making me laugh. Caroline, thank you for always running with me, venting about our days, and our forever friendship.

Dietary and Genetic Influences on Neural Tube Defects

Kristin Renee Fathe, Ph.D.

The University of Texas at Austin, 2014

Supervisor: Richard H. Finnell

Neural tube defects (NTDs) are a world health issue, affecting approximately 1 in every 1000 live births. These congenital defects arise from the improper closure of the neural tube during development, resulting in significant, life-threatening malformations of the central nervous system. Although it has been observed that supplementing women of child-bearing age with folates greatly decreases the chances of having an NTD affected baby, unfortunately these defects still occur. It is accepted that these complex disorders arise from a combination of genetic, environmental, and dietary influences. One such dietary influence is the one-carbon metabolism metabolite, homocysteine. Homocysteine is a byproduct of methylation reactions in the cell that exists in an inverse homeostasis with folate. Homocysteine can also undergo a transformation that allows it to then react with exposed lysine or cysteine residues on proteins, in a process known as N-homocysteinylation or S-homocysteinylation respectively. High levels of homocysteine have been long correlated with many disease states, including NTDs. One potential mechanism by which homocysteine confers its negative effects is

through protein N-homocysteinylation. Here, a novel and high-throughput assay for N-homocysteinylation determination is described. This assay is shown to be accurate with mass spectrometry then shown to be biologically relevant using known hyperhomocysteinemia mouse models. This assay was then applied to a cohort of neural tube closure staged mouse embryos with two different genetic mutations that have previously been shown to predispose mice to NTDs. The genotypes explored here are mutations to the *LRP6* gene and the Folr1 gene, both of which have been described as folate-responsive NTD mouse models. It was seen that maternal diet and embryonic genotype had the largest influence on the developmental outcome of these embryos; however, the inverse relationship between folate and homocysteine seemed to be established at this early time point, emphasizing the importance of the balance in one-carbon metabolism. One of these genes, *LRP6*, was then explored in a human cohort of spina bifida cases. Four novel mutations to the *LRP6* gene were found and compared to the mouse model used in the previous study. One of the mutations found in the human population was seen to mimic that of the LRP6 mouse model, therefore expanding the potential of this NTD model.

Table of Contents

List of Tables xiii

List of Figures xiv

Chapter 1: Introduction 1

1.1 Mouse Embryonic Development 1

1.2 Neural Tube Defects 3

1.2.1 Genetic Effectors of NTDs 5

1.2.2 Dietary Effectors of NTDs 7

1.2.3 Environmental Effectors of NTDs 9

1.3 Wnt Signaling 14

1.3.1 Low Density Lipoprotein Receptor-Related Protein 6 18

1.4 FOLATE (One-Carbon) Metabolism 20

1.4.1 Folate Proteins 25

1.4.1.1 Folate Receptor Alpha 25

1.4.1.2 Folate Receptor Beta 31

1.4.1.3 Folate Receptor Gamma 31

1.4.1.4 Folate Binding Protein 32

1.4.1.5 Proton Coupled Folate Transporter 32

1.4.1.6 Reduced Folate Carrier 33

1.4.2 Homocysteine 34

1.5 The Immune System 40

1.5.1 The Complement Cascade 41

1.5.2 Immunity and NTDs 44

1.6 Mouse Models 45

1.6.1 Folr1 (Folbp1/FRα) Mouse 46

1.6.2 LRP6 Mouse Models 47

1.7 Concluding Remarks 49

Chapter 2 Biological Application and Adaptation of a Chemical N-Homocysteinylation Determination Assay 50
2.1 Introduction 50
2.2 Materials and Methods 63
2.2.1 Bradford Assay 63
2.2.2 Polymerase Chain Reaction (PCR) 63
2.2.3 Homocysteinylation of Proteins 64
2.2.4 N-Homocysteinylation Detection in Samples 64
2.2.5 Reaction with Biotinylated Aldehyde 65
2.2.6 Dot Blot Detection 66
2.2.7 Mass Spectrometry 66
2.2.8 Mouse Husbandry 67
2.2.9 Mouse Genotyping 68
2.2.10 Mouse Sample Collection 68
2.3 Results 69
2.3.1 Confirmation of Stoichiometry of Assay 69
2.3.2 Confirmation of Chemistry using Mass Spectrometry 69
2.3.3 Confirmation of High-Throughput Adaptation 70
2.4 Conclusion 79

Chapter 3 Examining Genetic and Dietary Effects on the Metabolic Status of Developing Embryos 82
3.1 Introduction 82
3.2 Materials and Methods 89
3.2.1 Experimental Animals 89
3.2.1.1 Mouse Genotyping 89
3.2.2 Animal Sample Collection 90
3.2.3 Folate Determination 90
3.2.3.1 Sample Preparation 91
3.2.3.2 Competitive Binding ELISA Assay 91
3.2.4 N-Homocysteinylation Determination 92

3.2.4.1 Sample Preparation 92
3.2.4.2 N-homocysteinylation Labeling and Probing 92
3.2.4.4 Data Analysis 92
3.2.5 Statistical Analysis 93
3.3 Results 93
3.3.1 Characterization of Embryonic Sample Cohort 94
3.3.2 Statistical Analysis of Genetic and Dietary Effects on Developing Embryos 94
3.4 Conclusion 100
Chapter 4 LRP6 mutation examination in a human population 104
4.1 Introduction 104
4.2 Materials and Methods 115
4.2.1 Plasmid DNA 115
4.2.2 Bacterial Transformation and Plasmid Preparation 115
4.2.3 Co-Immunoprecipitation Assays 116
4.2.4 Subcellular Localization 117
4.2.5 Luciferase Assays 118
4.2.5.1 Wnt5a Conditioned Media 119
4.3 Results 119
4.3.1 Novel LRP6 Mutations Affect Binding to Chaperone Protein MESD 119
4.3.2 Novel Lrp6 Mutations Affect Sub-Cellular Localization 120
4.3.3 Novel Lrp6 Mutations Abrogate Canonical Wnt Signaling ..120
4.3.4 Novel Lrp6 Mutations Enhance Non-Canonical Wnt Signaling121
4.4 Discussion 127
Chapter 5 Future Directions and Conclusions 132
5.1 Future Directions 132
5.1.1 Adaptation Chemical N-Homocysteinylation Assay to Histological Marker 132
5.1.2 Functional analysis of target N-homocysteinylated proteins133

5.1.3 Increased Investigation into LRP6 and PCP signaling 133
5.2 Concluding Remarks 134
Appendix 1. Full Data Table from Chapter 3 137
Appendix 2. List of Abbreviations.....143
References.....146
Vita…….....171

List of Tables

Table 2.1 Homocysteinylthiolactone Modified Peptides in BSA 72

Table 3.1 Digenic Interaction of LRP6 and Folr1.....88

Table 3.2 Number of Embryos Used for Statistical Analysis by Category.....97

Table 4.1 Novel *LRP6* Mutations Identified in Human Spina Bifida Cases.109

List of Figures

Figure 1.1 Canonical Wnt Signaling Cascade 15
Figure 1.2 Non-Canonical Wnt Signaling Pathways 16
Figure 1.3 Folates: Water-soluble Vitamins B9.....22
Figure 1.4 Folate One-Carbon Metabolism 23
Figure 1.5 Endocytotic Mechanism of the Folate Receptor Alpha.....27
Figure 1.6 Folate Mimetic as Therapeutics.....30
Figure 1.7 Homocysteine Metabolism.....37
Figure 1.8 Protein Homocysteinylation 38
Figure 1.9 The Complement Cascade.....43
Figure 2.1 Reaction of an Aldehyde and a γ-Aminothiol 55
Figure 2.2 Aldehyde Reactive Aminothiols.....56
Figure 2.3 Enrichment for N-homocysteinylation Events with a Solid State.....58
Figure 2.4 Tagging of N-homocysteinylation Events with a Biotin Tag.....59
Figure 2.5 Methionine Cycle 62
Figure 2.6 Linear Range Created for N-homocysteinylation Assay.....71
Figure 2.7 (A-D) Representative Mass Spectra 75
Figure 2.8 Mass Spectrometry Coverage Maps.....76
Figure 2.9 BSA with Reacted Surface Lysines.....77
Figure 2.10 Use of Chemical N-Homocysteinylation Assay.....78
Figure 3.1 Folate Receptor Alpha Shows Decreased Function with Increased Homocysteinylation 85
Figure 3.2 Dietary Influences of Dam N-homocysteinylation and Folate.....96

Figure 3.3 Estimated Marginal Means of Embryonic Folate, N-homocysteinylation, and Somites....98
Figure 3.4 Statistical Analysis of Embryonic Outcomes....99
Figure 4.1 A Partial Alignment of Human *LRP6* with Seven Other Orthologous Sequences....110
Figure 4.2 Rare Novel LRP6 Mutations Identified in Human Spina Bifida Patients111
Figure 4.3 Co-Immunoprecipitation Between LRP6 Mutations and the Chaperone Protein MESD....122
Figure 4.4 Representative Images of Subcellular Localization of LRP6 Mutants.123
Figure 4.5 Quantitative Analysis of Subcellular Localization of LRP6 Mutants 124
Figure 4.6 Novel Y544C LRP6 Mutation Decreases Canonical Wnt Signaling .125
Figure 4.7 LRP6 Mutant Effects on Non-canonical Wnt Signaling Pathway 126

Chapter 1: Introduction

1.1 Mouse Embryonic Development

Mouse conception is marked, like in most mammals, when the egg in the female mouse is joined with sperm from a male mouse. For the first 4 days post conception, the fertilized egg (zygote) will travel toward the uterus and divide multiple times. At approximately 4 to 5 days post-fertilization (ED) in the mouse, the formation of a blastocyst is seen. The inner cell mass of this blastocyst is what will become the embryo (Johnson, 2009). At this time, the blastocyst will implant into the uterine wall to continue development. The blastocyst consists of an internal mass of cells that will give rise to the amniotic sac and the three germ layers, while the external cells will give rise to the maternally owned placenta. Gastrulation marks the next major step in embryogenesis, in which cells move and differentiate into the three germ layers: the endoderm, the mesoderm and the ectoderm (Tam & Behringer, 1997). The cells that differentiate into the ectoderm are fated to be the skin, portions of the mouth, some of the endocrine system, and the nasal passageways. The cells that differentiate into the mesoderm are fated to be muscular, skeletal, cardiovascular, connective tissues, and some of the urinary and reproductive systems. The cells that differentiate into the endoderm are fated to become the epithelium of the digestive tract, the liver, the pancreas, the respiratory system, and portions of the urinary and reproductive systems (Detrait et al, 2005).

At approximately ED 7.5 in the mouse, the neural plate begins to form. Here, the ectoderm thickens and forms the neural plate, which is located right above the notochord, a long cylindrical structure comprised of mesoderm cells. At this point, a process called convergent extension becomes the predominant morphogenetic

process, where epithelial cells constrict and elongate the entirety of the neural plate. The processes involved in convergent extension are very complex, but many of them are regulated by Planar Cell Polarity (PCP) genes (Copp et al, 2003; Wallingford, 2005). After the elongation of the neural plate, the cells associated along the notochord morphologically change and median hinge point forms (Eom et al, 2013). At this point in development, the median hinge point associates with the notochord below it and pulls the middle of the neural plate down causing neural folds to form. The dorsolateral hinge points on each of the neural folds then bend following the restructuring of cells to form a wedge shape, and this allows for the neural folds to meet and fuse (Eom et al, 2013; Golden & Chernoff, 1995). In mice, the neural tube closes at 3 different initiation closure points, and each zip toward each other closing the entirety of the neural tube (Golden & Chernoff, 1995). This process is known as primary neurulation. After this, secondary neurulation occurs, where the lower, or caudal portions of the spinal cord form. This process differs from primary neurulation because a canal is formed within the tissue that then connects to the rest of the spinal column (Greene et al, 2009). These primary and secondary neurulation events occur throughout mammalian species in a very similar manner. Any failure to completely close the neural tube at any of these closure points results in a neural tube defect (NTD).

The anterior neural pore closes by ED 9 or 9.5, while the posterior neural pore remains open until ED 10 or 10.5. Once neural tube closure is completed, the somites, which began appearing at ED 8, will continue to form until ED 14. The somites will subsequently contribute to the vertebrae, skeletal muscle, and skin cells (Hodge, 2010; Slack, 2013). Throughout this stage of development through around ED 13 or 14, the developing embryo/fetus is in a stage of organogenesis, where all

major organ systems a vertebrate has are formed. Following this, and until birth, the embryo undergoes histogenesis, the formation and differentiation of specific tissue types. The normal gestational period for mice averages between 18 and 22 days, depending on the strain of the animal.

1.2 Neural Tube Defects

Neural tube defects (NTDs) are congenital malformations that affect the Central Nervous System (CNS). According to the World Health Organization, NTDs affect between 1 and 10 in every 1000 pregnancies, depending on the geographic location and ethnic group of the mothers. In the United States, it has been noted that Hispanics have the highest rate of NTDs (1.12/1000), whereas African Americans and Asians have the lowest rates, under 1/1000 births (Mitchell, 2005). In other areas of the world; however, these numbers are greatly increased. In the Shanxi province of China for example, in 2003, there was a reported NTD prevalence of 13.9/1000 births (Li et al, 2006). No matter what the rate of NTDs is in various areas of the world, these are defects that come with a great emotional, physical, and monetary burden to those affected and those close to an affected individual.

Neural tube defects arise from the improper closure of the neural tube during early pregnancy. Neural tube is the phrase used for the developing CNS, or brain and spine, in chordates. The term NTD encompasses a number of conditions including, spina bifida, anencephaly, craniorachischisis, encephalocele, and iniencephaly (Kondo et al, 2009). Spina bifida is a lesion in the spinal column, whereas anencephaly is the lack of part of the skull or brain. Craniorachischisis is the condition described when an anencephaly and spina bifida event occur together and the neural material is exposed from the skull and continues to be open to the

spine. Anencephaly and craniorachischisis are both lethal conditions upon birth or even before. Spina bifida is the most common NTD and although it can be surgically closed, it is far from being repaired and the defect has lasting negative effects on the individual's quality of life. The impact that spina bifida has on a child usually depends on the location and the severity of the lesion involved. Generally speaking, spina bifida patients do not have proper innervation below the lesion in their spinal cord; therefore, the complications include not only the loss of function of their legs, but their urinary tract and bowels are also poorly controlled (Kondo et al, 2009). Spina bifida is also often accompanied by hydrocephalus, which can be controlled with the use of a shunt throughout life (Copp & Greene, 2013). Most recent advances in medicine involve surgery to repair spina bifida lesions *in utero.* These are specialized surgeries, but are thought to prevent some neural damage during development and have been reported to improve overall outcomes for these children (Johnson et al, 2006). Encephalocele is a more rare NTD where a portion of the skull is open and allows for the brain and covering membranes to project from this hole. Inienchephaly is a distortion of the spine that manifests as a fetus with a head bent backwards in a star-gazing appearance and the skin is directly connected to the chest. Iniencephaly is a very rare NTD, although more commonly seen in Asian populations, where upon birth these affected infants do not usually live longer than a matter of hours (Botto et al, 1999; Copp et al, 2013). In human pregnancies, neural tube closure occurs 28 days post conception or ED 28 (Botto et al, 1999). In mouse models, the neural tube completes closure at ED 9.5 to 10 (Gray & Ross, 2011). The variety of NTDs described above result directly from the failed closure at specific points of the developing spinal column or brain.

The physical defects that result in NTDs during development have been fairly well described; however, the reasons why these malformations actually occur largely remain mysterious. It has been seen that no one factor can be ascribed to most NTD patients. The principal factors that are considered when looking at the etiology of NTDs includes: genetic factors, nutritional factors, and environmental factors (maternal exposure and maternal environment).

1.2.1 Genetic Effectors of NTDs

One factor that may cause or even pre-dispose people to NTDs is their genetic makeup. In the age of genetic engineering (genome editing), mouse modeling is a very useful tool to help study which genes may be involved in NTDs. Over 240 mouse models of NTDs currently exist (Harris & Juriloff, 2010). Unfortunately, the insight gained by these mouse models does not always easily translate into the human model. When reviewing all of the existing mouse NTD models, Harris and Juriloff (Harris & Juriloff, 2007; Harris & Juriloff, 2010) made a few important conclusions. Not all of these models reflect a dietary responsiveness to folate, and some of them are even responsive to different small molecule treatment. Indeed, many of these models have not even been tested for folate responsiveness. In addition, around 90% of the mouse models manifest with only an NTD and secondary symptoms to this NTD (other health problems can be directly traced to be caused by the NTD). Only around 15% of human NTDs are like this, indicating that human NTD cases are generally more complicated and most likely multi-factorial, even within a single individual. In addition, there have been some genes identified to be mutated in humans with an NTD that do not produce an NTD phenotype when these genes are knocked out in mice (Au et al, 2010). Of the

plethora of mouse models, there are a few biological pathways that seem to be the most promising on which to focus. The era of whole genome sequencing has allowed for a multitude of case-control studies to be performed, and in turn for researchers to identify single nucleotide polymorphisms in selected genes from NTD patients. The genes involved in folate, one-carbon metabolism, and those involved in non-canonical Wnt signaling, or the Planar Cell Polarity (PCP) pathway, have proven to be key genes associated with neural tube defects (Bharathselvi et al, 2013).

Of the one-carbon metabolism related genes, 5,10-methylene tetrahydrofolate reductase (MTHFR) has been one that has been studied intensely (Greene et al, 2009). The MTHFR knockout mouse manifests with hyperhomocysteinemia, aortic lipid deposits, and growth retardation, but depending on the genetic background, no NTDs (Chen et al, 2001). In humans, the C677T mutation found in the MTHFR gene has been heavily studied. This mutation shows a decrease in the MTHFR enzyme function by 35-40% of normal enzymatic function (Frosst et al, 1995). An analysis of the literature showed an increased chance of having an NTD with this mutant allele, but only in Europeans of non-Latin lineage (Amorim et al, 2007). A second mutation found in the MTHFR gene in spina bifida patients is A222V, which resulted in high levels of homocysteine and lower levels of folate (van der Put et al, 1995). Single nucleotide polymorphisms in the Methylene Tetrahydrofolate Dehydrogenase 1 (MTHFD1) gene have also been associated with significantly increased risks of an infant having an NTD (Etheredge et al, 2012). MTHFD1 has also proven to be an essential gene for mouse development, and when only one copy of this gene is present, mice show altered one-carbon metabolism (Macfarlane et al, 2012). Mutations in multiple enzymes in the mitochondrial glycine cleavage system have also been identified in NTD cases,

but not in control samples (Narisawa et al, 2012). Along with the many mouse models that exist where disruption of the folate genes displays as an NTD, the association of mutations in these genes in human patients emphasizes the necessity of proper one-carbon metabolism during gestation.

The second category of genetic emphasis for NTD studies has been the PCP pathway. The fact that PCP genes govern the process of convergent extension directly associates them with proper neural tube closure (Wodarz & Nusse, 1998). It was first noted that when Vangl2, Celsr1, Ptk7, Dvl1/2/3, or Scrib were mutated or knocked out in the mouse, craniorachischisis rates would increase (Copp & Greene, 2013). In humans, mutations in Vangl1 have been identified in a population of spina bifida patients and these mutations were seen to abolish binding with Dvl1/2/3. More recently, the PCP genes of Celsr1 and Scrib have been associated with a population of spina bifida cases as compared to wildtype controls (Lei et al, 2013; Lei et al, 2014). Despite these genetic trends in mouse models and human data sets, it is important to note that NTDs are still considered to be multi-factorial in origin, and other effectors must be investigated in parallel with genetic interrogations.

1.2.2 Dietary Effectors of NTDs

There is no single prevention method known for NTDs. The existing paradigm for ameliorating this public health issue is by encouraging women of child-bearing age to supplement their diets with adequate folic acid. In the late 1970s and early 1980s, Dr. Richard Smithells became the pioneer of the studies of interaction of folate and NTDs (Schorah, 2009). In 1980, Smithells et al showed preliminary data that folate might reduce the chances that a mother will have a child

affected with an NTD. These studies were continued throughout the 1980s (Smithells et al, 1983; Smithells et al, 1989) and validated the initial findings that mothers who were supplemented with folates reduced their risk for having NTD affected pregnancies. Currently, public health panels in different countries handle the issue of recommending folic acid to mothers differently. In the United States for example, the government recommends women of child bearing age to consume 0.4mg of folic acid per day and additionally fortifies grains with folic acid (Shane, 2003). In Great Britain, the government recommends women take 0.4mg of folic acid a day also, but the government does not supplement grain foodstuffs, whereas in the rest of the European Union, 0.2 mg of folate a day is recommended (Sen et al, 2001). In the United States, Canada, and Chile, all countries with mandated folic acid fortification of grains, the number of babies born with NTDs has significantly been reduced since this mandated fortification began (Eichholzer et al, 2006) (Honein et al, 2001). Although there is significant evidence from population based treatment with folic acid, the exact mechanism by which folic acid prevents neural tube defects remains unknown (Wallingford et al, 2013). It is easy to imagine why folic acid is necessary for proper neural tube closure: a time where cells are rapidly dividing needs the one carbon units that folic acid supplies. In fact, it is seen that in certain genetically modified mouse models, additional folate supplementation can partially protect against some NTDs (Fleming & Copp, 1998). It has also been suggested that one of the essential roles of folate in preventing NTDs is its role in DNA methylation. Potentially, the epigenetic regulation by sufficient folate is responsible, in part, for the proper development of an embryo (Greene et al, 2011).

1.2.3 Environmental Effectors of NTDs

The complex interactions of diet and genetics are constantly being studied and manipulated in attempts to better understand the etiology of NTDs. One must also consider maternal exposures. These exposures do not necessarily have to be what mothers consume, but what they encounter while pregnant and the environment that they provide for their developing embryo. There are a number of factors that mothers may be exposed to, or that may compromise the *in utero* environment that the embryo develops in, that have proven to be crucial in describing risk factors for NTDs. For example, the regionally higher rates of in-home coal burning in high-risk areas of China prompted many studies on this constant exposure, to determine if it could be a contributing factor as to why there are so many children born with NTDs in the Shanxi province. It was indeed seen that mothers who live in constant exposure to the combustion byproducts of coal had an elevated risk for NTDs (Li et al, 2011). Additionally, it has been more recently demonstrated that organic pollutants in the environment will increase the risk for NTDs when mothers are constantly being exposed (Correa et al, 2008; Ren et al, 2011). Occupational exposure to radiation, heavy metals, and certain chemical by-products has also been correlated to higher risk for giving birth to children with NTDs (Maldonado et al, 2003; Sever, 1995). Even the act of living in areas with higher levels of air pollutants has been shown to increase risk for NTDs (Padula, 2014). Studies such as these though tend to be debated in the literature, with a split in findings when reviewing population-based analysis of human subjects (Brender et al, 2006) (Jin et al, 2014; Suarez et al, 2012). Many animal studies have shown that exposure to heavy metals will increase the risk for birth defects (Saadeldien et al, 2012) (Padmanabhan, 1987; Webster & Messerle, 1980). Not all exposures that

are harmful for developing infants are physical entities, however. The long established risk factor, maternal hyperthermia (Bennett et al, 1990; Finnell et al, 1986) is not to be overlooked. The risk for NTDs can be elevated by almost two-fold (Moretti et al, 2005) when the internal body temperature reaches only 100^{o}F. Maternal use of hot tubs and even practicing hot yoga are discouraged for pregnant women (Chan et al, 2014).

One of the most well-known environmental causes of NTDs was highlighted when there was an NTD cluster in 1990 on the Texas-Mexico border (Missmer et al, 2006). It was thought that this increased rate of NTDs was due to corn that was contaminated with Fumonisins, as horses in the area had previously been afflicted with leukoencephalomalacia (Hendricks et al, 1999). Fumonisin B1 is a toxin produced by two different molds (Sadler et al, 2002). It is a well characterized toxin that is a common contaminant of corn. Exposure to this toxin has been associated with various pathologies including liver and kidney toxicity and leukoencephalomalacia in horses (Gelineau-van Waes et al, 2005). It has been previously reported that the risk for NTDs increases with exposure to Fumonisin B1 in a dose-dependent manner until fetal death is observed (Suarez et al, 2012). Mechanistically, Fumonisin B1 was shown to inhibit sphingosine N-acetyltransferase, therefore inhibiting the synthesis of different sphingolipids in cells. Since sphingolipids are used in many biological processes from signaling to structural building, it is thought that their disruption will lead to problems during development, even potentially causing NTDs (Sadler et al, 2002).

Valproic acid (VPA) is a small molecule drug that is used to treat migraine headaches, epilepsy, and bipolar disorder. VPA was discovered in the 1960s to have efficacy in seizure treatment (MEUNIER et al, 1963) and was subsequently approved

by the FDA in 1978 for use in the United States to treat epilepsy. More recent applications have been prescribing VPA for use helping bipolar disorder and migraine headaches, thus widening the group of women of reproductive age that are using VPA as a therapeutic. Years of scientific research about the teratogenicity of VPA (Robert & Guibaud, 1982) (DiLiberti et al, 1984; Lammer et al, 1987) culminated in a warning in 2009 by the US FDA that *in utero* exposure to VPA increases the chances that a baby will have a variety of congenital malformations including NTDs. In fact, it has been reported that mothers taking VPA will have a 2 to 16-fold higher chance of giving birth to a child that is affected with a congenital malformation (Hill et al, 2010) (Jentink et al, 2010). Neither the exact mechanism of action for the efficacy of VPA nor the mechanisms of action for the teratogenicity of VPA are known. It is thought that VPA has multiple targets, including increasing the neurotransmitter gamma-aminobutyric acid and even directly inhibiting voltage-gated sodium channels (Rosenberg, 2007). In addition, the exact mechanism of teratogenicity of VPA is unknown. It has been hypothesized that VPA serves as an HDAC inhibitor that may have anti-angiogenic effects during development (Phiel et al, 2001), serves to create folate-depleted conditions (Schwaninger, 1999), sequesters Coenzyme A through its metabolism, and generally increases bodily levels of oxidative stress (Hsieh et al, 2012). In addition to the more commonly prescribed VPA, a second anti-convulsant drug has been shown to increase the risk of having an NTD affected pregnancy when mothers are using this drug known as carbamazepine during pregnancy. Carbamazepine is a derivitized iminostilbene that is used in the treatment of epilepsy, bipolar disorder, and trigeminal neuralgia (Jentink et al, 2010). The mechanism of teratogenicity of this drug is also still relatively unknown, but it is thought to be mediated by an arene oxide intermediate

(Madden et al, 1996). Carbamazepine has been seen to be a risk factor for NTDs and other congenital malformations (Hill et al, 2010).

The maternal environment in which the embryo is developing is also of great concern. In addition to external stimuli that the embryo may encounter secondary to the mother's exposure, there are also steady states maintained by mothers that are directly related to an increased risk for developing NTDs. Maternal obesity has been shown to increase the risk of having a NTD affected pregnancy by at least 2 fold (Shaw et al, 1996). In addition to obesity, maternal type II diabetes has also been shown to increase the risk for babies born to affected mothers to have a higher risk of congenital malformations (King, 2006). Although no direct mechanism has been demonstrated for the pathogenesis caused during development of a mother affected with type II diabetes, some more general hypotheses have been discussed. The current general consensus is that the disruption of glucose and fat energy balance lead to mitochondrial stress and an increase in reactive oxygen species (ROS) (Reece, 2012). The creation of ROS has been shown to increase apoptosis and deviations in development in many model organisms (Hill et al, 2013). An increase in oxidative stress has also been directly correlated to NTD risk (Groenen et al, 2004; Han et al, 2011). Other researchers suggest that the increase in risk for NTDs when mothers have diabetes is due to altered epigenetic regulation (Sukanya et al, 2012). It has been shown that methylation status has been changed in key genes during a diabetic state (Ling et al, 2008). The differences in methylation patterns seen in diabetics are not only thought to allow for more or different gene transcription, but it has also been proposed that these epigenetic changes may influence the DNA that offspring receives (Villeneuve & Natarajan, 2010). Not only could the development be disregulated *in utero* by maternal signals, the DNA of the

baby itself could be changed due to the diabetic status of the mother. Another factor that links both diabetes and obesity is increased basal levels of inflammation (Das, 2004). In obesity, and type II diabetes, there is an excess of adipose tissue. This adipose tissue, which traditionally was thought of as only an excess energy store, is now being thought of as an endocrine tissue. Adipocytes release regulatory molecules now known as adipokines (MacDougald & Burant, 2007). These adipokines are signaling molecules responsible for satiety, insulin sensitivity, and more. In addition, it has been shown that adipocytes play a key role in both innate and adaptive immunity, both of which have been implicated in NTDs (Huh et al, 2014).

Despite the number of different factors that have even been discussed here that contribute to the risk for NTDs, it remains that NTDs are multi-factorial in nature. The first point of evidence is that folate greatly reduces the risk for having a child with an NTD, but does not completely abolish this possibility. Another marked example of this is that wildtype mice that are fed a low folate diet do not present with an increased risk for NTDs, whereas when the genotype is also manipulated, you begin to observe an increased risk for NTDs (Burren et al, 2008). In addition, it is seen that some single allele mutations will not increase the risk for an NTD, but when paired with another mutation, there is an increased risk for an NTD (Ross, 2010). Some mouse models only express an NTD phenotype in response to environmental stimuli when they already have a genetic mutation (Wlodarczyk et al, 2001). It is therefore important to study all possible facets of the etiology of NTDs.

1.3 WNT SIGNALING

More than 3 decades ago, the *Wingless* gene was manipulated in *Drosophila* and the same gene, a relatively unstudied proto-oncogene, Int-1, was reported in the mouse (Bejsovec, 2013). In 1991, the name Wnt was coined by Nusse et al as a combination of wingless and int, thus the start of a new nomenclature for this important gene family. The Wnt genes are highly conserved throughout species, and it is now known that vertebrates have 19 Wnt genes (Nusse & Varmus, 2012). The Wnts were discovered when investigating their potential role in cancer, but more research has shown that they have a critical role in development, and also various disease states such as multiple types of cancer and diabetes (Logan & Nusse, 2004). The Wnt proteins themselves are a group of soluble glycoproteins ranging from 300 to 400 amino acids in length that have a highly conserved region of modified cysteine residues (Cadigan & Nusse, 1997). The Wnt proteins serve as signals to various cell surface receptors to begin a cascade of signal transduction to the target cell. There are three major paths of Wnt signaling that are known: canonical β-catenin. Non-canonical planar cell polarity (PCP) and non-canonical calcium regulation (Habas & Dawid, 2005).

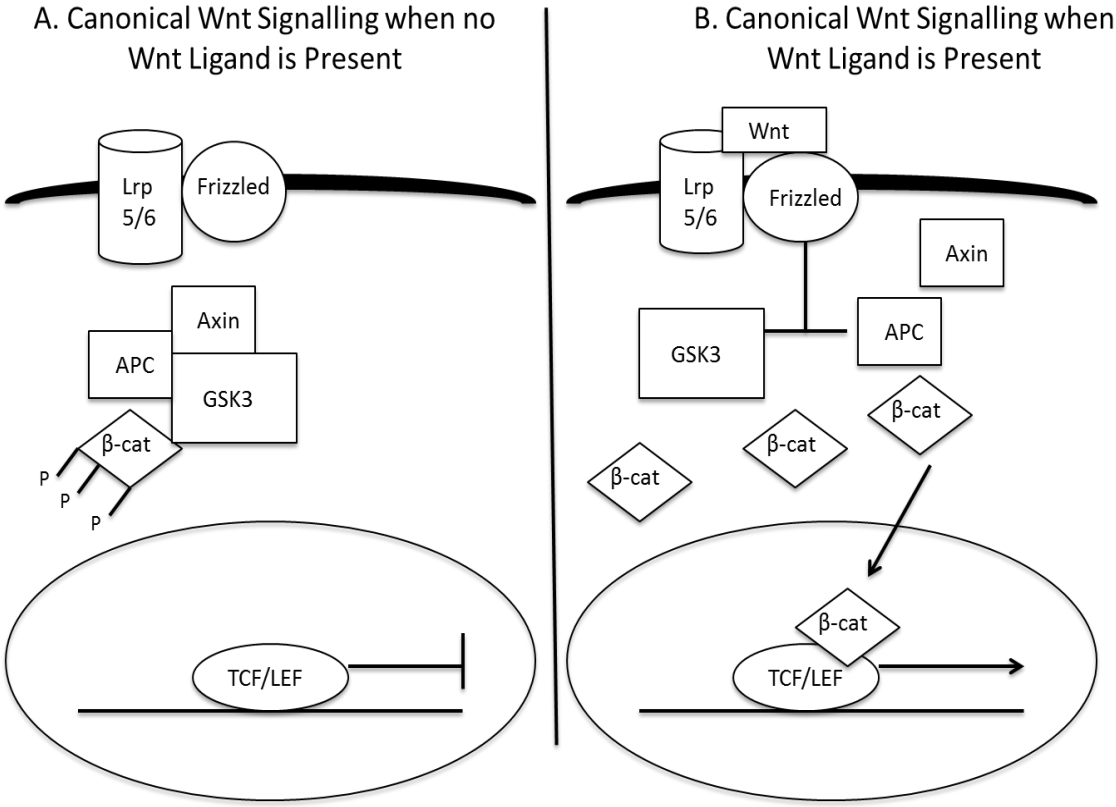

Figure 1.1 Canonical Wnt Signaling Cascade

Panel A shows an inactive Wnt signaling cascade. Here, no ligand binds to the cell surface receptors and β-catenin is phosphorylated and degraded. Panel B shows an active Wnt signaling cascade. Here β-catenin does not get phosphorylated and is allowed to translocate into the nucleus and turn on TCF/LEF dependent genes.

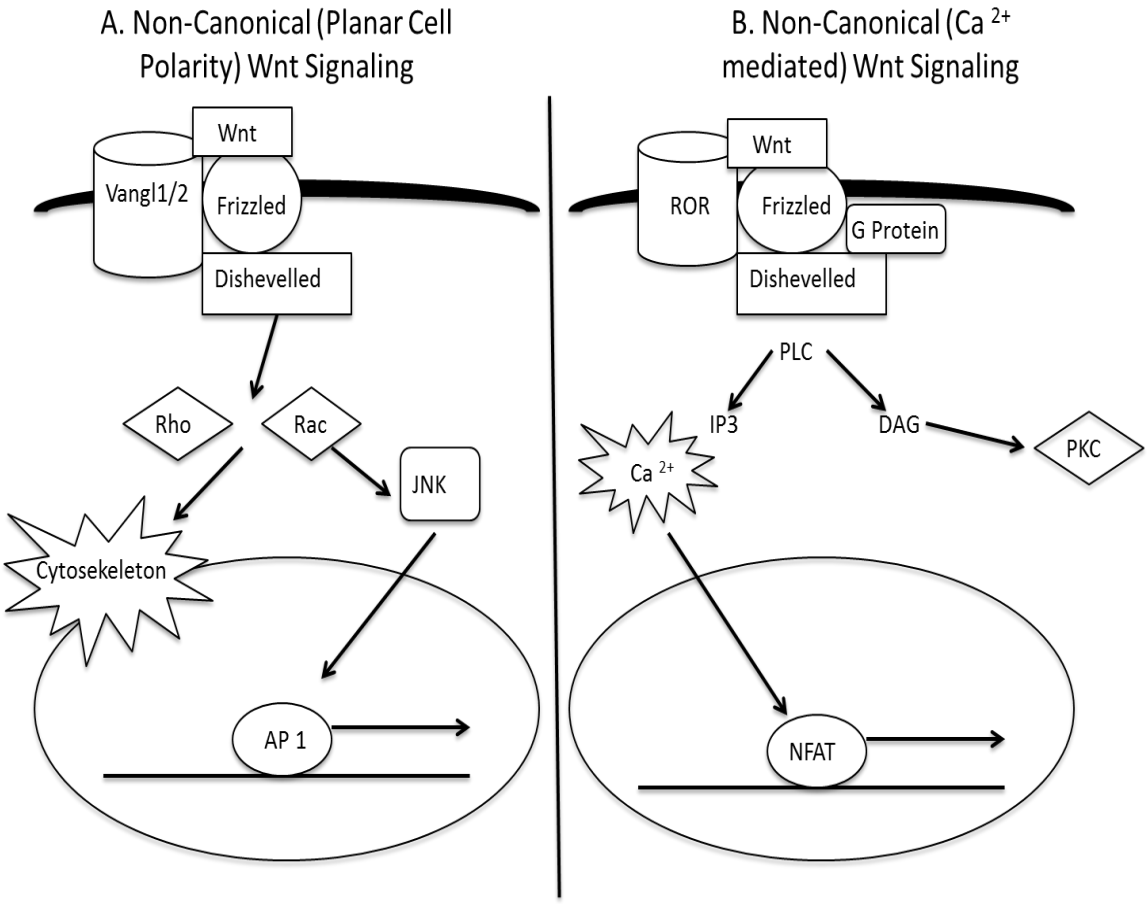

Figure 1.2 Non-Canonical Wnt Signaling Pathways

Panel A shows the PCP pathway that will either help with cytoskeletal remodeling or transcribe AP1 dependent genes. The Calcium pathway shown in panel B will either activate PKC or transcribe NFAT dependent genes.

Figure 1.1a illustrates the canonical Wnt signaling pathway. This pathway is characterized by protein receptor complex that is embedded in the cell membrane that is made up of Frizzled and low density lipoprotein receptor-related protein 6 (MacDonald et al, 2009). The pathway only turns on when this complex binds one of the extra-cellular Wnt proteins, most commonly Wnt1, Wnt3a, and Wnt 8 for canonical Wnt signaling (Niehrs, 2012). When this pathway is not active, Glycogen Synthase Kinase 3 (GSK3) steadily phosphorylates beta-catenin. This phosphorylation event causes beta catenin to be tagged for degradation (Klaus & Birchmeier, 2008). A protein complex known as the destruction complex will dock on the phosphorylated beta catenin. This complex will polyubiquinate the beta-catenin, causing it to be found and destroyed by a proteasome (Kimelman & Xu, 2006) (Kim et al, 2009). In the presence of a Wnt ligand (Figure 1.1b), beta-catenin is not degraded and translocates into the nucleus. In the nucleus, beta-catenin is allowed to bind TCF/LEF (T-cell factors/leukocyte enhancer factor) and activates transcription of specific genes (Rao & Kühl, 2010). Proper Wnt signaling is essential during development in patterning and control of organogenesis (Komiya & Habas, 2008).

Figure 1.2a illustrates the non-canonical (PCP) Wnt signaling pathway. The PCP pathway is also known as the beta-catenin independent pathway. The pathway starts out when Wnt proteins bind the PCP frizzled/disheveled receptor complex. Most commonly Wnt5a and Wnt 11 will bind this complex to begin non-canonical Wnt signaling (Niehrs, 2012). Wnt binding activates a cascade of Rho GTPases and protein kinases (Rao & Kühl, 2010). The GTPases can directly influence cytoskeletal elements and the protein kinases can cause transcriptional changes in the nucleus (Niehrs, 2012). The PCP pathway is known for regulating the polarity of cells within

a thin layer of cells. Essential developmental phenomenon, such as the orientation of cilia and the process of convergent extension are dependent upon the PCP pathway (Jones & Chen, 2007) (Rao & Kühl, 2010).

The calcium dependent Wnt signaling pathway is a second beta-catenin independent signaling pathway (Figure 1.2b). Here, a Wnt protein binds frizzled complexed with an ROR 1/2 co-receptor. This, in turn, activated phospholipase C, which cleaves phospholipids to create inositol 1,4,5-tri-phosphate (IP3) and 1,2 diacylglycerol (DAG). IP3 causes calcium ion release from the endoplasmic reticulum, which activates calmodulin-dependent protein kinase III. DAG activates protein kinase C. Then both these kinases can then activate diverse transcription factors such as NFAT and NEMO, which can regulate tissue movements and specifications and inhibit beta-catenin signaling (De, 2011; Komiya & Habas, 2008).

1.3.1 Low Density Lipoprotein Receptor-Related Protein 6

Low Density Lipoprotein receptor-related protein 6 (LRP6) is one of the transmembrane receptor proteins involved in Wnt Signaling. LRP6 was first described in 1998 (Brown et al, 1998) as a member of the low density lipoprotein receptor family. The low density lipoprotein receptor family is a group of membrane proteins that are responsible for binding and promoting the endocytosis of specific proteinaceous ligands (Nykjaer & Willnow, 2002). This family of proteins is characterized by a generic set of motives including a high percentage of cysteines, extracellular LDLR repeats and EGF repeats spaced by YWTD domains (Brown et al, 1998). LRP6 and LRP5 are very closely related members of this family. These two proteins are approximately 70% homologous in amino acid content and share a similar structure including 4 beta-propeller domains and 3 low density lipoprotein

ligand binding domains on the extracellular portion of the protein and one transmembrane anchor (Joiner et al, 2013). Mutations in human LRP5 and 6 proteins have been associated with bone defects, heart disease and Alzheimer's disease (Joiner et al, 2013; Williams & Insogna, 2009).

Both the LRP5 and 6 proteins require a chaperone protein to escort them from the endoplasmic reticulum to the plasma membrane. This chaperone, known as mesoderm development protein (MESD) in mice, and Boca in *Drosophila*, is a highly conserved protein across species (Culi & Mann, 2003). When MESD is knocked out in mice, you see a high rate of embryonic lethality that is similar to the deletion of Wnt3a (Hsieh et al, 2003). This suggests that MESD is essential for Wnt signaling because without it, one of the major receptor proteins cannot make its way to the cell membrane and become functional (Herz & Marschang, 2003). This is further evidenced by cell culture localization studies that show MESD is required for LRP6 to be properly located in the plasma membrane (Gray et al, 2013).

LRP6 is most commonly known for its crucial role in Wnt signaling as a co-receptor for the Wnt protein ligands in the canonical Wnt signaling pathway (Figure 1.1). More recent reports have shown that LRP6 may have a vital role in the non-canonical, PCP pathway as well (Allache et al, 2014; Bryja et al, 2009; Gray et al, 2013). The reciprocal effects of canonical and non-canonical Wnt signaling are beginning to be investigated, and it was seen that sometimes when a mutation in LRP6 decreased canonical Wnt-signaling, this was countered by an increase in PCP signaling (Allache et al, 2014). In addition, when LRP6 was either deleted from a mouse model, or mutated, the embryos did not develop properly and have mis-localization of GTP-RhoA, indicating a malfunction in PCP signaling (Gray et al, 2013). Although the intricacies of the role of LRP6 in both canonical and non-

canonical Wnt signaling still need to be fully elucidated, it is clear that this protein plays essential roles during neural development.

1.4 FOLATE (ONE-CARBON) METABOLISM

Folate is the general term that refers to the family of water-soluble B vitamins used in one-carbon metabolism. The transfer of any single carbon group in the body requires the donation of this carbon from a folate derivative, and therefore these processes are collectively known as one-carbon metabolism. A folate is a compound that contains a pteridine ring connected to a paraaminobenzoic acid, and a number of glutamic acid residues (Kim, 2007) (Locksmith & Duff, 1998). This polyglutamate tail is added to folates when they enter cells, so the newly entered folates remain inside the cell. The polyglutamate tail also helps the enzymes that will use these folates to better bind their substrates (Appling, 1991).

Mammals cannot synthesize folates *de novo*, and therefore must consume folates in their diet. The most well-known of the folates, folic acid, is the synthetic, oxidized form of the vitamin (Figure 1.3) (Lucock & Yates, 2009). Folic acid is a highly stable molecule and easy to produce, thereby making it the ideal vitamin to supplement foodstuffs with (Ohrvik & Witthoft, 2011). Folic acid is not a bioactive form of the folate family. When folic acid enters the cell, it is reduced by various enzymes. The reduced products are tetrahydrofolate (THF) and dihydrofolate (Figure 1.3b). Carbon units can then be added to the N5 and N10 positions, or bridge both. The resulting products are 5-methyl-THF, 5,10-methylene-THF, 5,10-methenyl-THF, 5,10-formimino-THF, 5-formyl-THF and 10-formyl-THF (Preedy et al, 2013). Naturally occurring dietary folates are reduced forms of folate, such as 5-methyltetrahydrofolate. Dietary folate sources include citrus fruit, dark leafy

greens, and legumes (Ohrvik & Witthoft, 2011). The instability of these natural forms of folate, however, does cause a large loss of the bioavailable compounds during food preparation, mostly through heating or oxidation (Bailey, 1995). It has also been noted that the bioavailability of folic acid is higher than that of natural sources, most likely because of its high affinity for many of the folate transport proteins (Hannon-Fletcher et al, 2004).

The importance of these bioactive folates is their place in all of one carbon metabolism. Figure 1.4 shows a brief overview of all of the places in cellular metabolism where folates are critical. One of the most important roles of folates is in nucleotide biosynthesis. When the body is synthesizing purines, 10-formyl-THF is required for a one-carbon donation. In addition, the only source of thymidine is by the methylation of deoxyuridine monophosphate (dUMP) to create deoxythymidine monophosphate (dTMP) using 5,10-methylene-THF (Nazki et al, 2014). Folates are therefore necessary for the synthesis DNA, an essential process for all cells. Folates are also required for methylation reactions. Most directly, 5-methyl-THF is required to recycle homocysteine back into methionine. Methionine can then be converted to s-adenosylmethionine (SAM), which is used in any number of reactions to methylate DNA, RNA, lipids, and proteins (Crider et al, 2012). DNA methyltransferases can use SAM to methylate cytosines and act in a regulatory manner (Anderson et al, 2012). Methyl groups can also be added to histone proteins and work to regulate transcription of DNA. It has even recently been shown that folic acid can change the structures of chromatin and therefore directly help regulate which genes are transcribed (Ichi et al, 2012). It is easily noticed why folate is such an essential vitamin; folate is required to simply make DNA and also for many other regulatory processes that we are just beginning to understand.

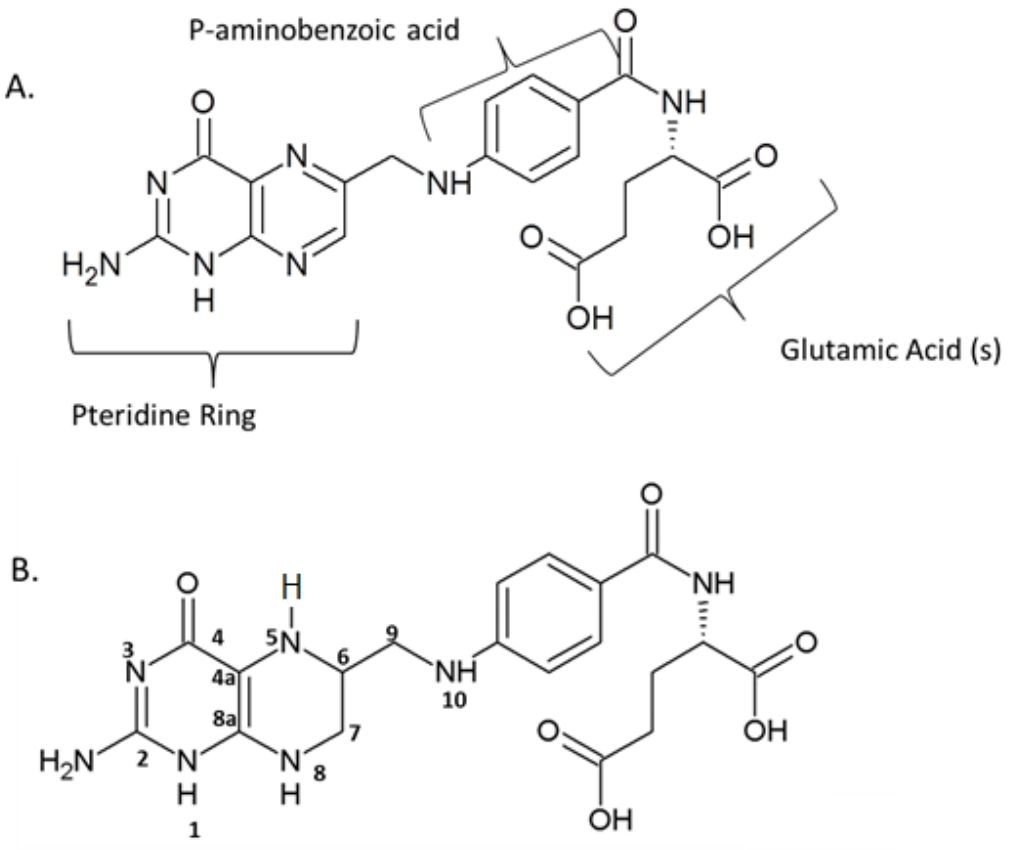

Figure 1.3 Folates: Water-soluble Vitamins B9

Panel A illustrates the oxidized and synthetic form of the folates, folic acid. Folates generally consist of a pteridine ring, a para-aminobenzoic acid, and any number of glutamic acid residues. Panel B illustrates the reduced form of a folate, tetrahydrofolate. This is the molecule that will be the acceptor and donor for the following one carbon units at N5 and/or N10:

Methanol CH_3-OH	5-Methyl-THF
Formaldehyde CH_2=O	5,10-Methylene-THF
Formic Acid HCOOH	5,10-Methenyl-THF
	5,10-Formimino-THF
	5-Formyl-THF
	10-Formyl-THF

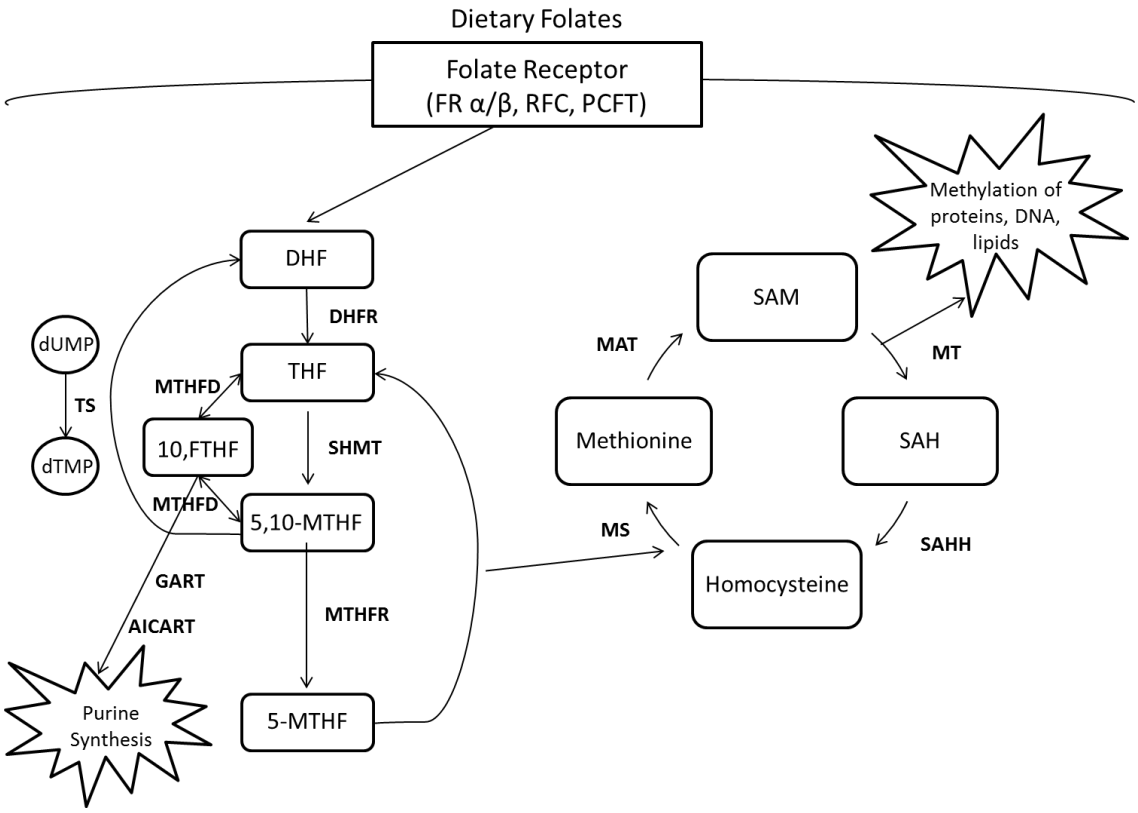

Figure 1.4 Folate One-Carbon Metabolism

Figure Caption Continued Page 24

Figure 1.4 Folate One-Carbon Metabolism

Folates enter the cell through cell surface folate receptors. These can be either the high affinity folate receptors (FRα/β), reduced folate carrier (RFC), or the proton coupled folate transporter (PCFT). Dihydrofolate (DHF) will be reduced to tetrahydrofolate (THF) using dihydrofolate reductase (DHFR). THF can be converted to 5,10-methylenetetrahydrofolate (5,10-MTHF) using serine hydroxymethyl transferase (SHMT) and converting serine to glycine. 5,10-MTHF can be converted to 5-methyltetrahydrofolate (5-MTHF) using methylene tetrahydrofolate reductase (MTHFR). 5-MTHF can then be used for a one carbon donation to homocysteine to synthesize methionine via methionine synthase (MS), therefore recreating THF. 5,10-MTHF can also be recycled to DHF in order to turn dUMP into dTMP using thymidylate synthase (TS). 5,10-MTHF can be reversibly turned back to THF with a 10-formyltetrahydrofolate (10-FTHF) intermediate, using methylenetetrahydrofolate dehydrogenase (MTHFD). 10-FTHF can be used in purine synthesis using the enzymes aminoimidazolecarboxamide ribonucleotide transferase (AICART) and glycinamide ribonucleotide transformylase (GART). Once methionine is remade from homocysteine with the one carbon donation from 5-MTHF, it can be turned into S-adenosyl methionine (SAM) using Methionine adenyltransferase (MAT). Methionine can also be consumed and enter this portion of the cycle. Methyltransferase (MT) can then be used to donate methyl groups to lipids, proteins, or DNA, creating S-adenosyl homocysteine (SAH) as a byproduct. S-adenosyl homocysteine hydrolase (SAHH) will then create homocysteine, where the methionine cycle then merges again with the folate cycle.

1.4.1 Folate Proteins

There are specialized proteins that allow for cells to uptake folates from the circulating blood. These proteins are known as the high affinity folate receptors and the folate transporters. The high affinity folate receptors are between 70 and 80% homologous in sequence (Shen et al, 1995). In humans the high affinity folate receptors include Folate Receptor Alpha (FRα), Folate Receptor Beta (FRβ), Folate Receptor Gamma (FRγ). The high affinity folate receptors readily bind folates and their Kd values for most folates are in the nanomolar range (Rijnboutt et al, 1996). There are also two known folate transporters, the Reduced Folate Carrier (RFC) and the Proton Coupled Folate Transporter (PCFT). The folate transporters are distinguished by their much lower binding affinities for folates, as they have Kd values in the micro to millimolar range (Sabharanjak & Mayor, 2004). The functions and expression patterns of these different folate transporters and receptors are unique.

1.4.1.1 Folate Receptor Alpha

Folate Receptor α (FRα) is known to use an endocytotic mechanism to allow folate to enter cells. The details by which the folate receptors are organized and readied for endocytosis are still being debated. It has been postulated that FRα is usually localized to caveolae (invaginations in the cellular membrane with increased lipid and protein content) or potentially lipid rafts, but more evidence is needed to reach a definitive conclusion (Sabharanjak & Mayor, 2004; Wu et al, 1997). The working scheme of FRα endocytosis is seen in Figure 1.5. In short, folates bind to the cell surface receptors, which are taken into the cell in an endocytotic vesicle.

The pH in the vesicle dramatically drops and the folate is released from FRα. A folate transporter (putatively, PCFT) will then allow for the folate to exit the vesicle into the cytosol where it will become polyglutamated and remain for use (Kamen & Smith, 2004). FRα is primarily found in epithelial tissues in humans, including the kidney and choroid plexus, although it is most highly expressed in the placenta (Antony, 1996). Due to the necessity of FRα in the placenta during development, it is considered to be the most developmentally relevant FR.

FRα is also notably expressed in many cancers. Malignant tumors in reproductive tissues, brain, colon, and breast tissues have all been seen to have higher than normal levels of FRα (Salazar & Ratnam, 2007). The variable expression patterns of FRα in tumors, including the *de novo* expression of FRα in some tumor tissues, along with the very specific and limited expression patterns of FRα in healthy tissue, make it a potential target for cancer therapeutics (Wu et al, 1999). Some potential methods that are being explored in order to exploit the rather high and particular expression of FRα in tumors are folate-conjugated drugs, radionucleotides conjugated to anti- FRα antibodies, and various vaccinations in order to induce auto-immunity to FRα (Lu et al, 2004). The NIH clinical trials database shows that there are many of these treatments currently in human clinical trials.

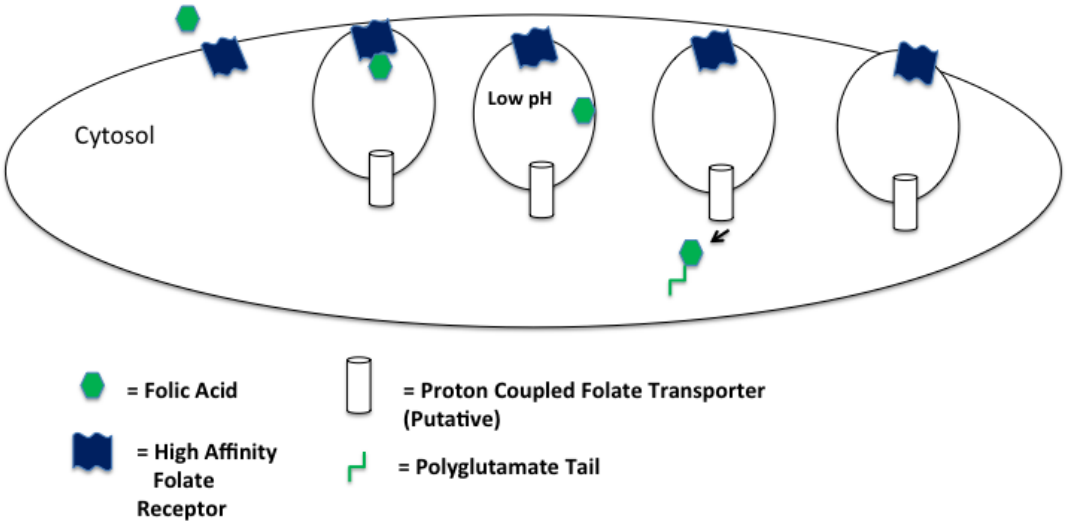

Figure 1.5 Endocytotic Mechanism of the Folate Receptor Alpha

FRα functions through an endocytotic mechanism. The surface high affinity folate receptor binds folate, and then becomes endocytosed. The pH of this vesicle lowers greatly and folate is released from the FR. Folate is transported out through a second folate transporter, thought to be PCFT, and polyglutamated. The receptor is then recycled back to the cell surface.

The most notable therapeutic use of FRα; however, does not directly exploit the transport protein, but a downstream enzyme. Methotrexate (MTX) is a folic acid mimetic approved by the FDA for multiple therapeutic uses (Figure 1.6). MTX has been shown to inhibit the enzyme dihydrofolate reductase (DHFR) (Endresen & Husby, 2001). When methotrexate is present in the bloodstream, it will bind to FRα on cell surfaces and compete with folic acid for these receptors. Although MTX has a binding affinity around 100 fold lower than folic acid to FRα, humans are therapeutically treated with enough MTX to disrupt the normal folate metabolism of a cell highly expressing FRα (Damaraju et al, 2005). When MTX is taken into cells, it binds DHFR rather tightly and does not allow folic acid entering the cells to be converted to the functional tetrahydrofolate form of the vitamin (Cronstein, 1997). This modification to the DHFR enzyme therefore does not allow for folic acid or any oxidized folate to enter the cell as a functional vitamin, thereby classifying MTX as a competitive inhibitor to DHFR. The lack of one-carbon units severely inhibits cellular growth and will kill the cells with high FRα expression, such as high or novel expressing cancer cells. MTX is trademarked under the brand names of Rheumatrex© and Trexall©. Methotrexate is currently approved for use to help treat psoriasis, rheumatoid arthritis, and certain cancers.

More recently, FRα has been implicated as having a role itself other than just a transport protein. In a 2010 report, it was noted that FRα was not only found in the plasma membrane of the cell, but also within the nuclear membrane (Bozard et al, 2010). Work done after this study showed that FRα can also translocate to the nucleus. It was seen that with increased amounts of folic acid present, FRα was seen to more readily translocate to the nucleus. In the nucleus, FRα has the ability to act as a transcription factor (Boshnjaku et al, 2012). Boshnajaku et al then

demonstrated that FRα can bind to cis-regulatory elements of promoters and regulate the transcription of certain genes. This new area of investigation emphasizes the importance of FRα, and may begin to shed light on the necessity of the protein, even when not all NTDs are folate responsive. It also opens a new avenue of research in the efficacy of folic acid; do increased amounts of folic acid benefit the growing embryo by not only their usual role as a vitamin, but also by increase the regulation of genes by FRα.

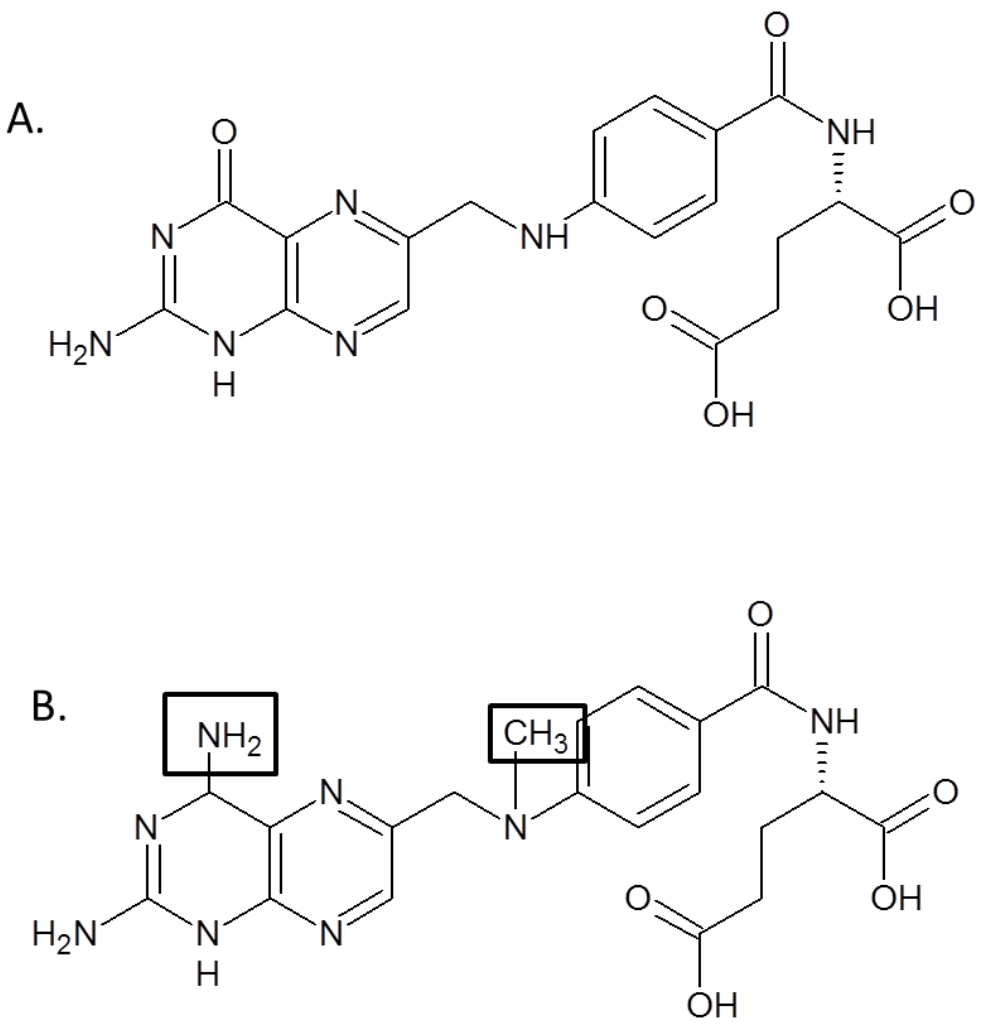

Figure 1.6 Folate Mimetic as Therapeutics

Panel A shows the structure of folic acid. Panel B shows the structure of the common folate mimetic Methotrexate. Methotrexate has the same structure as folic acid, with two different substituents, boxed in panel B. Methotrexate has a higher affinity for dihydrofolate reductase than natural folates, and is used for treatment of various cancers, rheumatoid arthritis, and psoriasis.

1.4.1.2 Folate Receptor Beta

Similar to FRα, Folate Receptor β (FRβ) is a glycophosphatidylinositol (GPI) anchored high affinity folate receptor. FRβ has an expression pattern that differs from FRα; FRβ is expressed mostly in placenta and non-epithelial malignant cells (Ross et al, 1994). In contrast to the FRα mouse models, the genetically modified mouse model without a Folr2 (FRβ) gene shows no gross developmental defects. The Folr2 mouse models that are homozygous for the mutation do show an increased susceptibility to teratogens such as sodium arsenate and VPA (Spiegelstein et al, 2003; Wlodarczyk et al, 2001). Unlike FRα, which is essential for proper development, FRβ does not appear to be, although errors in this protein may increase risk for NTDs when other factors that also increase NTD risk are present. FRβ has historically been identified as being overexpressed in certain types of cancer, such as leukemia (Ross et al, 1999). Upregulation of FRβ have also been noted in inflammatory disorders such as rheumatoid arthritis (Chen et al, 2005). More recently, FRβ has been described as a marker and potential drug target for tumor associated macrophages (Kurahara et al, 2012). As with FRα, FRβ has been implicated as either a marker or a target for/in many different disease states, and significant research energy is being dedicated to the specific targeting of both of these receptors.

1.4.1.3 Folate Receptor Gamma

Human folate receptor gamma (FRγ) (Wang et al, 1998) is a soluble high affinity folate receptor family member, as it lacks the signal peptide for a GPI anchor. FRγ has two common isoforms including the full-length transcript and a splice

variant commonly known as FRγ' (Shen et al, 1994; Shen et al, 1995). Together, these proteins are generally considered to be the soluble forms of the high affinity FRs in humans (Lu et al, 2004). Similar to the soluble FBP that is well studied from bovine milk, FRγ has a binding affinity around 0.4 nM (Shen et al, 1995). FRγ remains the least studied of the high affinity folate receptors in humans.

1.4.1.4 Folate Binding Protein

Folate Binding Protein is the generic term to refer to any of the high affinity folate receptors. In humans, any soluble, or unanchored, folate receptor can be referred to as a folate binding protein. More commonly, the term FBP is used to refer to the commercially available bovine FPB (bFPB). This is a commonly used reagent in many folate assays. FBP is found in mammalian milk and is thought to assist with folate provision and uptake while animals are suckling (Nygren-Babol & Jägerstad, 2012).

1.4.1.5 Proton Coupled Folate Transporter

The Proton Coupled Folate Transporter (PCFT) was first described in the literature nearly a decade ago as a heme transporter (Shayeghi et al, 2005). Shortly after, it was reported that this gene actually coded for a protein that was functional in transporting folates (Qiu et al, 2006). PCFT has a high affinity for folates at a rather low pH, functioning optimally at a pH of 5.5. This folate transporter is expressed mainly in the kidney, liver, placenta, small intestine, choroid plexus, and spleen (Qiu et al, 2006). The notably high expression of PCFT at the apical brush border in the duodenum is not surprising due to the dietary intake of folates that need to be absorbed and the locally low pH (Zhao et al, 2009a). It has been proposed that PCFT is the protein responsible for allowing folate to exit the

endosomic vesicles following FRα-mediated folate uptake (Figure 1.5) (Zhao et al, 2009b).

PCFT null mice survive through weaning age, but will die at around 50 to 60 days of age (Salojin et al, 2011). Intraperitoneal injection of these mice with folates will allow for them to survive past this time point into adulthood. It is hypothesized that this phenomenon is a result of the weanling mice ingesting plenty of extra folate (bound by milk folate binding protein) while suckling, but developing severe deficiencies after weaning (Salojin et al, 2011). These data reiterated the importance of the PCFT protein in the uptake of folate, and the mouse model was determined to closely resemble the symptoms of human folate malabsorption in the severe hematological problems that these mice develop (Salojin et al, 2011). Loss of function mutations in this gene have been associated with hereditary folate malabsorption in a few human patients, a condition characterized by lower folate levels in the cerebral spinal fluid than the circulating blood, mental retardation, ataxia, and megaloblastic anemia (Shin et al, 2011; Zhao et al, 2009b). It has been hypothesized that PCFT plays an essential function in allowing folates to cross the blood brain barrier, explaining the human patients with mutations in this gene (Geller et al, 2002).

1.4.1.6 Reduced Folate Carrier

The reduced folate carrier (RFC) is a bi-directional folate transport protein with an affinity for reduced folates on the order of 1 μM, but an affinity for the oxidized substrate folic acid around 100 fold lower (Ifergan et al, 2008). This protein is encoded for by the SLC19A1 gene and has 12 transmembrane passes with both its N and C termini located in the cytoplasm (Zhao et al, 2009b). The other

gene family members SLC19A2 and SLC19A3 code for two thiamine transporters (Ganapathy et al, 2004). Although there is evidence of RFC mRNA in all human tissues, the highest levels of expression of the RFC is seen in placenta, liver, and the epithelial tissues in the small intestine (Chiao et al, 1997; Zhao et al, 2001). The exact mechanism of RFC transport has not yet been elucidated, but it is classified as an organic anion transporter. The proposed mechanism is that RFC helps move folates through the plasma membrane by allowing anions to go down their concentration gradient and allowing folates to enter the cells. It has been shown that a variety of different organic anions can bind RFC and move through the protein *in vitro*, although phosphate anions are thought to be a major player in this type of folate transport. (Matherly et al, 2007; Zhao et al, 2002; Zhao et al, 2009b).

Using mouse models, RFC was shown to be a critical developmental protein. Animals completely lacking the RFC gene die *in utero* by ED 9.5. These embryos could be rescued by dosing the dams with 1mg/day folic acid, but all of the null animals died by day 12 due to no erythropoiesis (Gelineau-van Waes et al, 2008; Zhao et al, 2001). The RFC protein is seen to be upregulated when cells are dividing, but once they become senescent, the amount of RFC is reduced (Hamid et al, 2009). This requirement of RFC for growing cells and its ubiquitous expression patterns emphasize its importance in folate transport.

1.4.2 Homocysteine

Homocysteine is a non-protein incorporating amino acid that is a natural product of methionine cycling (Figure 1.7a). When methionine is turned into S-adenosyl methionine and then used for a one carbon donation (for methylation of various macromolecules), the byproduct of this reaction is homocysteine.

Homocysteine can then be converted back to methionine using a one-carbon donation by 5-methyltetrahydrofolate (Jakubowski, 1999; Jakubowski, 2001). Homocysteine can also be disposed of through two other methods (Figure 1.7b and c). In order to keep homocysteine from being misincorporated into proteins, methionyl t-RNA synthetase will bind homocysteine and activate it by attaching an ATP. The homocysteinyl adenylate will cyclize into homocysteine thiolactone (HTl) when the ATP is lost (Jakubowski, 1991; Jakubowski, 2000). Homocysteine can also be converted to cysteine through a series of transsulfuration reactions. Here, homocysteine may combine with serine using the enzyme cystathionine beta-synthase (CBS) to form cystationine. This is then converted to cysteine using the enzyme cystationine gamma-lyase (CSE) (Paul & Snyder, 2012). This pathway can further continue and synthesize the ubiquitous anti-oxidant glutathione (Deplancke & Gaskins, 2002).

The editing byproduct of methionyl t-RNA synthetase, HTl, is a very chemically reactive thiolactone ring. This compound has been linked to various human pathologies that will be described in depth later. Unsurprisingly, the body has a few pathways to rid itself of this reactive molecule. Once HTl has been made, it can be converted back to homocysteine using the enzyme paroxonase 1 (Getz & Reardon, 2004), an enzyme known as bleomycin hydrolase (BLH) has been seen to hydrolyze HTl (Zimny, 2008), and some HTl has been seen to be renally excreted (Chwatko & Jakubowski, 2005). If HTl is not enzymatically destroyed, nor excreted from the body, it can react with an amino group from a lysine or the sulfhydryl from a cysteine. When HTl reacts with either a lysine or a cysteine on the surface of a protein, it is a post-translational modification known as protein homocysteinylation (Selhub, 1999). When the HTl reacts with a cysteine, this is known as S-

homocysteinylation, and when the HTl reacts with a lysine, this is known as N-homocysteinylation (Figure 1.8). The mechanism of protein homocysteinylation is a simple chemical reaction that proceeds at physiologic pH and is not catalyzed by an enzyme. The reaction of HTl with an exposed lysine on a protein has been kinetically predicted to occur readily in the conditions of human plasma (including total protein and lysine bulk there) (Garel & Tawfik, 2006). In fact, it is estimated that around 70% of circulating homocysteine is N-linked in the plasma (Glowacki & Jakubowski, 2004). Reports such as this make it obvious that although there are mechanisms in place to rid the body of HTl, some of this reactive compound remains and attaches to proteins. Although reports on the average amount of circulating plasma HTl have had a large range, more recent reports show these numbers are in the nanomolar range (Chwatko & Jakubowski, 2005), with the bulk of it actually protein bound.

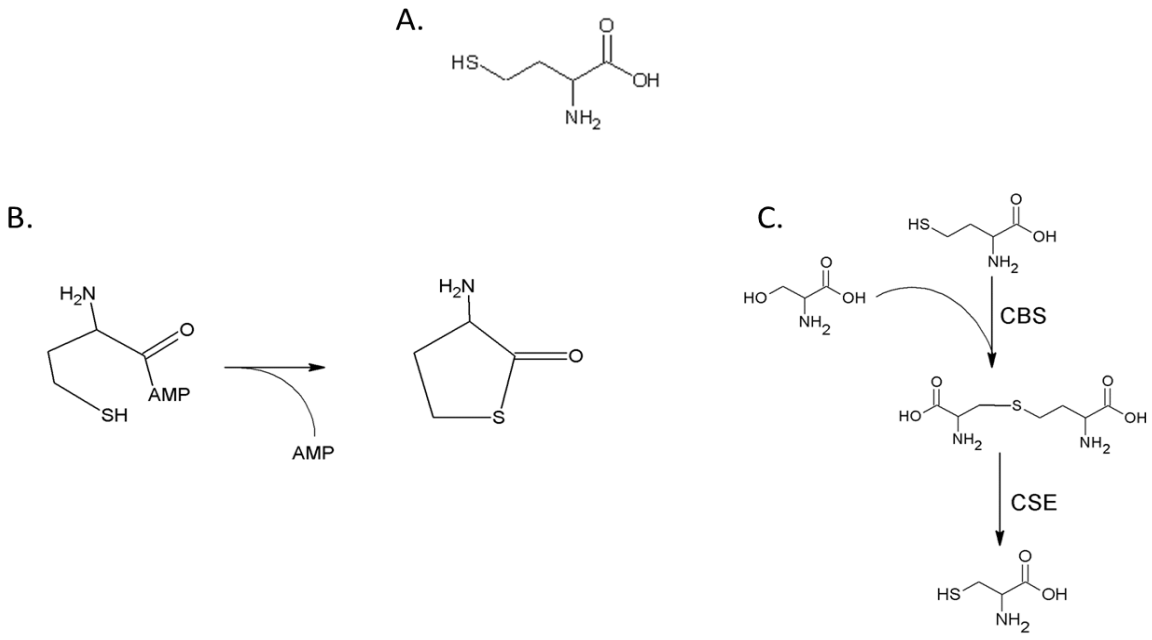

Figure 1.7 Homocysteine Metabolism

The non-protein incorporating amino acid homocysteine is seen in panel A. This small molecule can be cyclized into homocysteine thiolactone via an ATP dependent proofreading function of methionyl tRNA synthetase (panel B). Homocysteine can also be converted to cysteine using a series of transsulfuration reactions dependent upon the enzymes cystathionine beta-synthase (CBS) and cystationine gamma-lyase (CSE) seen in panel C.

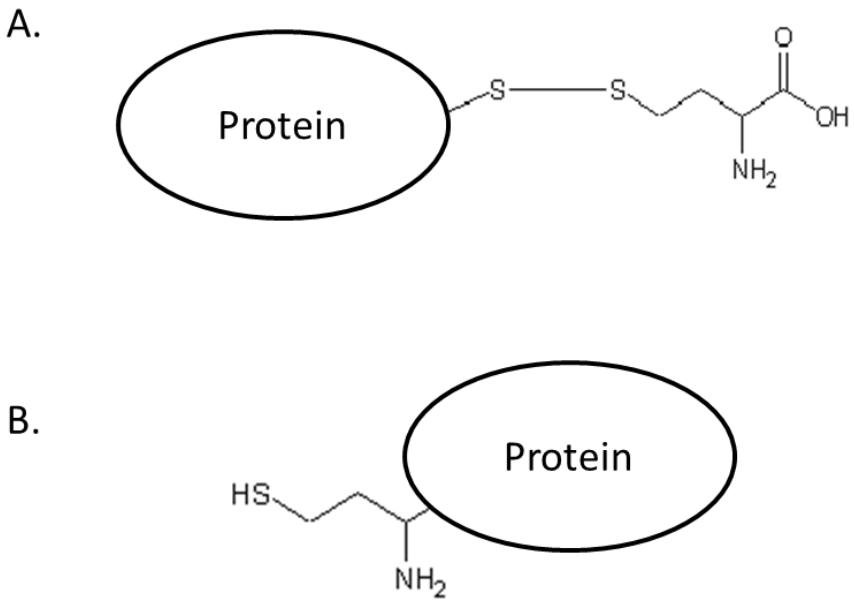

Figure 1.8 Protein Homocysteinylation

Panel A illustrates S-homocysteinylation, where a homocysteine creates a disulfide bond with an open cysteine on the protein surface.

Panel B illustrates N-homocysteinylation, where a homocysteine thiolactone covalently attaches to a lysine residue on the protein surface.

It has long been reported that high levels of homocysteine in plasma are correlated to many different health conditions, such as cardiovascular disease, neural tube defects, and stroke (Jakubowski, 2004; Yang et al, 2012). Although many correlative studies have been performed, the exact mechanisms by which these negative effects are conferred by homocysteine are still unknown. One hypothesis is that buildup of the reactive form of homocysteine, HTl, causes an increase in protein homocysteinylation, which can cause protein malfunction or autoimmune responses. If a homocysteinylation event occurred at either an active site residue or an entrance to the catalytic area of an enzyme, it is easy to imagine how this could disrupt protein function. In addition, as with any sort of post-translational modification, the addition of a homocysteine group could alter the structure and overall charge of a protein. It has been demonstrated that N-homocysteinylation events do indeed encourage protein aggregates *in vitro*, which may alter the functionality of these proteins, or simply cause plaques (Khodadadi et al, 2012; Paoli et al, 2010). Another deleterious result of this post-translational modification could be an immune response by the body to a foreign looking protein. N-homocysteinylation events are proceed in a non-enzyme dependent fashion and are not known to be required for any function. Proteins with these modifications may not be recognized by the body's immune system and an autoimmune response may be started. Antibodies against N-homocysteinylated lysines have been detected in multiple cohorts of human serum. These autoantibodies are seen to increase with increasing levels of serum homocysteine thiolactone and are also correlated with various disease states (Undas et al, 2004; Undas et al, 2006) (Jakubowski, 2005).

High maternal homocysteine levels during pregnancy are seen to have teratogenic effects (van Mil et al, 2010) (Murphy & Fernandez-Ballart, 2011). In

animal models, the introduction of homocysteine is seen to induce higher rates of NTDs (Rosenquist et al, 1996). Correlative data have also shown that women with NTD affected pregnancies have higher plasma homocysteine levels than those with unaffected pregnancies (Hague, 2003; Mills et al, 1995; Vanaerts et al, 1994). In addition, increased homocysteine levels are often correlated with lowered folate levels, as would be indicated by the methionine cycle (Selhub et al, 2000). One potential mechanism of homocysteine induced NTDs is that N-homocysteinylation of key developmental proteins may disrupt their functions and increase the overall state of inflammation in the mother via an autoantigenic response. In addition, it may exacerbate conditions of low folate in the developing embryo, a known risk factor for developing NTDs.

1.5 THE IMMUNE SYSTEM

In humans, the immune system is what helps protect individuals from dangerous outside invaders to our bodies. Beyond simple physical barriers such as skin and mucus, the cellular level of the innate immune system and the adaptive immune system coordinate to keep intruders out (Aderem & Ulevitch, 2000). The innate immune system is comprised of all physical barriers to the body such as skin, chemical barriers such as the low stomach pH or secreted peptidases, and the complement system. The innate immune system is the body's first defense to a foreign object. The adaptive immune system is mostly made of lymphocytes that identify an object and over time, create a response to this specific object, an antibody response. This is appropriately also known as the acquired immune system because over the course of time, your body increases its ability to respond to pathogens it has already encountered. The major players in acquired immunity are

B and T lymphocytes. There are types of white blood cells that circulate through the body in the blood and lymphatic system. T cells signal for the death of intruders and B cells are what are associated with antibodies against specific invaders (Delves & Roitt, 2000).

The innate immune system is what the body uses when there is a new and present danger that of the body needs to protect itself from. The adaptive immune system is complex, and it takes time to create specific responder cells. The innate immune system allows for the more immediate destruction of foreign invaders based on a set of specific recognition techniques (Janeway & Medzhitov, 2002). The body can distinguish between self and non-self with some common differences such as lipopolysaccharide cell membranes or short sequences of DNA specific to bacteria. Once one of these invaders is identified, it can be destroyed through phagocytosis (macrophages surrounding and killing the cell) or by the complement cascade (Medzhitov & Janeway, 2002).

1.5.1 The Complement Cascade

The complement cascade refers to the series of events that occurs when the body's innate immune system responds to a potential enemy (A.S. & B.S., 1996). The complement proteins are serum soluble proteins that signal for cell death and inflammation. These proteins, innate to all humans, are known as C1 through C9. The complement cascade can be divided into three different categories: classical, alternative, and lectin, all of which have the same end point. The classical pathway starts with an IgM or IgG (non-specific antibody isotypes) responding to an antigen and C1 binding to this complex. The binding of C1 signals for C3 convertase to be formed, which will allow for the production of C3a and C3b. The alternative pathway

starts when an immature C3 sees a pathogen and then a C3 complex is formed, allowing for the production of C3a and C3b. The lectin pathway is very similar to the classical pathway, but the recognition step starts when a mannose binding lectin binds a mannose on the membrane of a foreign body. C3a and C3b are then formed from C3 convertase. After the formation of C3a and C3b, all of the pathways merge. C3a signals for inflammation. C3b binds to the bacterial surface, and will cause the bacterium to be tagged for phagocytosis by macrophages (a process called opsonization). C3 convertase can also combine with another protein to make C5 convertase. This forms C5 and C5b. C5a is a chemo attractant, enhancing inflammation, whereas C5b can also signal for the formation of a membrane attack complex (Figure 1.9). The membrane attack complex is the nomenclature for the series of proteins that will assemble at the pathogen surface in response to C5b. These proteins are responsible for creating holes in the foreign cell membrane, and thereby killing the pathogen. (Delves & Roitt, 2000).

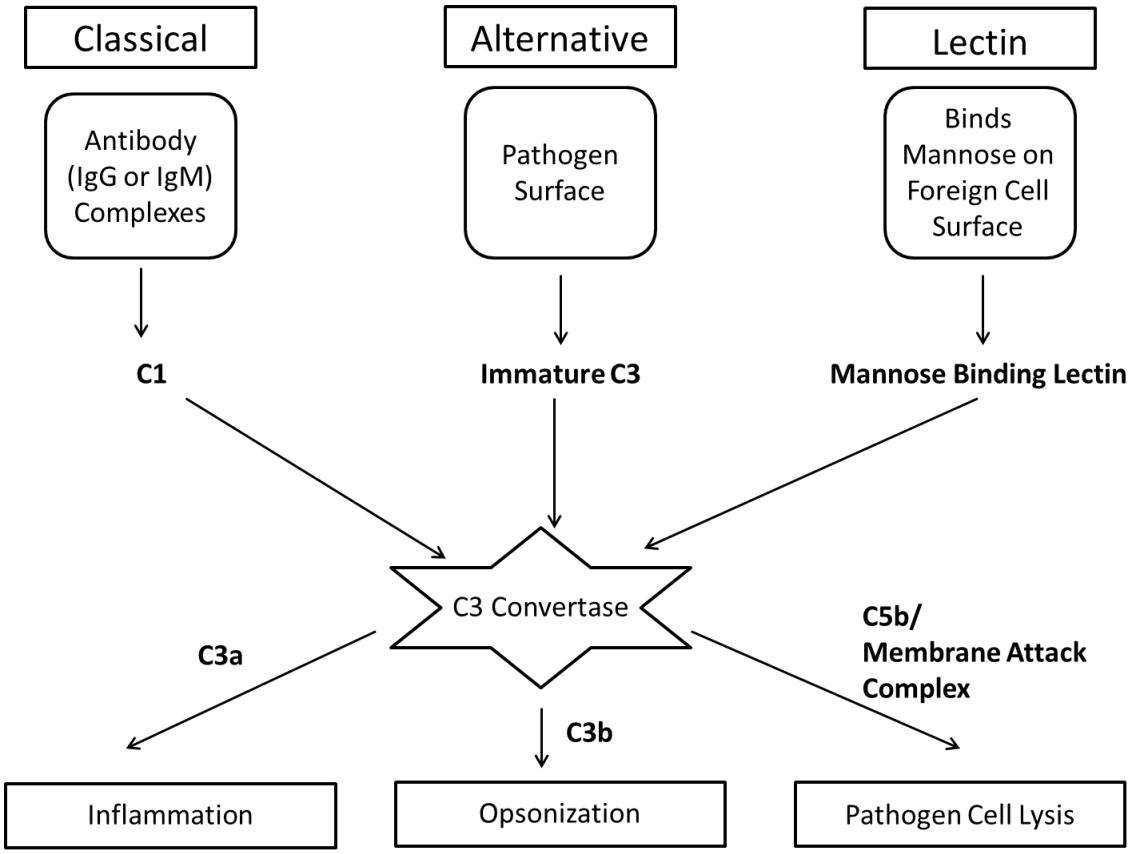

Figure 1.9 The Complement Cascade

One of the body's natural immune defenses is the complement cascade. The complement cascade has three branches; the classical, the alternative, and the lectin, all of which meet at C3 convertase and signal for inflammation and pathogen destruction.

1.5.2 Immunity and NTDs

The connection between various states of increased inflammation and the risk for bearing children with NTDs has been previously discussed in regards to obesity and diabetes. Another state of increased inflammation occurs during an immune response. There has been much conflicting evidence about natural immune response elevation and risk for NTDs. The great interest in this area was started by a study published in 2004 by Rothenburg and colleagues. In this study, it was reported that autoantibodies against folate receptors were found in the serum of women who previously had NTD affected pregnancies at significantly higher levels than those women who had unaffected pregnancies (Rothenberg et al, 2004). These autoantibodies were also seen to block the amount of folate that was allowed to bind to the receptors when tested *in vitro*. It is possible that if mothers have antibodies blocking folate from binding their folate receptors, not enough folate will reach the developing embryo, even if the mom has supplemental folate in her diet. The increased risk of NTDs therefore may be a direct result of the lack of folate available for the developing embryo. It has also been noted that autoantibodies against the folate receptor that block folate binding are elevated in persons with cerebral folate deficiency (Ramaekers et al, 2005). This condition is marked by normal circulating folate levels, but decreased levels of folate in the cerebral spinal fluid. It is hypothesized that the antibodies detected in these patients may block enough of the folate receptors in the choroid plexus (the blood-cerebral spinal fluid-barrier) to cause such a condition (Ramaekers et al, 2005). This reiterates the importance that such antibodies may play in the etiology of NTDs. Other studies have also confirmed this outcome in different time points during the pregnancy including from mid-gestation serum draws (Cabrera et al, 2008). There have also

been opposing reports with larger case control groups that show no significant elevation in autoantibody levels (Molloy et al, 2009), which calls in to question the validity of these claims, although these samples were also not taken mid-gestation.

A second hypothesis is that the innate immune system is directly related to the events of neural tube closure itself. It has been more recently suggested that the immune system itself may play a direct role during neural tube development. Various proteins involved in immune response and regulation are expressed in the neural tube of animal models at the appropriate time of neural tube formation and closure (Denny et al, 2013b). Beyond the various immune factors that have been seen to be localized to areas of the developing neural tube, the complement cascade proteins are beginning to emerge as important players during embryonic development. C1, C3 and C9 were seen to be present in the neural plate during development in *Xenopus* (McLin et al, 2008). The complement factor C5 has been shown to be expressed in the mouse neural tube during development (Denny et al, 2013a). Additionally, NTDs are observed when mice are given an antagonist of the C5a receptor (Woodruff et al, 2005). These data indicate that there may be a significant role being played by the complement cascade and other innate immune modulators during development that may be completely separate from the role for which they are most commonly known.

1.6 Mouse Models

In scientific research, it is critical to have model systems in which one can perform experimental science before this research can be translated to humans. Many different model systems exist from many different species, but one of the most popular mammalian model systems is *mus musculus*, or the house mouse. For the

investigation of specific genes and their coded proteins, it is essential to be able to manipulate these model systems, and ideally create stable genetically modified tools. In the 1970s, the first genetically modified mouse was reported. Unfortunately, this mouse did not show germ line transmission of its modified genetics (Jaenisch & Mintz, 1974). In the early 1980s it was reported that the ability to alter specific genes in mice could have the potential of creating a new lineage of mice that would transfer the transgene from generation to generation (Gordon & Ruddle, 1981) . Since the discovery of this tool, genetically modified mice have expanded in their number and potential applications. Current technologies in the mouse modeling system include gene knock-outs, animals that totally lack a specific gene, gene knock-ins, animals that over express genes of interest, and conditional animals, those where you can turn off certain genes in certain tissues (Simmons, 2008). In fact, currently there are over 200 genetically modified mouse models that express an NTD phenotype (Harris & Juriloff, 2007; Harris & Juriloff, 2010).

1.6.1 Folr1 (Folbp1/FRα) Mouse

The Folr1 mouse, or the genetically modified folate receptor alpha knockout mouse, is one of the many mouse models that are used in the realm of NTD research. Specifically, the Folr1 mouse allows for animal modeling of the ablation one of the major transporters of folate into cells. The Folr1-/- mice die *in utero* before neural tube closure is completed (Piedrahita et al, 1999). The null mice display cranial neural tube closure malformations and also facial malformations. Folr1 -/- mice can be rescued by maternal supplementation with folates and after weaning, can survive on their own. The heterozygous mice show no obvious phenotype and have only slightly lowered circulating folate levels (Piedrahita et al, 1999).

In addition to the obvious lack of folate in developing embyros, the Folr1 mice show a marked alteration in the expression of critical signaling molecules during development. This change in expression of various genes is one thought to be one reason why such drastic malformations are seen (Tang & Finnell, 2003). This is specifically interesting when considering newer research that has indicated that Folr1 can serve as a folate responsive transcription factor (Boshnjaku et al, 2012). The lack of a folate receptor may not only allow for sufficient folate transport to the developing embryos, but may also change the transcription of genes enough during development that such devastating phenotypes are seen.

1.6.2 LRP6 Mouse Models

There are three mutations to the *LRP6* gene that result in three different mouse models currently described in the literature. The LRP6 conventional knock out mouse completely prevents a functional LRP6 protein from ever being made. These mice exhibit skeletal and limb defects, spina bifida, micro-ophthalmia, and urogenital malformations. The homozygous loss-of-function mice die at birth (Pinson et al, 2000). Interestingly, it is believed that the homology between the LRP5 and LRP6 proteins is what allows the LRP6 null mice to survive as far as birth. It has been seen that mice with both LRP5 and LRP6 knocked out have much earlier lethality, dying during gastrulation (Kelly et al, 2004). This emphasizes the importance of the LRP6 protein both because it has a redundant partner and because of the damaging effects when one or both of these proteins is not present.

The LRP6 Cd mouse has been described in the literature as a spontaneous mutation known as the crooked tail mouse for many decades (Morgan, 1954). The homozygous Cd/Cd mutants manifest in various ways. Around 30% of these

animals die *in utero* or immediately at the time of birth, 20% have exencephaly, and the rest will be very runted with profound skeletal defects that are visible as crooks in the mouse's tail (Carter et al, 1999). Even the heterozygous animals can present with crooked tails, but the exact phenotype for these animals can vary greatly depending on the genetic background of the animal. More recently, this mouse mutant was seen to respond positively to dietary folic acid treatment, by reducing the recurrence rate of exencephaly by 55% (Carter et al, 1999). This makes the Cd mouse a very valuable tool for studying NTDs, as it mimics the human folate response nicely. After these studies describing the Cd mouse as a folate response mutant, genetic mapping determined that the Cd mutant was genotypically described as a G494D amino acid substitution (Carter et al, 2005). The mouse has canonically been described as a hypermorphic Wnt signaling mutation. The Cd mutation does not allow for the proper binding of Dkk1 to LRP6, therefore not allowing for the Wnt signaling pathway to be negatively regulated (Carter et al, 2005). The most recent studies involving the Cd mutation; however, demonstrate that this mutation does not allow for MESD to bind LRP6. The abrogated binding of LRP5/6 to its chaperone protein MESD have been studied in cell culture models and have shown that this mutation does not allow proper membrane translocation for LRP5/6, but also decreases the ability of LRP6 to serve as a canonical Wnt signaling receptor (Gray et al, 2013).

The LRP6 Ringleschwanz (Rs) mouse was discovered as a spontaneous point mutation in the *LRP6* gene (R866W) (Kokubu et al, 2004). The Rs mutants were phenotypically characterized by a decrease in overall bone mass and dysregulation during somitogenesis. The Rs mouse was later determined to be an LRP6 hypomorph (Kubota et al, 2008). The LRP6 Rs mouse shows a lessened binding to

the chaperone protein MESD and reduced canonical Wnt signaling (Kubota et al, 2008). This mouse is a useful tool for studying the role of LRP6 in bone morphologies, as it does not have as damaging effects as the total knock out mouse model.

1.7 Concluding Remarks

The complex etiology of NTDs still remains unknown. It is apparent that folates are crucial in preventing the bulk of these congenital malformations, but even in an age of food fortification in the United States, approximately 1 in every 1000 live births are still affected by NTDs. Research has focused on genetic, environmental, and dietary causes of NTDs. The complexities of the human body and the developmental and metabolic pathways therein are the focus of current research. Using techniques such as dietary and genetic manipulation of model organisms, scientists are constantly learning new pieces of information that may help shed light on possible prevention strategies for these costly and physically and emotionally challenging defects.

Chapter 2 Biological Application and Adaptation of a Chemical N-Homocysteinylation Determination Assay

2.1 INTRODUCTION

It is imperative that the correlation between the multitudes of health problems and high levels of homocysteine in the human population be further explored. Homocysteine exists in the human body in many forms: protein-bound, free form, and in disulfides. For patients, homocysteine concentrations are usually determined as levels of total homocysteine (Gilfix et al, 1997). The results of these most common assays will give the sum total of all the forms of homocysteine in the body together, with no distinction between the different states in which homocysteine may exist. Although the assays for determining levels of total homocysteine are well established (Ueland et al, 1993), it would be clinically useful to distinguish between the various species of homocysteine in order to further mechanistically characterize the correlation between homocysteine levels and its associated disease states. One hypothesis as to why high homocysteine levels are deleterious is based on the chemical reactivity of HTl. It is thought that when HTl reacts with either lysines or cysteines on proteins, these homocysteinylation events may disrupt protein structure or function (Jakubowski, 1999), cause the proteins to aggregate and form plaques (Ravnskov & McCully, 2009), or become autoantigenic (Undas et al, 2004). The modification of cysteine residues in proteins with homocysteine occurs through a reversible disulfide bond (Ueland et al, 1996). At any point, a cysteine residue could form a disulfide bond with another cysteine, a homocysteine, or a cysteinylglycine molecule. These bonds are not a result of HTl covalently attaching to a protein; they are simply reversible disulfide bonds (Hortin et al, 2006). The labile nature of these S-homocysteinylation events is one of the

reasons that there is a greater interest in lysine bound homocysteine. Whereas S-homocysteinylation events are dynamic, there is no reported mechanism in the body that can rid a protein of a covalently bound N-homocysteinylation event. In addition, there have been reports that lysine bound homocysteine specifically is associated with protein malfunctions and autoantigenicity, over the other forms of homocysteine in the body (Jakubowski, 2005; Jakubowski, 2008; Perla-Kajan et al, 2008; Undas et al, 2004). Elevated levels of homocysteine have been seen to increase vascular stiffness (Devi et al, 2006) and inflammation (Hofmann et al, 2001), both of which are thought to be results of N-homocysteinylation. Despite the numerous correlative studies, the mechanism by which hyperhomocysteinemia is harmful still remains elusive. It is necessary to be able to differentiate between the various forms of homocysteine in the body in order to determine if N-homocysteinylation events really are responsible for many of the negative effects seen in people with hyperhomocysteinemia.

After proteins are synthesized in the cell, they can be decorated with various sugars and functional groups. These additions are known as post-translational modifications (PTMs). Proteins contain many PTMs, but lysine is one of the amino acids that can be subject to a significant amount of different PTMs. Lysines can be subject to acetylation, ubiquitination, SUMOylation, methylation, butylation and more (Lu et al, 2011). All of these modifications are added to proteins enzymatically. There are actually very few non-enzymatically governed PTMs *in vivo*. Two of these non-enzymatic modifications include lysine glycation and lysine homocysteinylation (N-homocysteinylation) (Ansari et al, 2011). N-homocysteinylation proceeds by chemistry favored at ambient body conditions as already discussed, while lysine glycation refers to the addition of a glucose molecule

to the amino group on a lysine via a Schiff base intermediate (Ansari et al, 2011). There are numerous ways to detect the various PTMs that exist on lysines and the other amino acids. One very common way of detecting PTMs is using either single or tandem mass spectrometry (Larsen et al, 2006). Mass spectrometry allows for the determination of various PTMs with a high degree of sensitivity and can determine relative levels of these PTMs. Detection of PTMs using mass spectrometry; however, is costly, time consuming, and highly technical. Only one sample can be run at a time and these samples usually require enrichment when investigating either less abundant PTMs or proteins (Witze et al, 2007). Other methods of identifying PTMs include 2D gel electrophoresis (Wilkins et al, 1996), antibodies specific to certain PTMs, or incorporation of radiolabelled atoms and autoradiographic detection (Seo & Lee, 2004). Often 2D electrophoresis must be coupled with mass spectrometry, and the incorporation of radiolabelled atoms is subject to the normal detection limits of film based autoradiography assays (Carter, 2012). In addition, there are commercial antibodies available for the detection of some PTMs, but not all, with the range in the specificity of these antibodies varying greatly.

If one is specifically interested in examining only N-homocysteinylation events, the methods are significantly limited in number and ease of accessibility. Traditional experimental methods usually only allowed for the determination of the total homocysteine population, not distinguishing between any of the existing forms. These methods included a derivitization of the homocysteine molecules, a separation using high performance liquid chromatography, gas chromatography, or capillary electrophoresis, and were usually followed by detection using fluorescence or ultra-violet spectroscopy. These methods are able to determine total

homocysteine levels with a limit of detection around 1-0.01 μM (Nekrassova et al, 2003). Additionally, recent reports have also shown colorometric assays to determine total homocysteine, but these cannot distinguish between protein bound and free homocysteine (Wang et al, 2004). Mass spectrometry, which has been useful in identifying other PTMs, has also been helpful in identifying N-homocysteinylation events. Successful mass spectrometry techniques include liquid chromatography followed by tandem mass spectrometry (Marczak et al, 2011). Recently, there have been a few reports in the literature of the generation of polyclonal antibodies against homocysteinylated lysines (Perla-Kajan et al, 2008; Tyagi et al, 2012) (Bossenmeyer-Pourié et al, 2013). These antibodies have shown some success, but have fairly high levels of non-specific binding, are not widely published, and are not commercially available.

In 2009, Zang et al (Zang et al, 2009) published a novel method for determining N-homocysteinylation sites using a chemical reaction. This method is based on a specific and stoichiometric aldehyde based reaction (Zang et al, 2009). It has been established that aldehydes will specifically react and cyclize with β or γ aminothiols (Das et al, 2012). The product of a reaction between an aldehyde and a β or γ aminothiol is a 1,3-thiazine adduct as seen in Figure 2.1 (WRISTON & MACKENZIE, 1957). This specific chemical reaction is useful because an N-homocysteinylated lysine is actually a γ-aminothiol. The only other biologically relevant aminothiol would be an N-terminal cysteine residue, which would be a β-aminothiol (Figure 2.2). Interestingly, β-aminothiols are fairly rare in biology. Using a proteome-wide survey, it was seen that less than 0.5% of all human proteins have an N-terminal cysteine residue (Giron et al, 2009). This means that in all proteins there is only a 0.5% chance of reacting with an N-terminal cysteine instead

of the intended homocysteinylated lysine target when using aldehyde chemistry. Also, it is reported that the majority of proteins are subject to modifications by N-terminal acetyltransferases, which would acetylate the N-terminus of a peptide (Starheim et al, 2012). Indeed, it is seen that N-terminal cysteines are substrates for many of these acetylation reactions (Hwang et al, 2010). The acetylation of an already rare N-terminal cysteine would not allow for reaction with an aldehyde, as there would no longer be a β-aminothiol. In addition, the chemical microenvironment created by these γ-aminothiols assists with the success of this chemistry. Whereas the amine groups in native proteins are usually protonated and Schiff base formation will not happen, the amine on a γ-aminothiol will become easily deprotonated at only slightly acidic conditions (Jakubowski, 2006). This allows for the successful and biologically irreversible formation of a 1, 3-thiazine adduct when N-homocysteinylation events are exposed to an aldehyde in mildly acid and reducing conditions.

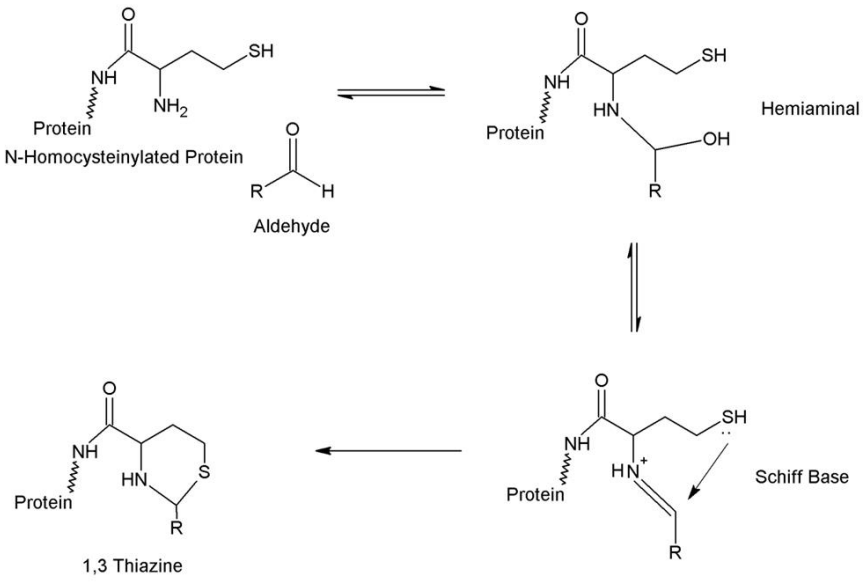

Figure 2.1 Reaction of an Aldehyde and a γ-Aminothiol

This reaction scheme illustrates the reaction between a γ-aminothiol and an aldehyde. First the lone pair on the nitrogen will attack the carbonyl carbon creating a hemiaminal. Water can then reversibly leave from this hemiaminal, forming a Schiff Base intermediate. The lone pair on the sulfur will attack the double bonded carbon, irreversibly creating a 1, 3 thiazine adduct.

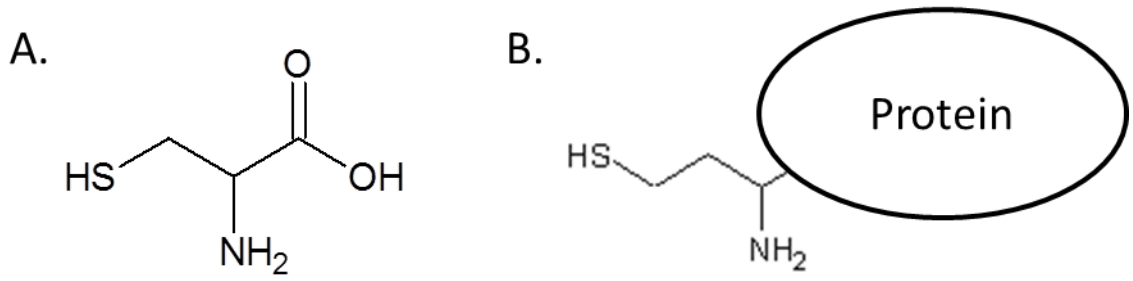

Figure 2.2 Aldehyde Reactive Aminothiols

Image A represents an N-terminal cysteine. This β-aminothiol would be seen if there was a cysteine at the N-terminus of a protein.

Image B represents an N-homocysteinylation event on a protein. This is a γ-aminothiol. Both of these naturally occurring aminothiols are reactive with aldehydes, however the presence of β-aminothiols is relatively rare and their reactivity is decreased when they are acetylated.

Although there are other methods that exist to determine levels and locations of N-homocysteinylation events as previously described, the method explored here has many advantages. This assay is highly specific, can be quantitative, and proceeds at room temperature with only mildly acidic conditions. This chemistry can allow for enrichment using an aldehyde solid state (commercially available from Applied Biotechnologies) (Figure 2.3). Enrichment of crude sample so that it only contains N-homocysteinylated proteins greatly expands the amount and kinds of analysis that can be done. The enrichment for only N-homocysteinylated proteins allows for proteome wide analysis of these events using mass spectrometry. Techniques such as searching for proteome-wide modifications are often more difficult with mass spectrometry because these modifications, if not enriched, will blend into the background noise because of their relatively low prevalence. Furthermore, aldehydes are a rather simple functional group that can be easily attached to various probes. A commercially available biotinylated aldehyde (Peptides International) allows for streptavidin probing using the traditional enzymatic (horse radish peroxidase) or fluorescent/infrared probes (Figure 2.4). In addition, the use of secondary streptavidin probing can allow for the adaptation of this assay to a high throughput biological system as described here.

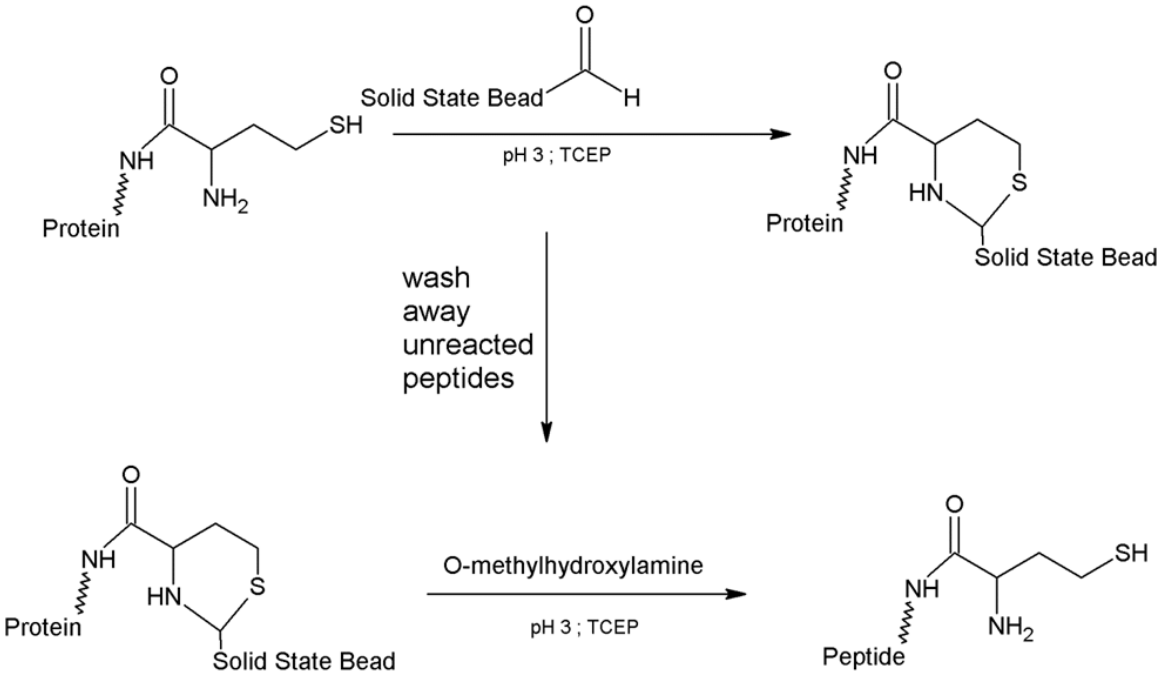

Figure 2.3 Enrichment for N-homocysteinylation Events with a Solid State

Beads substituted with aldehyde functional groups on the outside will allow for capture of N-homocysteinylation events on proteins. The release of any captured peptide with O-methylhydroxylamine will allow for the determination of the protein with mass spectrometry or further probing with antibodies.

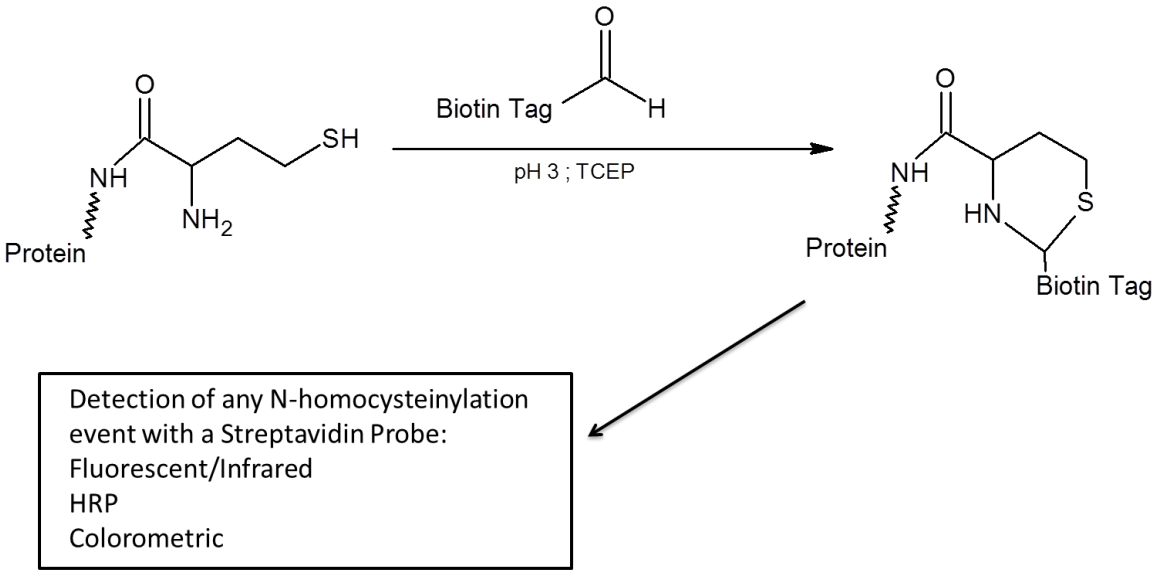

Figure 2.4 Tagging of N-homocysteinylation Events with a Biotin Tag

Tagging N-homocysteinylated proteins with a biotin tag will allow for the probing of these proteins in multiple ways by exploiting the very high affinity interaction between biotin and streptavidin.

The use of aldehyde bead enrichment and mass spectrometry allowed for the confirmation of the accuracy of this chemical assay for detection of N-homocysteinylation events. In addition, the adaption of this assay to a high-throughput dot blot scheme compatible with a variety of biological samples was tested using two well characterized mouse models. The 5,10-methylenetetrahydrofolate reductase (MTHFR) mouse model has been previously discussed in respect to mutations in this gene being linked to human NTD cases. This enzyme is responsible for the conversion of 5,10-methylene tetrahydrofolate into 5-methyl tetrahydrofolate. The enzyme product, 5-methyl tetrahydrofolate, is essential for the one carbon unit that can convert homocysteine back into methionine (Figure 2.5). Traditionally, this is why mutations of the MTHFR gene are thought to be associated with human hyperhomocysteinemia patients (Varga et al, 2005). The Mthfr knock-out mouse model is characterized by up to a 10-fold increase in plasma homocysteine levels, a global decrease in methylation, and increased lipid deposits in the aortas (Chen et al, 2001). The heterozygotes are phenotypically normal, but display altered one-carbon metabolism. The homozygotes appear runted with cerebral pathologies (Chen et al, 2001). The Pcft knockout mouse, which has been previously described, also shows elevated homocysteine levels in both the heterozygous mice and the homozygous knock out mice. Both the Pcft and Mthfr mice showed elevated levels of protein N-homocysteinylation (Jakubowski et al, 2009). The method of determination of N-homocysteinylation used for this initial study with the Mthfr and Pcft mice was to first allow N-homocysteinylation events to be liberated into HTl under highly acidic conditions (pH=0) in the presence of a reducing agent. The HTl was then separated with HPLC and derivatized with o-phthaldialdehyde under alkaline conditions. This

complex can then be detected with a fluorometer (Chwatko & Jakubowski, 2005) (Jakubowski et al, 2009). The use of these two mouse models, with known elevated levels of total homocysteine and N-homocysteinylation, allowed for proof of principle of the assay described here, that requires no more reagents than those used for a traditional western blot. The format is also such that all of the samples can be treated at once in a 96-well plate, rather than being run one at a time like the method previously described.

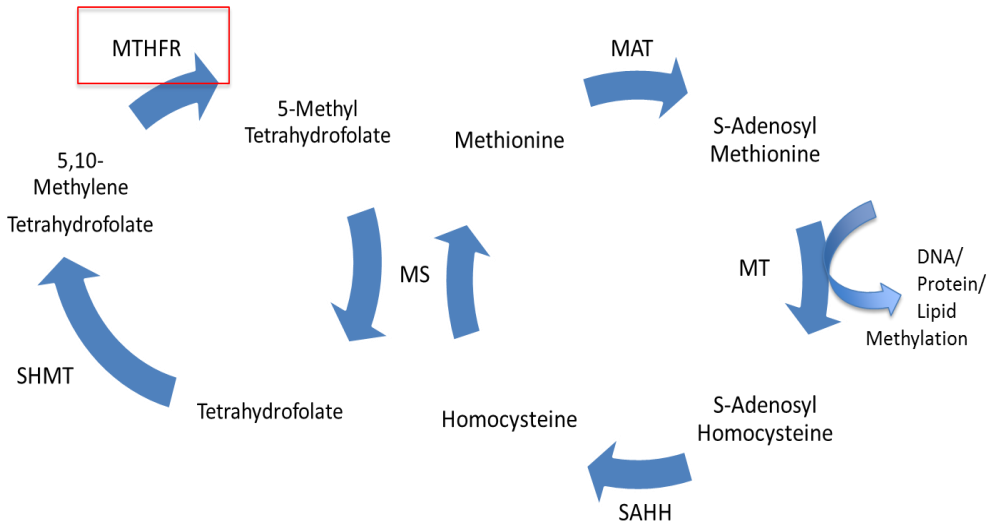

Figure 2.5 Methionine Cycle

Illustrated here is the methionine cycle, where homocysteine is made. The only way to convert homocysteine back to methionine is with 5-methyl tetrahydrofolate, which is created by the enzyme MTHFR. Enzyme abbreviations: Methionine adenyltransferase (MAT), Methionine Synthase (MS), Methyltransferase (MT), S-adenosyl homocysteine hydrolase (SAHH), Serine hydroxymethyl transferase (SHMT).

2.2 MATERIALS AND METHODS

2.2.1 Bradford Assay

To determine total protein concentration for any sample presented in this entire body of work, the Bradford method was used (Bradford, 1976). A 12 point standard curve was established using known concentrations of Bovine Serum Albumin (BSA)(Sigma Aldrich) in a 96 well plate. Protein samples were diluted properly to fit within the range of the standard curve. Bradford reagent (BioRad) was added to both the samples and the standard curve. Plates were read at 595nm using a SpectraMax Plus plate reader (Molecular Devices). Protein samples were interpolated into the standard curve to determine total protein concentrations.

2.2.2 Polymerase Chain Reaction (PCR)

All PCR protocols described in this body of work used the same standard set of reagents and same general protocol with various annealing temperatures. Crimson Taq Reagent Set (New England Biolabs) was used to set up reactions per manufacturer's instructions. The reactions were performed in a Biorad T100 thermal cycler under the following conditions:

Temp	Time	Cycle
95°C	5 minutes	1
95°C	30 seconds	Repeat 38 times
Variable (Annealing)	1 minute	
72°C	1 minute	
72°C	10 minutes	1

2.2.3 Homocysteinylation of Proteins

In order to force an N-homocysteinylation event on any protein, protein samples were incubated with 5mM HTl in 100mM Ammonium Bicarbonate and 10mM tris (2-carboxyethyl)phosphine (TCEP) hydrochloride at pH 7.8 overnight in the dark at room temperature. Excess HTl was removed using dialysis into 50mM potassium phosphate and 1mM TCEP with a 10kDa cut off cassette (Pierce). Dialysis buffer was changed 3 times over the course of 24 hours. For stoichiometry assays, stoichiometric ratios of HTl to the moles of protein were used. For the bFBP, 1µmol/mL (or 28g/mL protein) was dissolved in reaction buffer with progressively increasing amounts of HTl, starting at 0.001:1 molar ratio with the bFBP, a starting concentration of 0.0002mg/mL or 1nmol/mL of HTl. The range went from 0.001:1 through 1:1 using 1 to 10 dilutions.

2.2.4 N-Homocysteinylation Detection in Samples

BSA (Sigma Aldrich) was prepared using the method previously described for the forced homocysteinylation of proteins. The reacted protein was digested overnight at 37°C while gently shaking with sequencing grade trypsin (Promega) in

a 95mM ammonium bicarbonate, 1mM TCEP, and 10% acetonitrile buffer. The trypsin reaction was stopped using 5% formic acid. Excess solvent was removed using a speed vacuum (Eppendorf). Aldehyde beads (POROS AL, Applied Biosystems) were first primed for use following the manufacturer's instructions. In short, the beads were washed on a spin column 3 times with water. This was followed with the beads being washed 3 times with binding solution (150mM citric acid, 20mM TCEP, 20% acetonitrile). The previously trypsinized protein solution was dissolved in binding solution and allowed to mix with the pre-conditioned beads overnight while rocking at room temperature. The next day, the beads were washed 3 more times each with 3 different washing solutions: wash 1 (150mM citric acid, 10mM TCEP, 20% acetonitrile), wash 2 (150mM citric acid, 2M NaCl, 10mM TCEP, 5% acetonitrile), and wash 3 (150mM citric acid, 20mM TCEP, 50% acetonitrile). The beads were then given 3 final washes with the binding solution. The peptides of interest were then eluted using 2 different steps. First the beads were incubated in the first elution solution (100mM citric acid, 20mM TCEP, 20% acetonitrile, 400mM O-methylhydroxylamine) overnight. The next morning, this was collected and saved. Two subsequent hour long elutions were then performed with the second elution solution (400mM O-methylhydroxylamine, 50% acetonitrile, and 10mM TCEP). All the elution steps were combined and allowed to evaporate excess liquid using a speed vacuum. These samples were then prepared for mass spectrometry (2.2.7).

2.2.5 Reaction with Biotinylated Aldehyde

Lysates or plasma were standardized for total protein (Using Bradford Method) in a 96-well plate. The samples were incubated with 200uM biotinylated

aldehyde (Peptides International) overnight at room temperature away from the light in a 50mM citric acid and 500uM TCEP buffer. Samples were segregated from excess reagents in a 10kDa molecular weight cut off plate (Pall). At this point the samples were ready for dot blot analysis.

2.2.6 Dot Blot Detection

1 μL of sample was spotted onto a nitrocellulose membrane using a multi-channel pipette. The samples were allowed to adhere and dry onto the membrane for 10 minutes. The membrane was blocked for one hour at room temperature using a 5% powdered milk solution in TBS-T. The membrane was washed 3 times for 10 minutes each with TBS-T. The membrane was then incubated in the dark for 45 minutes with anti-streptavidin antibody (1:10000; Li-Cor Biosciences) in TBS-T with 0.01% sodium dodecyl sulfate. Membranes were imaged using the Li-Cor Odyssey. Odyssey software was used for analysis. The 96-well plate with round spot template was used to determine the average integrated pixel intensity for each spot.

2.2.7 Mass Spectrometry

The trypsin digested BSA was analyzed by LC-MS/MS using the Proxeon Easy-nLC II coupled to the Thermo Velos Pro as previously described (Takata et al, 2013). Prior to HPLC separation, the peptides were desalted using Millipore U-C18 ZipTip Pipette Tips following the manufacturer's protocol. A 2 cm long x 100 μm I.D. C18 5 μm trap column (Proxeon EASY Column) was followed by a 75 μm I.D. x 15 cm long analytical column packed with C18 3 μm material (Dionex Acclaim PepMap 100). Buffer A was composed of 0.1% formic acid in water and Buffer B 0.1% formic acid in acetonitrile. Data was acquired for 38 min using an HPLC gradient of 5% B to

45% B over 30 min with a flow rate of 300 nl/min. The data dependent method consisted of an MS scan followed by CID MS/MS of the top 10 precursor ions. The mass range was m/z 300-1700, with 2.0 amu isolation width for MS/MS, collision energy 35, and dynamic exclusion after 2 counts for 60 sec. Raw data was processed using SEQUEST embedded in Proteome Discoverer v1.4.0.288 using the following parameters: full trypsin digest with maximum 2 missed cleavages and variable modifications oxidation of methionine and lysine homocysteinyl thiolactone (mass addition C_4H_7NOS, monoisotopic mass 117.024835, average mass 117.1695), searching the SwissProt all species database dated July 22, 2013 (455,256 entries). The mass accuracy was set to 1.2 Da average mass for precursor ions and 0.8 Da monoisotopic for fragment ions. A decoy database was generated from the SwissProt database and used for calculating peptide probabilities. X!Tandem (GPM, version CYCLONE (2010.12.01.1) database searches were performed embedded in Scaffold 4 Q+ v.4.3.0 (Proteome Software) on a subset database using the same search parameters as SEQUEST with additional variable modifications of pyroglutamic acid modification of glutamine on peptide N-teminus, and ammonia loss on peptide N-terminus. Scaffold was used for validation of peptide identifications with confidence filtering of 90% confidence to 99.99%.

2.2.8 Mouse Husbandry

Mice were housed in the Dell Pediatric Research Institute's animal facility. The animals were maintained on a 7 am to 7 pm light/dark schedule. All animals were fed *ad libidum*. Animals on non-specified diet were fed milled chow (PicoLab Diet 20 no. 5053, Lab Diet). All animals were maintained according to institutional rules (IACUC protocols AUP 2013-0051 and AUP 2014-00276).

2.2.9 Mouse Genotyping

Tails of mice were clipped at weaning age (3 weeks). 200µL tail digestion buffer (Viagen Biotech) and 2 µL Proteinase K (Viagen Biotech) were added to each tail. Tails were digested overnight at 65°C in a shaking bath. The next day, the proteinase K was inactivated by heating the samples to 95°C for 10 minutes. Tails were vortexed to break up remaining tissues and centrifuged at 12000xG for 5 minutes to pellet any particulate matter. This crude sample of DNA was used for genotyping. The MTHFR mice were genotyped for the mutant allele using the primer set 5'-GAC TAC CTG GCT ATC CTC TCA TCC-3' and 5'-AGC CTG AAG AAC GAG ATC AGC AGC-3', whereas the wildtype allele was detected with 5'-GAC TAC CTG GCT ATC CTC TCA TCC-3'and 5'-GAA GCA GAG GGA AGG AGG CTT CAG-3'. Both the MTHFR primer sets used a standard genotyping PCR protocols with an annealing temperature of 56°C. The PCFT mutant gene was detected using 5'-GCA GCG CAT CGC CTT CTA TC-3' and 5'-CTT GAC CAC AAC TGT CCA TGT GC-3', whereas the wildtype allele was detected using 5'-CCC AAC TCC AAA FCF CAG GTT CAT-3'and 5'-TCC AGA TGG GAA AGA AGA GGT-3'. Both the PCFT primer sets used a standard genotyping PCR protocols with an annealing temperature of 61.5°C. All primers used were purchased from IDT DNA custom oligo service.

2.2.10 Mouse Sample Collection

Plasma was collected using the submandibular punch method (Heimann et al, 2010). Blood was held in EDTA coated K2 tubes (BD Bioscoiences) and spun at 5000XG for 10 minutes and the supernatant was collected. Livers were extracted from euthanized animals. Livers were manually minced then rinsed with ice cold PBS three times to wash away excess blood. Liver pieces were homogenized in RIPA (Radio immunoprecipitation assay) buffer with protease inhibitors (Roche) using a

Tissue Tearor (Cole-Parmer). Lysates were spun at 4°C for 20 minutes at 12000 RPM. Fat was removed from the top of the tube with a Kimwipe (Kimberly Clark Scientific) and the supernatant was collected. These samples were then run through biotin tagging for N-homocysteinylation events described in 2.2.5, and detected with a dot blot as described in 2.2.6.

2.3 RESULTS

2.3.1 Confirmation of Stoichiometry of Assay

Using bFBP and increasing stoichiometric ratios of HTl, it was seen that the an increase in the ratio of HTl:protein will give an according increase in average integrated pixel intensity from this N-homocysteinylation assay. After the ratio of 1:1 HTl to protein was reached, the signal had reached a maximum (data cut from this image). Figure 2.6 shows the linear range only of the dot blot and the accompanying linear regression.

2.3.2 Confirmation of Chemistry using Mass Spectrometry

LC-MS/MS was used to confirm the modification of only the lysine residues in BSA. The modification was seen as a +117.02 Da to a lysine peak. Four modification sites were detected at 99.99% confidence. Three additional homocysteinylation sites were detected with greater than 90% confidence. Protein identification information about the 7 sites is contained in Table 2.1. Representative MS/MS for each confidence threshold are shown in Figure 2.7 (A-D). The reacted BSA compared to the control non-reacted BSA coverage information at 90% is seen in Figure 2.8. There are 7 lysines that are homocysteinylated at 90% confidence in the reacted BSA sample, whereas none are seen to be homocysteinylated in the control non-reacted BSA sample. Additional modifications that were seen were an ammonia

loss from a glutamine, and an oxidation of a methionine. In addition, Figure 2.9 shows that the lysines that were homocysteinylated mapped to the surface of the BSA protein, as would be predicted. This is a chemical reaction, so the lysines must be exposed to the substrate while in solution.

2.3.3 Confirmation of High-Throughput Adaptation

Use of known mouse models allowed for the confirmation that this assay could be adapted to a high throughput dot blot format without losing any specificity or sensitivity. All preparation and analysis was performed with samples collected and held in 96 well plates. Figure 2.10b shows the confirmation that livers from PCFT null mice had significantly higher levels of N-homocysteinylation than those of their heterozygous counterparts. Figure 2.10a shows that plasma from the MTHFR heterozygous mice had a significantly higher level of N-homocysteinylation than do their wildtype counterparts. The significance was tested in both cases by a student's two-tailed t test.

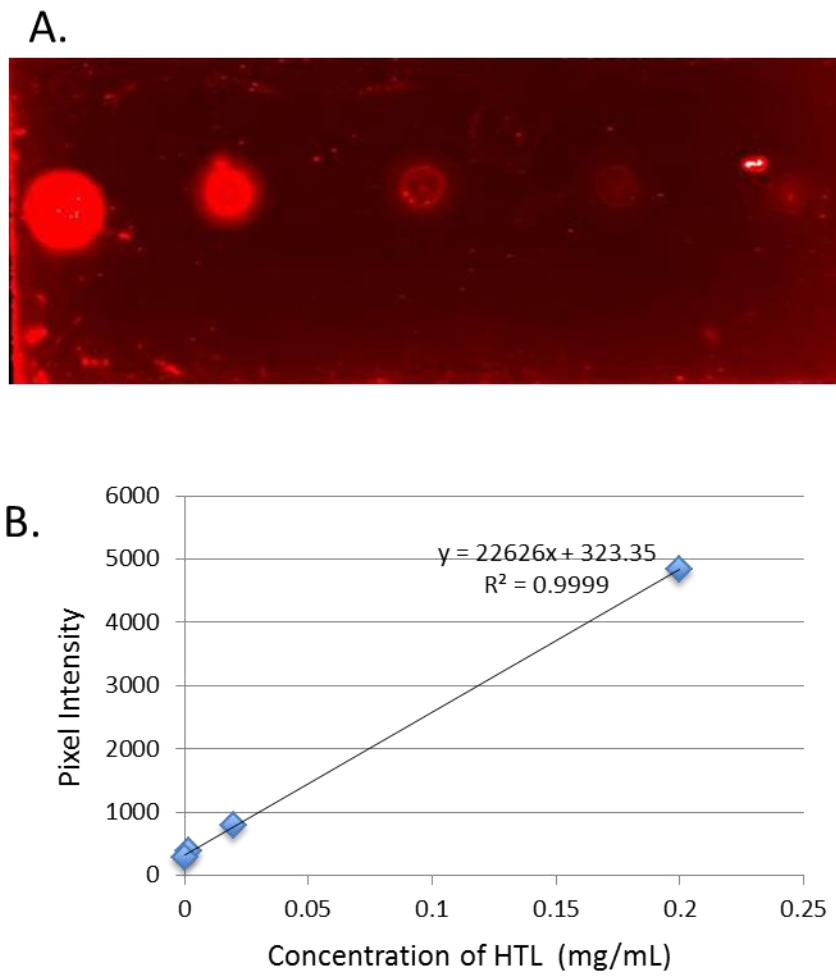

Figure 2.6 Linear Range Created for N-homocysteinylation Assay

Panel A shows the raw data from a dot blot of bFBP with decreasing amounts (10 fold dilutions) of HTl reacted with the protein. Panel B shows the linear range of pixel intensity (qualitative representation of total N-homocysteinylation) versus the concentration of HTl added.

Table 1: Homocysteinylthiolactone Modified Peptides in BSA

Sequence	Probability	SEQUEST XCorr	SEQUEST deltaCn	X! Tandem	Modifications	Observed	Actual Mass	Charge
(R)DTHkSEIAHR(F)	94%	2.9490924	0.21142247	2.7212465	HCysThiolactone (+117)	437.9558	1,310.85	3
(R)DTHkSEIAHR(F)	92%	2.6278703	0.25118622	1.251812	HCysThiolactone (+117)	438.0332	1,311.08	3
(K)KFWGkYLYEIAR(R)	100%	4.054633	0.30478325	4.853872	HCysThiolactone (+117)	846.7354	1,691.46	2
(K)KFWGkYLYEIAR(R)	100%	4.7147555	0.32283342	4.468521	HCysThiolactone (+117)	846.787	1,691.56	2
(R)ALkAWSVAR(L)	98%	1.8117387	0.08630793	1.853872	HCysThiolactone (+117)	1,118.67	1,117.66	1
(K)YICDNQDTISSkLK(E)	100%	3.8147483	0.28284302	6.309804	HCysThiolactone (+117)	873.2189	1,744.42	2
(K)YICDNQDTISSkLK(E)	98%	3.1571016	0.1478094	3.0457575	HCysThiolactone (+117)	873.3038	1,744.59	2
(K)qNCDQFEkLGEYGFQNALIVR(Y)	100%			6.79588	Ammonia-loss (-17), HCysThiolactone (+117)	1,286.96	2,571.91	2
(R)LCVLHEkTPVSEKVTK(C)	93%	4.114283	0.18710856	1.4814861	HCysThiolactone (+117)	644.0059	1,929.00	3
(R)LCVLHEkTPVSEKVTK(C)	91%	3.7546747	0.16047297	1.2218487	HCysThiolactone (+117)	643.6296	1,927.87	3
(K)ATEEQLkTVMENFVAFVDK(C)	100%	2.541721	0.28919214	9.721247	HCysThiolactone (+117)	1,158.84	2,315.67	2

Table 2.1 Homocysteinylthiolactone Modified Peptides in BSA

The peptides that were found in a BSA sample reacted with homocysteine thiolactone and enriched by an aldehyde solid state to show the confidence of the reaction chemistry. All reacted lysines (indicated by a k) mapped to the surface of the BSA crystal structure and have a >90% confidence.

A. >99.99% confidence

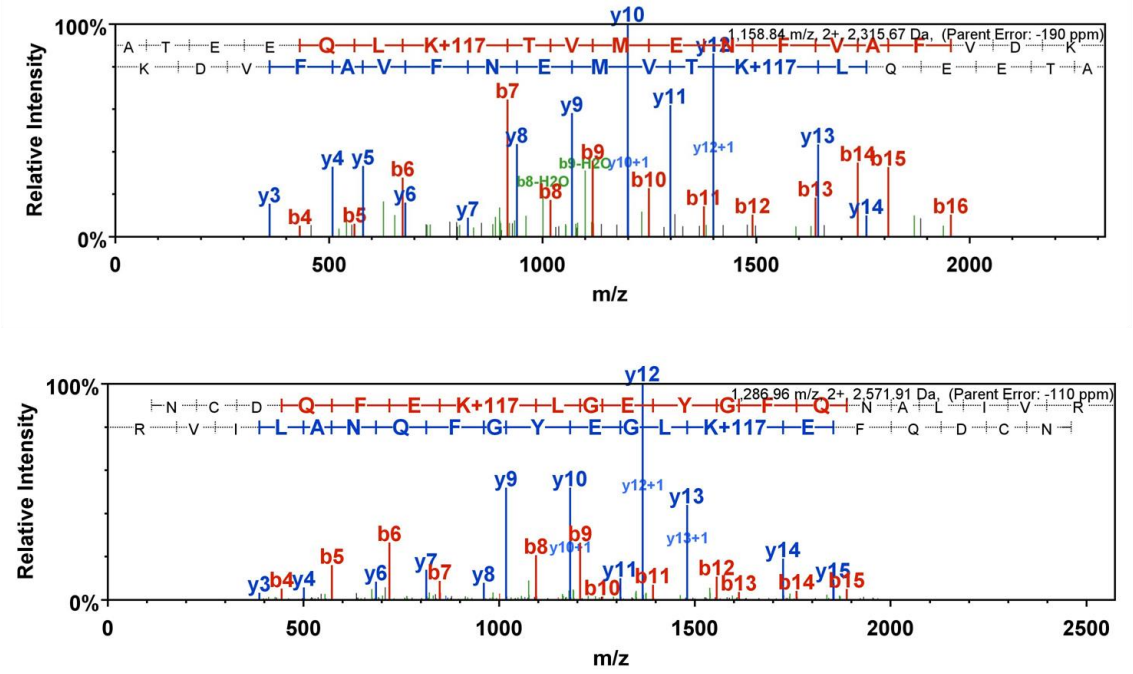

Figure 2.7 (A-D) Representative Mass Spectra

Continued on Page 74

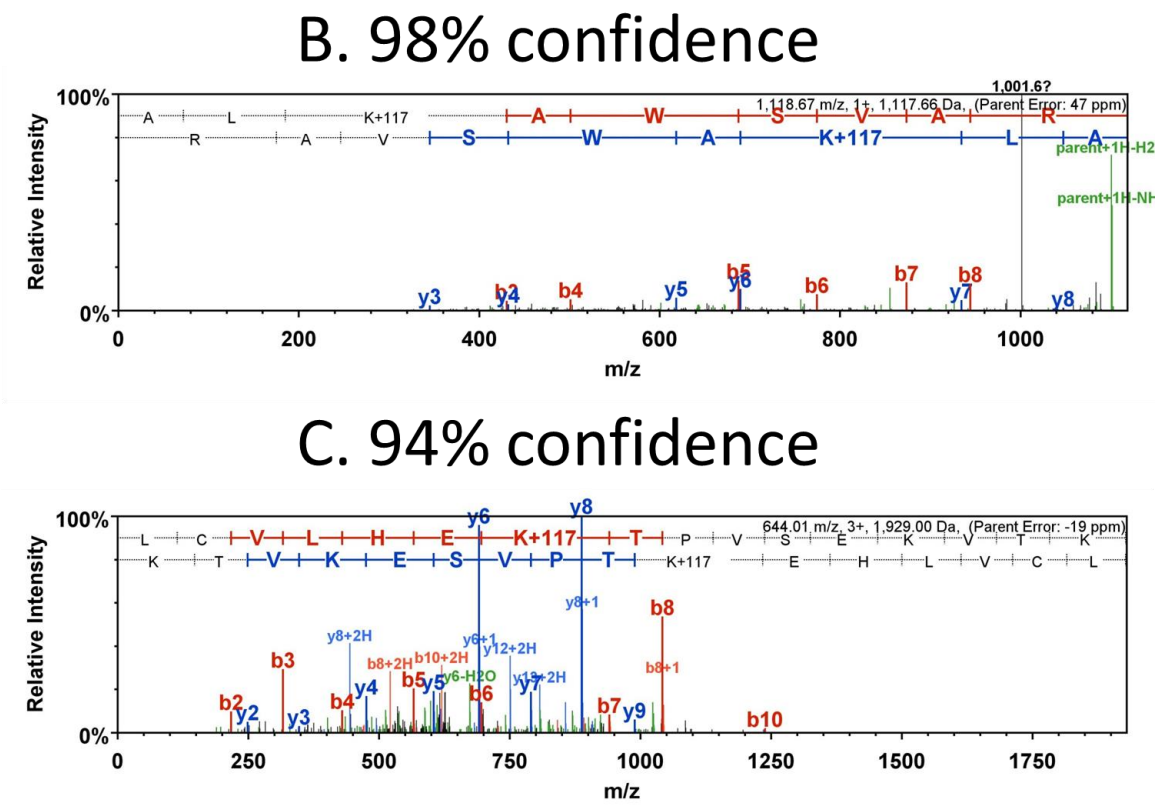

Figure 2.7 (A-D) Representative Mass Spectra

Continued on Page 75

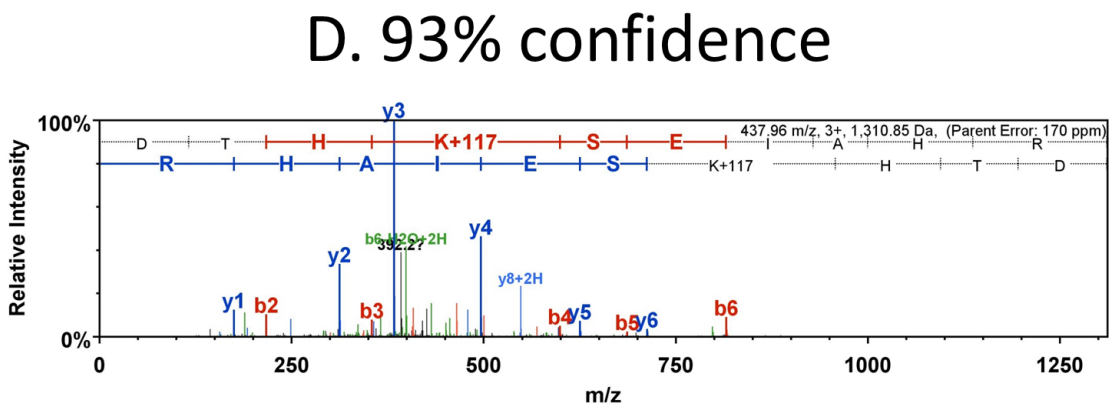

Figure 2.7 (A-D) Representative Mass Spectra

These representative spectra show the molecular weight shifts from a homocysteinylated lysine at various confidence levels. The K+117 shifts represent the addition of a homocysteine to a lysine. The relatively low background and large peaks for the homocysteinylated lysine are representative of the quality of the spectra used for analysis.

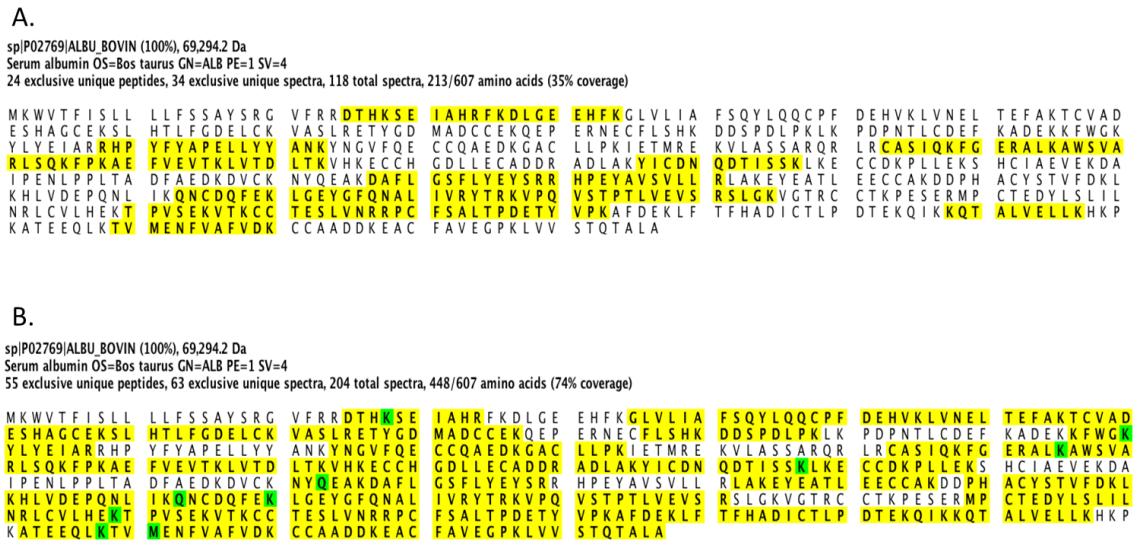

Figure 2.8 Mass Spectrometry Coverage Maps

Panel A shows the non-reacted BSA peptide subjected to enrichment for N-homocysteinylation events. None were seen. The coverage is due to non-specific binding or manual error in preparation.

Panel B shows the HTl-reacted BSA peptide subjected to enrichment for N-homocysteinylation events. The highlighted Ks show a homocysteinylated lysine. All PTMs had a localization probability of 100%. Both maps shown are at a 90% confidence threshold.

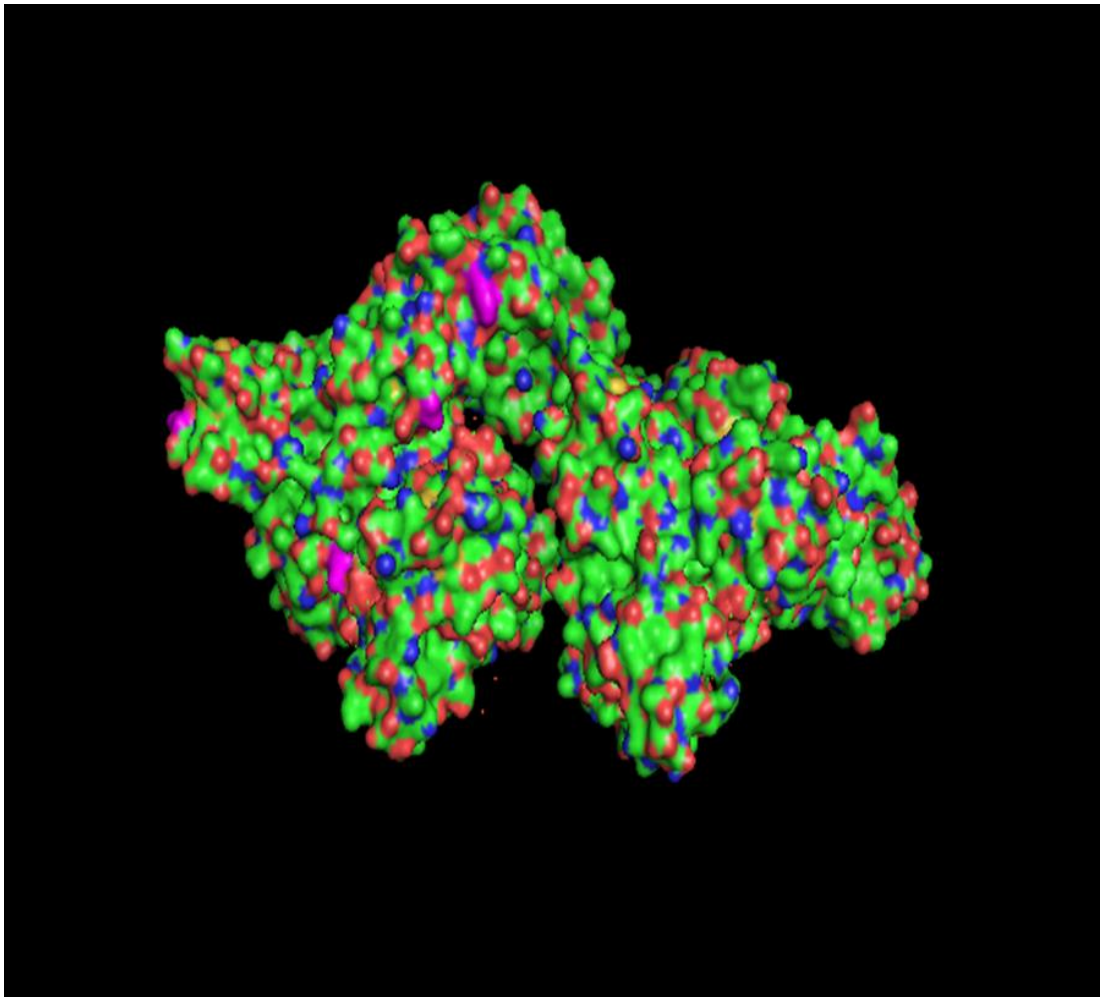

Figure 2.9 BSA with Reacted Surface Lysines

The lysines that were seen to be N-homocysteinylated by MS/MS are pictured in magenta in this space filling model of serum albumin from Bos Taurus (PDB: 3V03). As expected, the modified lysines map to the surface of the protein.

A.

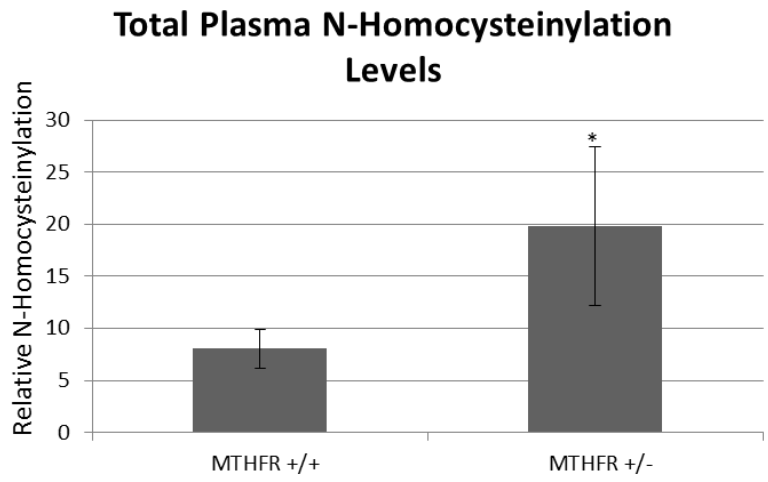

B.

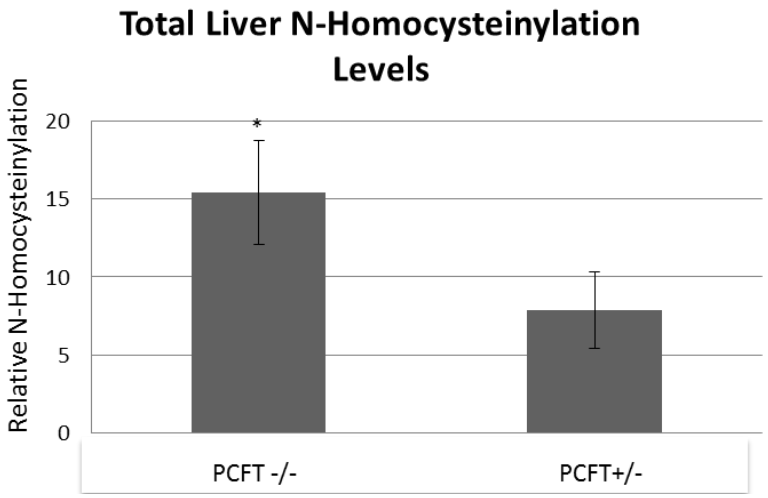

Figure 2.10 Use of Chemical N-Homocysteinylation Assay

Dot blot method of N-homocysteinylation assay was tested in both plasma and whole liver tissue. For each chart, N=5 age and sex matched mice. The asterisks indicate a $p<0.05$ significance with a two-tailed t-test.

2.4 CONCLUSION

The successful adaptation of a specific and stoichiometric assay for determination of N-homocysteinylation has been demonstrated here. The ability to adapt a highly specific chemical method for the determination of N-homocysteinylation to a high throughput dot blot method that is compatible with biological samples is a great success. The large number of disease states that have been correlated to high levels of homocysteine need to be further explored with a mechanistic hypothesis in mind. The tool developed here will allow for the further investigation into the idea that N-homocysteinylation is the reason that high homocysteine levels are associated with disease states. The versatility of this assay gives the opportunity to further explore the role of N-homocysteinylation in disease states. As shown by the stoichiometry, this reaction could be quantitative if using purified proteins. It would be possible to create a standard curve with known amounts of HTl added to the protein of interest then interpolate the unknown into this curve. The assay will also qualitatively determine total amounts of N-homocysteinylation in whole samples, which will be the application applied throughout this study. In addition, the mild conditions of this reaction will allow for histological applications by tagging N-homocysteinylation events with biotin tag then counter staining with an antibody of interest. Even whole mount staining on early staged embryos or permeablized tissues could be used to identify localized areas of high N-homocysteinylation. The assay presented here will allow for a multitude of studies that may help in the understanding of how high levels of homocysteine are related to such a large number of disease states.

The confirmation of the specific chemistry using mass spectrometry highlights the functionality of selecting for N-homocysteinylation events using aldehyde beads. The confidence with which N-homocysteinylated lysines were selected for indicates that this would be a good method for determining total proteome homocysteinylation events. Most of the reports that use mass spectrometry as a technique to identify N-homocysteinylation events use an *in vitro* method with a single purified protein (Stroylova et al, 2012; Zhao et al, 2010). Currently, the *in vivo* studies that present N-homocysteinylation data focus on human serum albumin (Marczak et al, 2011). This is the most abundant protein in human serum, therefore it will be easy to identify even PTMs on albumin with mass spectrometry (Bruschi et al, 2013). However, if one is interested in a number of proteins that may not be as abundant, these less common proteins will be not seen over the background noise. In addition, it is possible to strip samples of common proteins like albumin (Gundry et al, 2009) and antibodies can be removed from serum with many commercially available kits. After these procedures, if samples are enriched for only N-homocysteinylation events, the most common proteins with these PTMs, not just the most common proteins, would be able to be identified using mass spectrometry.

The use of both tissue and plasma from known mouse models that present with elevated homocysteine levels allowed for the aldehyde chemistry introduced here to be validated with biological samples, both tissue and plasma. Both the MTHFR heterozygous and the PCFT homozygous mouse samples were shown to have statistically increased levels of N-homocysteinylation, as would be expected. The agreement between these data and the previous determination of the levels of N-homocysteinylation in these mouse models serves as proof of principle for this

aldehyde reaction assay. These results, along with the mass spectrometry data, show that the adaptation of this chemical method worked, and can now be applied to a set of samples, in a high throughput fashion.

Chapter 3 Examining Genetic and Dietary Effects on the Metabolic Status of Developing Embryos

3.1 INTRODUCTION

Using genetic and dietary manipulation of the mouse model system, specific factors (target genes, metabolites, or external stimuli) and their importance in development can be explored. In the present study, maternal metabolism and its impact on the environment for the developing embryo, were manipulated through three different defined diets. Additionally, target genes were explored by using two mouse knockout models with spontaneous neural tube defects (NTDs) that are responsive to supplemental folic acid. The experimental diets allowed for the manipulation of maternal one-carbon metabolism balance. A high folate diet (10 ppm folic acid) allowed for ample amounts of folate and a balance in levels of total homocysteine. A diet supplemented with extra L-methionine (1% L-methionine) will increase flux through the methionine cycle, and will therefore increase the levels of maternal serum homocysteine (Troen et al, 2008). A final diet was used, as a control diet, and this diet had "normal" levels of folate (2 ppm folic acid). The effects that these diets have on the maternal environment and the developing embryo were the focus of the experiments reported in this chapter. Beyond just the relationship between folates and development, a high methionine diet allows for the relationship between protein N-homocysteinylation and development to be more fully explored.

The hypothesis that the PTM, N-homocysteinylation, has deleterious effects on proteins has been previously discussed both in the Introduction and in Chapter 2. Nearly all of the work performed in the field of protein N-homocysteinylation has been conducted in adult tissues. It has been seen that N-homocysteinylation can

cause an autoimmune response (Undas et al, 2004; Undas et al, 2006), can cause protein aggregates (Paoli et al, 2010; Stroylova et al, 2012), and can cause proteins to malfunction (Beltowski et al, 2005). To the knowledge of the author, no literature has been published describing N-homocysteinylation status during development, especially in a neural tube closure staged embryo. Herein we begin to explore on what level these PTMs affect developing embryos. One possibility is that protein N-homocysteinylation could affect maternal proteins that are critical for embryonic development, causing these proteins to malfunction and lead to embryonic abnormalities. A second possibility is that protein N-homocysteinylation could cause an autoimmune response in mothers that increases the overall maternal inflammation levels. Increased corporal levels of inflammation such as that which occurs in diabetes and obesity have been related to an increased risk for NTDs (Shaw et al, 1996; Wallingford et al, 2013). Additionally, autoimmune responses, such as autoantibodies against essential proteins such as FRα, have been associated with interfering with protein function and with an increased risk for NTDs (Cabrera et al, 2008; Rothenberg et al, 2004). The disruption of maternal proteins, such as the placentally expressed FRα, may change the nutrient supply available to the developing embryo, exacerbating the maternal low folate and high homocysteine levels in the *in utero* environment. In addition to autoantibodies, previously unpublished data from the Finnell laboratory shows that FRα itself loses functionality when it becomes homocysteinylated. Figure 3.1 shows that with increasing amounts of HTl, FRα will bind less of its folate substrate. Therefore, it can be expected that when FRα is homocysteinylated in the placenta, less folate will be bound and the developing embryo will be under exacerbated low folate conditions. In fact, the human FRα has 13 lysine residues, most of which are

surface exposed (PDB ID: 4LHR), allowing FRα to be an ideal target for potential N-homocysteinylation events. The FRα knockout mouse is an example of the great maternal importance of this protein during development, so if its function is disrupted, there may be dramatic embryonic effects (Piedrahita et al, 1999) . These data validate the idea that N-homocysteinylation can disrupt maternal proteins that are essential to development.

It remains to be determined if N-homocysteinylation can have a direct effect on embryonic tissues at the early stage of neural tube closure. The addition of HTl to a protein lysine is a chemical reaction that proceeds readily at body temperatures; therefore, an embryo does not have to have any specific enzymes expressed for these modifications to take place (Garel & Tawfik, 2006). It is possible at any time for a homocysteinylation event to occur, regardless of what proteins an embryo is, or is not yet producing. On the other hand, there are no enzymes that can rid proteins of these modifications, so it is generally thought that N-homocysteinylation events will increase over time, especially in proteins with low turnover rates (McCully, 2007; Undas et al, 2004). Potentially, developing embryos do not have a great impact from N-homocysteinylation in themselves because there is simply not enough time to have accrued significant amounts of these PTMs. To date, there is no study that has explored N-homocysteinylation levels in neural tube closure staged embryos, a study which could be the link between hyperhomocysteinemia and NTDs.

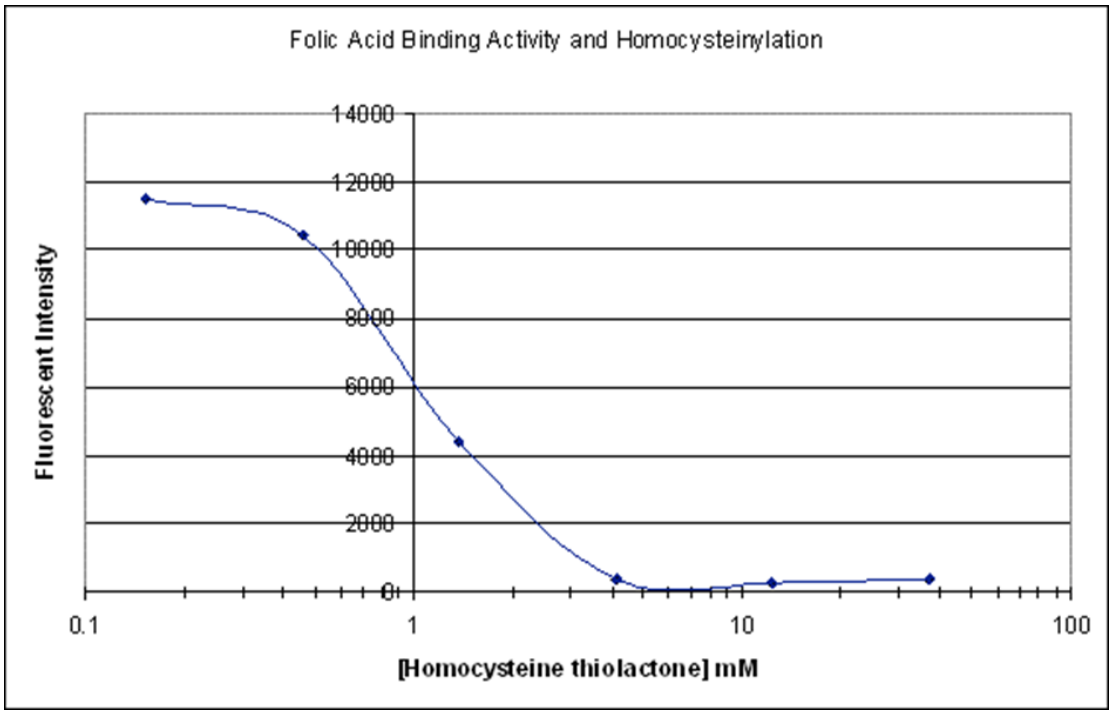

Figure 3.1 Folate Receptor Alpha Shows Decreased Function with Increased Homocysteinylation

Folate receptor isolated from placenta was subjected to increasing concentrations of homocysteine thiolactone at 37^{o} C for 4 hours in 100 mM sodium phosphate pH7.5 and 0.2 mM EDTA. As the concentration of homocysteine thiolactone increases, the amount of folic acid binding decreases, as reflected by the decrease in fluorescent intensity.

In addition to the three dietary factors explored here, two genetic manipulations were also investigated. As previously discussed, two major areas of focus regarding the genetic factors that may predispose an embryo to a NTD are mutations in either the Wnt signaling pathway, or the one-carbon metabolism pathway. The overlap between these two pathways is something that is more recently being explored. Recent literature has speculated that variable levels of folic acid will methylate DNA accordingly; high levels of folic acid will lead to hypermethylation and low levels of folic acid will lead to hypomethylation. The resulting hyper or hypomethylation will epigenetically regulate the expression of key genes, even those involved in Wnt signaling. One such example of this regulation is seen in a study that implicated elevated homocysteine levels in the inhibition of cardiac cell growth via increased Wnt signaling (Linask & Huhta, 2010). It was hypothesized that the low folate levels that coincided with the elevated homocysteine levels actually increased Wnt signaling, therefore suggesting an inverse relationship between folate and Wnt signaling (Linask & Huhta, 2010). In addition, it has been observed that folic acid supplementation will rescue the LRP6 Cd mouse mutant, which is traditionally considered a mouse model for hyperactive Wnt signaling. In contrast, the LRP6 knockout mouse model has an increased number of NTDs when supplemented with folate (Gray et al, 2010). This data again suggest that high levels of folate may suppress Wnt signaling in an unknown way. Another overlap between Wnt signaling and one carbon metabolism is the digenic interaction seen between the Folr1 and the LRP6 Cd mice. As seen in Table 3.1, while both the single heterozygous mice show no penetrance of NTDs, the compound heterozygous animals manifest with around a 40% penetrance of NTDs (Data from ME Ross and RH Finnell not published). In order to further explore the

interaction of the folate pathway and the Wnt signaling pathway, the LRP6 Cd mouse model and the Folr1 mouse model were used here to investigate the importance that genetic factors may have in neural tube closure, and the interaction between these two genes and one carbon metabolism.

The idea that NTDs do not arise from one single factor has been well established in the Introduction. The examples of this are widespread; from the range of mutations that have been identified in some human NTD cases, but not others, to genetically altered mice that do express an NTD until further stressed by a second environmental factor. For example, the Folr2 mice do not manifest with NTDs without stimulus, but are sensitive to arsenic induced NTDs (Wlodarczyk et al, 2001). Studies such as this emphasize the importance of examining multiple gene variants with different dietary inputs. Until now, the lack of a facile and high-throughput assay to determine N-homocysteinylation levels on small samples has prevented any studies of N-homocysteinylation levels on neural tube closure staged embryos. The application of the assay discussed in Chapter 2 will allow for the determination of N-homocysteinylation in a large cohort of ED 9.5 mouse embryos from a combination of Folr1 and LRP6 Cd gene variants. The folate concentrations and the extent of N-homocysteinylation of maternal plasma were determined, along with the folate and N-homocysteinylation levels in whole embryonic tissues. The embryos were developmentally staged by somite counts, a well-established method of staging embryos after ED 8 (Bard et al, 1998; Downs & Davies, 1993). Finally, all of these endpoints were explored in light of variations in their genotypes and diet.

$Lrp6^{Cd/+}$ x $Folr1^{+/-}$

	WT:WT	Cd/+:WT	WT:Folr1+/–	Cd/+:Folr1+/–	P value **
observed	0/18	0/21	0/20	13/32 **	
NTD rate	0%	0%	0%	41%	>0.0001

Table 3.1 Digenic Interaction of LRP6 and Folr1

Either single heterozygotes of the LRP6 Cd mouse or the Folr1 mouse show no penetrance of NTDs. However, the compound heterozygotes however show a 41% penetrance of NTDs, a highly significant increase over either of the single heterozygous mice.

3.2 MATERIALS AND METHODS

3.2.1 Experimental Animals

Mice were housed in the Dell Pediatric Research Institute's animal facility. The animals were maintained on a 7 am to 7 pm light/dark schedule. All animals were fed *ad libidum*. LRP6 Cd/+ males were kept on milled chow (PicoLab Diet 20 no. 5053, Lab Diet) until introduced to females. Females had a 6-week diet washout period after they reached 6 weeks of age. The three test diets had the same formulation as the control diet (2ppm folic acid), with different levels of folate or methionine being the only variable. The high folate diet had 10 ppm folic acid and the high methionine diet had 1% L-methionine. They were all purchased from Research Diets with the ID numbers D05072701i, D05072702Bi, and D1108021i, respectively. After a 6-week washout period, females were housed 4 to a cage and were provided with the same experimental diets. A single male was added to each cage and vaginal plugs were checked daily. When a vaginal plug was found, females were separated and this was marked as ED 0. All animals were maintained according to institutional rules (IACUC protocols AUP 2013-0051 and AUP 2014-00276).

3.2.1.1 Mouse Genotyping

Samples from the adult mice and embryos were taken and prepared as described in Chapter 2. The Folr1 mice were genotyped using two sets of primers. The wildtype primers were 5'-AAG TGC AAG GCT GCA TGT GG-3' and 5'-CAT TCC GAT GTC ATA GTT CCG C-3', whereas the Folr1 null mutation was detected 5'-ATC GCC TTC TAT CGC CTT CTT GA C-3' and 5'-TGC ATT CCG ATG TCA TAG TTC CG-3'. Both the Folr1 primer sets used a standard genotyping protocol with an annealing

temperature of 62°C. The LRP6 Cd mouse was genotyped first by PCR amplification of the *LRP6* gene using the primers 5'-TGA CAA GCC ATC AAG CAG AG-3' and 5'-GCT CAG AGG CTA TGT GAA CCA-3'. The amplification of the *LRP6* gene used a standard genotyping PCR protocol with an annealing temperature of 62.5°C. The point mutation was then detected with a restriction digest using Blp1 (New England Biolabs). The Cd point mutation fails to be cut by Blp1, whereas the wildtype DNA will be cut.

3.2.2 Animal Sample Collection

Embryos were collected from dams after sacrifice by carbon dioxide asphyxiation and cervical dislocation. Embryos were harvested in ice cold PBS under a microscope (Leica). Yolk sacs were collected for genotyping and washed once before digestion in PBS. Yolk sacs were digested using 99µL of Viagen Tail Buffer and 1µL of Proteinase K following the same genotyping protocol as used for the adult mice. Embryos were genotyped for both Lrp6 and Folr1 alleles. Embryos were kept in 96 well plates at -80°C.

3.2.3 Folate Determination

Total folates in samples were determined using a competitive binding ELISA assay previously developed in the Finnell Laboratory (Cabrera et al, 2008). In short, commercially purchased bovine folate binding protein (bFBP) is allowed to attach to the surface of a 96-well plate. Samples and a horse radish peroxidase-tagged folate (HRP-FA) are then mixed together and added to the plate. When folates from a sample bind the bFBP, the HRP-FA is displaced. The more folate present in a sample, the less signal captured.

3.2.3.1 Sample Preparation

Plasma and whole tissue were both treated to release any protein bound folate and denature any remaining proteins in the sample. 10uL of sample was added to 50uL of TBS-T with 1% w/v ascorbate, pH 3. These samples were homogenized by vortexing and then boiled for 10 minutes. When samples returned to room temperature, 2uL of 5% NaOH was added to neutralize the solution. Samples were spun for 5 minutes at 14000XG. The supernatant of each tube was removed and kept in a new tube as the working sample for folate determination.

3.2.3.2 Competitive Binding ELISA Assay

A competitive binding ELISA assay was used to determine qualitative total folate measurements. Lyophilized bFBP (Sigma Aldrich) was dissolved in Phosphate Buffed Saline pH 7.8 (PBS) with 2.5% glycerol at a concentration of 50ng/μL. 1 μL of the bFBP was manually printed in the center of each well of an Immulon 2HB high binding 96-well plate (Thermo Fisher). The plates were covered with film and placed in an opaque incubation chamber at 4^{o}C overnight. The plates were then washed three times with 300 μL each well with Tris Buffered Saline pH 8 with 0.1% Tween-20 (TBST). This removed excess bFBP that did not attach to the plate. 10 μL sample (see folate sample preparation) was then mixed with 5 μL HRP-FA (Johnson and Johnson Vitros Diagnostic) and 35 μL Tris Buffered Saline (TBS), a total of 50 μL for each well. Samples were incubated on the plate for 1 hour at room temperature in an opaque chamber. Plates were then washed three times with 300 μL each TBST then twice with 300 μL each TBS. 50 μL of SuperSignal Femto Chemiluminescent substrate (Pierce) was added to each well. The competitive nature of this assay yields results that are inverse to the amount of folate present in any sample. Therefore, a higher signal (pixel intensity) translates to a lower amount of folate in

the original sample. The plates were imaged using the Quansys Biosciences camera and the data was processed using the Quansys Biosciences software.

3.2.3.3 Data Analysis

Data was collected using the Quansys program. Pixel intensity was gathered from each spot. Each sample was run in triplicate and the means for the average spot intensity were used for further analysis of each sample.

3.2.4 N-Homocysteinylation Determination

N-homocysteinylation of both maternal and embryonic samples was determined using the chemical method described in Chapter 2. After sample collection and description, samples were prepared and labeled in 96-well plates as follows.

3.2.4.1 Sample Preparation

Plasma was normalized to total protein and then reacted with biotinylated aldehydes. Embryos that were collected were then lysed in RIPA buffer with protease inhibitors (Roche) for 2 hours at 4^{o}C while rocking. Large matter was pelleted with centrifugation at 5000XG for 15 minutes. Supernatant was collected and used for further assays.

3.2.4.2 N-homocysteinylation Labeling and Probing

Labeling was performed as previously described for both plasma and embryo tissue. Probing was conducted using a dot blot as previously described in Chapter 2.

3.2.4.4 Data Analysis

N-Homocysteinylation values were qualitatively determined using the LiCor Odyssey software. Software 96-well plate template was used to determine the

intensity of each spot. Average integrated pixel intensity was used for further analysis. Each sample was run in triplicate and averages were used for final statistical analysis.

3.2.5 Statistical Analysis

Statistical analysis was performed in Microsoft Excel and SPSS (IBM). Microsoft Excel was used to determine overall average values for the folate and N-homocysteinylation of both the embryos and the dams. Two-tailed t-tests were also performed in Excel. SPSS was used with a data set consisting of mean values from triplicates from folate and N-homocysteinylation assays, along with maternal data, somite number, genotype, and diet. Linear mixed model analysis, multivariate analysis of variance (MANOVA), and inter-item correlation matrices were the analyses that were used in SPSS.

3.3 RESULTS

In order to verify that the test diets being used had the desired outcome, the relative N-homocysteinylation levels and folate concentrations were compared for the dams on the three different diets. The plasma from these dams showed that a significant elevation in N-homocysteinylation was seen when the dams were treated with the high methionine diet (Figure 3.2a). The N-homocysteinylation level for the high methionine diet was significantly higher than that of either the control diet or the 10ppm high folate diet. Additionally, it was seen that the dams fed the high methionine diet and the 2ppm folate diet had significantly lower folate levels than those fed the 10ppm folate diet (Figure 3.2b). As previously noted, the competitive ELISA assay used to determine folate levels has an inverse relationship with the actual amount of folate in the samples. Therefore in Figure 3.2b, the higher pixel

intensity seen in the high methionine and control diets translates to a lower amount of folic acid in the samples.

3.3.1 Characterization of Embryonic Sample Cohort

A total of 257 embryos were analyzed. Table 3.2 shows the total embryo population that was collected for analysis, grouped according to the different maternal diets and embryonic genotypes. The outputs from folate determination, N-homocysteinylation measurements and somite number for the embryos and their respective dams are presented in Appendix 1. Figure 3.3 illustrates the estimated marginal means (unweighted means for each category, not accounting for differences in numbers or other factors) for somite number for each genotype and diet combination. It is seen that the high methionine diet is the most deleterious to growth (somite number) for all genotypes. This along with the data shown that the dams of the high methionine diet have increased N-homocysteinylation levels indicates that these high homocysteinylation levels may be deleterious to the embryonic growth.

3.3.2 Statistical Analysis of Genetic and Dietary Effects on Developing Embryos

First, the relationship between embryonic levels of folate and N-homocysteinylation was described. Reliability analyses in both adult and embryonic samples were used to determine that N-homocysteinylation levels and folate levels were inversely related. A correlation coefficient of 0.982 (from an inter-item correlation matrix analysis) indicated that there was a high level of inverse correlation throughout the entire embryonic group between N-homocysteinylation and folate concentrations. A MANOVA test showed that both maternal diet and embryonic genotype exhibited significant effects on the embryonic somite number,

folate levels, and N-homocysteinylation levels (Wilk's Lamba Coefficient $p<0.05$). Further exploration was completed using linear mixed model analysis. This determined if there were any correlations between maternal N-homocysteinylation and folate, and embryonic N-homocysteinylation and folate or embryonic somite number. There were no statistically relevant correlations found between either maternal folate or N-homocysteinylation levels and embryonic folate, N-homocysteinylation, or even somite number. The data presented here (Figure 3.4) indicated that embryonic N-homocysteinylation and folate levels are dependent on maternal diet and embryonic genotype, not directly dependent on maternal levels of folate and N-homocysteinylation.

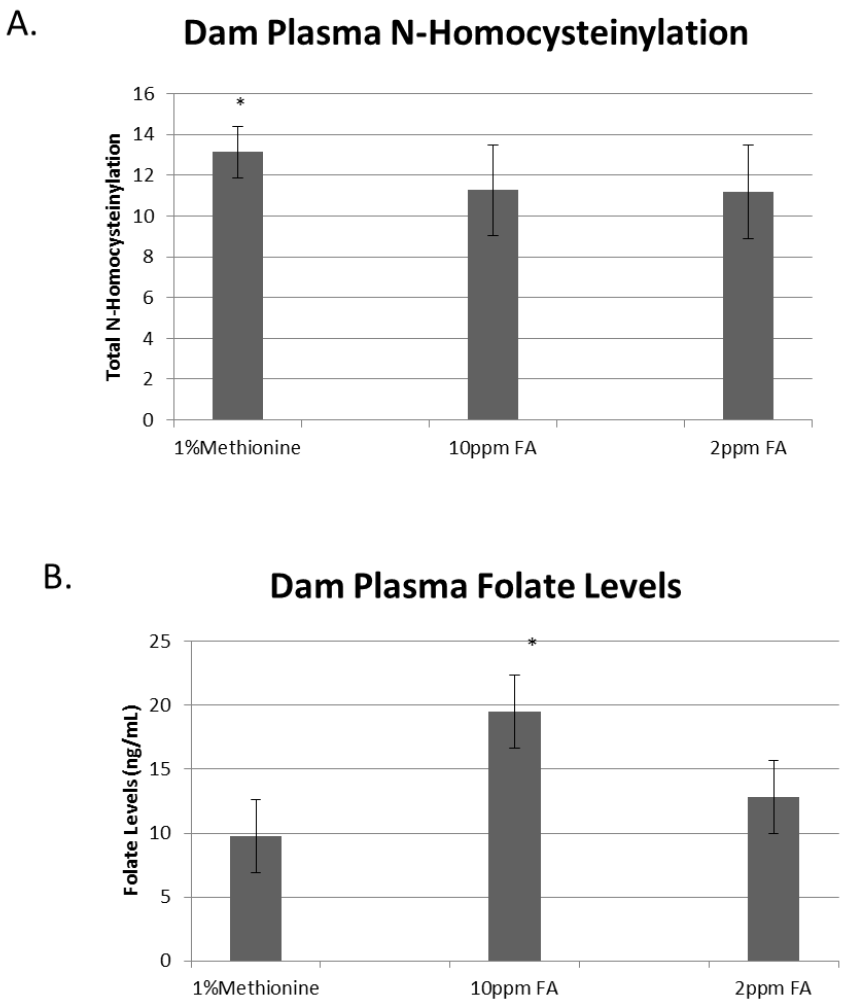

Figure 3.2 Dietary Influences of Dam N-homocysteinylation and Folate

Panels A and B show the relative N-homocysteinylation and folate levels in dam plasma after a 6 week washout period on three experimental diets. Asterisks indicate significance based on a two-tailed t-test ($P<0.05$).

Number of Embryo Subjects

		N
Genotype	Folr1 +/+; Lrp6 +/+	71
	Folr1 +/-; Lrp6 +/+	53
	Folr1 +/-; Lrp6 Cd/+	64
	Folr1 +/+; Lrp6 Cd/+	69
Diet	10 ppm Folic Acid	85
	2 ppm Folic Acid	81
	1% L-Methionine; 2ppm Folic Acid	91

Table 3.2 Number of Embryos Used for Statistical Analysis by Category

Embryos were described in binned groups of genotype and maternal diet. These embryos were those that had enough information to be used in the statistical analysis.

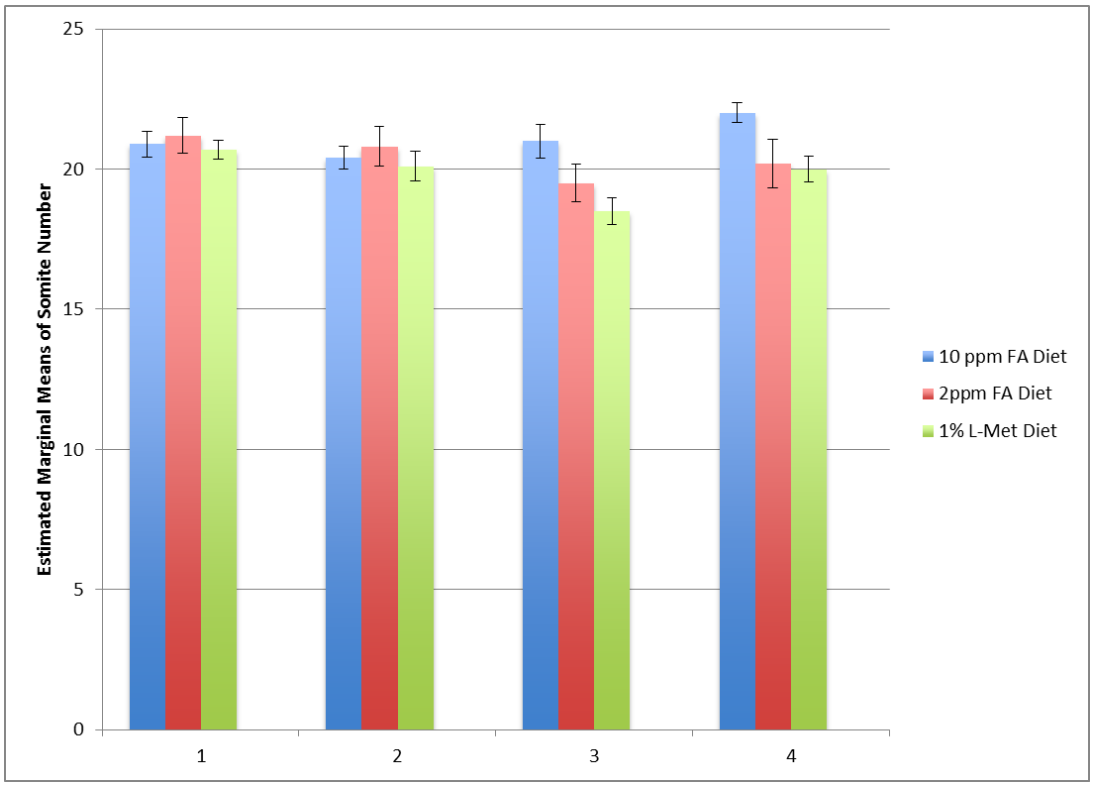

Figure 3.3 Estimated Marginal Means of Embryonic Folate, N-homocysteinylation, and Somites

The estimated marginal means for the somite number are illustrated in this figure. The diets are 1 (10ppm folic acid), 2 (2ppm folic acid), and 3 (1% methionine). The genotypes are 1 (Folr1 +/+; Lrp6 Cd +/+), 2(Folr1 +/-; Lrp6 Cd +/+), 3(Folr1 /+; Lrp6 Cd +/-), and 4 (Folr1 +/-; Lrp6 Cd+/-).

A.

MANOVA Analysis

	Wilk's Lambda
Embryo Genotype	0.034
Maternal Diet	0.031

B.

Significance from Mixed Model Analysis

	Dam N-Homocysteinylation	Dam Folate
Embryonic Folate	0.094	0.262
Embryonic N-Homocysteinylation	0.053	0.285
Somite Number	0.645	0.227

Figure 3.4 Statistical Analysis of Embryonic Outcomes

Panel A indicates that the embryonic genotype and maternal diet both significantly influenced the embryonic somite number, N-homocysteinylation levels, and folate levels. Panel B shows that there was a not a significant correlation between dam folate and dam homocysteine and any of the embryonic outcomes.

3.4 CONCLUSION

The assay that was previously described in Chapter 2 as being a robust and accurate way of determining N-homocysteinylation levels was applied to a set of neural tube closure staged embryos to determine specific responses to diet that might be modified by the genotype and how these factors might contribute to NTD susceptibility. These embryos were the product of crosses between two folate-responsive NTD mouse models, the Folr1 mouse and the Lrp6 Cd mouse. These two genes are of specific interest due to the digenic interaction seen in these mouse models (the compound heterozygotes display a marked increase in NTDs compared to the single heterozygotes), and the putative overlap between the folate and Wnt signaling pathways described in the Introduction. In addition, three different diets allowed for the balance of one carbon metabolism to be altered, with increased folate or increased methionine. Amongst these three diets, the embryos could be any combination of a Folr1 and Lrp6 Cd single heterozygous cross (Folr1 +/+ and Lrp6 +/+; Folr1 +/- and Lrp6 +/+; Folr1+/- and Lrp6 Cd/+; Folr1 +/+ and Lrp6 Cd/+).

It was seen that both embryonic genotype and maternal diet had a significant impact on embryonic folate, embryonic N-homocysteinylation, and also embryonic development as measured by somite number (MANOVA analysis, Wilk's Lamba Coefficient <0.05). As discussed in Chapter 1, both maternal diet and embryonic genotype have known associations with specific embryonic outcomes; therefore, it is not surprising that this significant impact was observed. An additional significant correlation of interest was that the embryos already had established an inverse relationship between N-homocysteinylation and folate levels. This common phenomenon of increased homocysteine levels when there are low folate levels has

been well established in adult rodent populations (Challet et al, 2013; Sugiyama et al, 2012; Tyagi et al, 2011). Indeed, the association between low folate levels and high homocysteine levels are commonly seen in adult human populations (Miller et al, 1994) as well as amongst children and teenage populations (van Beynum et al, 2005). However, this relationship has not yet been shown to be established at such an early point in development as neural tube closure. Working with early stage mouse embryos limits the amount of biological tissue one has to assay, thus many previously established methods of determining N-homocysteinylation may not have been feasible. Using the assay described in Chapter 2, N-homocysteinylation and folate levels could be determined quickly with the small amounts of available tissue from an embryo just after neural tube closure. The fact that this inverse relationship between N-homocysteinylation and folate has already been established at 9.5 days post conception highlights the importance of the *in utero* environment that is established by maternal diet and other potential factors. Measurements of s-adenosyl methionine and s-adenosyl homocysteine, two other metabolites in the methionine cycle, have revealed the importance of a well regulated methionine cycle in early embryonic development; however, the limitations on these study methods did not allow for such a large sample set to be evaluated (Burren et al, 2006; Dunlevy et al, 2006). Additionally, measurements of s-adenosyl methionine and s-adenosyl homocysteine simply describe the balance of methylation reactions from the methionine cycle, and these metabolites do not point directly to protein modification by HTl.

To date, no studies have been performed examining N-homocysteinylation of proteins at a point of development as early as neural tube closure. Only one study has been performed examining N-homocysteinylation levels in fetuses at ED 20 (one

day before the average day of birth) (Bossenmeyer-Pourié et al, 2013). This recently published article demonstrated that structural proteins in the stomachs of fetuses whose mothers were fed a methyl donor deficient diet had elevated levels of N-homocysteinylation (Bossenmeyer-Pourié et al, 2013). This research indicates that N-homocysteinylation of proteins in the developing embryo may also play a role in some of the negative outcomes seen with mothers who have elevated levels of homocysteine. The embryos collected in the study presented in this body of work were at a much earlier time point in development, prior to the onset of organogenesis. The chemical nature of this PTM, and the lack of any known removal system in the body, also make the early time point studied here extremely interesting from a developmental biology perspective. It is possible that simply insufficient homocysteinylation events have taken place to be significantly associated to the developmental outcomes of the embryos. It is also possible that the total protein N-homocysteinylation levels are not what matters the most, but rather it is the homocysteinylation of only specific proteins that is critical during development. Further studies that include multiple samples before and during neural tube closure should be performed. A developing embryo is changing constantly, which emphasizes the need to take multiple time points, a task that is now feasible with the method used in these experiments. In addition, these studies could be more easily interpreted by the isolation of specific regions of the developing embryo or by using this method as an adapted histological staining method. In the data presented here, the entirety of the embryo was analyzed together. Even studies using the "global approach" to metabolomics (Nicholson & Lindon, 2008), isolate specific tissue types to get a better perspective of what is happening in the body (Cabaton et al, 2013). Studies, such as this, where every

portion of an entire body is analyzed together do not allow for the elucidation of what areas and proteins are important when they are or are not homocysteinylated. These further tissue and protein specific studies need to be performed, as the data presented here failed to find a significant correlation between total embryonic N-homocysteinylation and somite number.

The overwhelming lack of data supporting or refuting the hypothesis that N-homocysteinylation is responsible for the negative effects that are correlated to high levels of homocysteine, make any data set a valuable addition to the field of research. Here, data including N-homocysteinylation levels and folate levels for a group of early staged embryos was generated using the technique described in Chapter 2. The success and ease with which these large amounts of data were generated shows promise for future studies. Multiple time points collected during the dynamic development of an embryo may help determine if there are specific points of increased N-homocysteinylation. Studies isolating specific regions of the developing embryos or using this chemical method as a stain and counterstaining for developmental proteins of interest or cell death will be necessary. Here, we showed that the maternal diet and embryonic genotype were the most significant predictors of not only embryonic growth, as measured by somite number, but also embryonic one-carbon metabolism. The balance between folate levels and N-homocysteinylation already established in these developing embryos indicates the importance of folate and N-homocysteinylation during development, not only maternally, but also for the embryo itself.

Chapter 4 LRP6 mutation examination in a human population

4.1 Introduction

The era of whole genome sequencing has allowed for the expansion of the types of studies that can be performed to help determine the etiology of various congenital defects. After the first few human genomes were sequenced in the early 2000s, it was predicted that single nucleotide polymorphisms (SNPs) were what provided the bulk of the genetic variety in human genomes (Feuk et al, 2006) (Redon et al, 2006). These SNPs are single base changes in the DNA and can either be inherited, or be the result of a spontaneous change of a single nucleotide. Depending on which nucleotide is changed, and the nature of the change, different types of errors can arise. SNPs can be synonymous, in that they do not change the amino acid sequence coded for, or non-synonymous, meaning that they will change the amino acid sequence. Synonymous SNPs will not change the protein that is coded for by a gene because of the degeneracy of the codons allows for some changes. Non-synonymous SNPs can be further characterized into missense mutations, where a new codon is made and a new amino acid is created, and nonsense mutations, where an aberrant stop codon is the result of the change. Both of these types of mutations change the sequence of the protein. It is also important to consider that only an estimated 2% of the entire human genome codes for proteins (Alexander et al, 2010). However, even if a SNP is not within the coding region of the protein, there still may be deleterious effects to the protein product

when RNA processing takes place (Millar et al, 2010). Any number or a specific placement of a SNP in a person's genome may translate to deleterious effects in their proteome and may manifest as a disorder.

Often, when whole genomes are sequenced, these data are processed and compared to existing databases of normal individuals (control DNA) in order to identify any SNPs a patient may possess. After identifying any number of SNPs that a person has, the relative importance of these SNPs must be assessed in relation to a specific condition present in the individual to determine if it is possibly causative. Often, major biological pathways associated with a specific condition will be investigated first for any mutations in genes crucial for these pathways. When investigating NTDs, the folate one-carbon metabolism related genes and the Wnt signaling genes are among the gene pathways currently serving as a focus of investigation. After finding SNPs of interest, they can be run through *in silico* analyses that can predict the ramifications of the amino acid change that was coded for by the SNP. These programs, such as PolyPhen, use database searching for homology of genes and protein structure information to determine if certain changes will probably damage the protein or not (Ramensky et al, 2002). The change of amino acid residues that are highly conserved over various species, a change in a domain that has a conserved folding pattern, or a drastic change in the chemical properties of amino acids usually indicate deleterious mutations. Although this *in silico* analysis is not always correct, it allows for a good starting place when

interpreting and managing the massive amounts of data (typically greater than 1 terabyte per person) that whole genome sequencing provides.

The number of different mutations in the mouse NTD mutant *LRP6* gene, the essential role of LRP6 in canonical Wnt signaling, and the putative role of LRP6 in non-canonical Wnt signaling, make *LRP6* a gene of interest in human mutation studies of NTDs. In fact, two of these NTD mouse models of the *LRP6* gene are the result of single nucleotide changes in the DNA. Recently human SNPs in *LRP6* have been associated with such disease states as coronary artery disease (Xu et al, 2014), early onset Crohn's Disease (Koslowski et al, 2012), and even NTDs (Allache et al, 2014). The data presented here represent the sequencing results of the *LRP6* gene from a group of spina bifida patients from the California Birth Defects Monitoring Program. The cases represent 192 infants with spina bifida and no other major birth defects, while the controls represent 190 non-affected infants. Among the 192 spina bifida cases, 82 are Non-Hispanic White, 54 are native US born Hispanics and 56 are foreign born Hispanics. Among the 190 controls, 81 are White Non-Hispanic, 54 are US born Hispanics and 55 are foreign born Hispanics. All samples were obtained with approval from the State of California Health and Welfare Agency Committee for the Protection of Human Subjects (the primary IRB). The *LRP6* gene was sequenced by Dr. Yunping Lei using PCR on the whole genome amplification product of each infant. These products were sequenced using an automated sequencer and were analyzed using the Mutation Surveyor software (Softgenetics).

Any mutations found in *LRP6* were validated by a second round of Sanger sequencing. Four novel *LRP6* gene mutations were identified in the cases that were not present in any of the controls.

The four novel mutations found in the gene and described herein, were also not present in three public databases: dbSNP, the 1000 genome project, and the NHLBI GO exome sequencing project. These four novel missense mutations that were found in the spina bifida cases and not any of the controls or public databanks are seen in Table 4.1. This table also provides the mutation in the DNA sequence, the predicted protein effects using the software PolyPhen, and if the amino acid that was changed is a conserved amino acid. The sequence alignments of the *LRP6* gene for the areas of interest are seen in Figure 4.1. All of the mutations are in conserved regions of the *LRP6* gene over 8 vertebrate species. The placement of the mutations in the LRP6 protein in relation to known features of the protein, along with the placement of the Cd mutation, is depicted in Figure 4.2. The amino acid change of alanine to valine at position 3(A3V) is in the signal region of the peptide, but not in the mature form of the protein, and is a substitution of a small hydrophobic to a slightly larger hydrophobic amino acid. The tyrosine to cysteine amino acid alteration at position 544 (Y544C) is in the critical YWTD beta-propeller repeat domain, and changes a large aromatic to a small and reactive amino acid. Both the proline to leucine at position 1482 (P1482L) and the arginine to leucine at position 1574 (R1574L) are in the cytoplasmic domain of the protein, not the extracellular

binding surface of the protein. It is however, important to note that the P1482L mutation is predicted to not be damaging, whereas the R1574L mutation is predicted to be possibly damaging. The proline to leucine change at 1482 is a small hydrophobic substituted with a small hydrophobic, whereas the arginine 1574 to leucine will change a negatively charged amino acid to a small hydrophobic. This may potentially interrupt some cytoplasmic binding partners that LRP6 is known to have.

Nucleotide Change	Protein Change	PolyPhen predict	Conserved
c.8C>T	p.Ala3Val	benign	**Yes**
c.1631A>G	p.Tyr544Cys	**probably damaging**	**Yes**
c.4445C>T	p.Pro1482Leu	benign	**Yes**
c.4721G>T	p.Arg1574Leu	**possibly damaging**	**Yes**

Table 4.1 Novel *LRP6* Mutations Identified in Human Spina Bifida Cases

Four novel mutations in the *LRP6* gene identified in 192 spina bifida cases, but not in controls. All of the mutations are evolutionarily conserved throughout vertebrates and two are predicted to be damaging by PolyPhen *in silico* analysis.

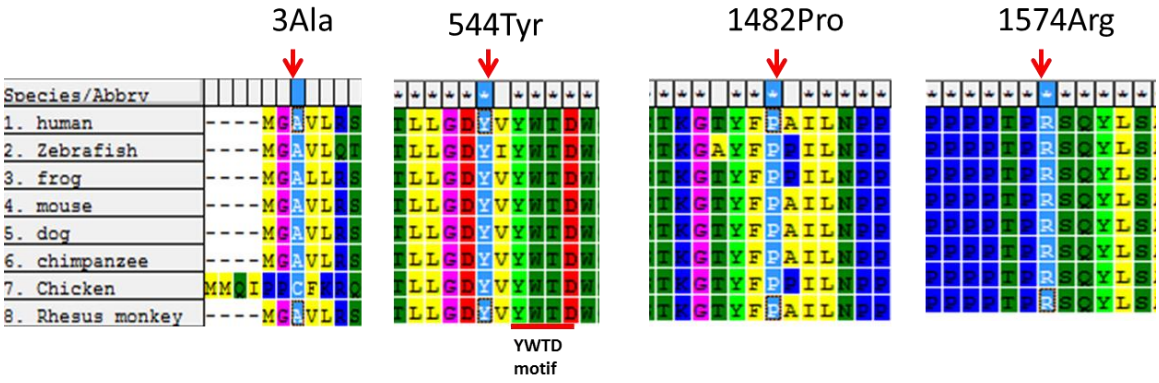

Figure 4.1 A Partial Alignment of Human *LRP6* with Seven Other Orthologous Sequences

The Lrp6 variants found in NTD patients affect conserved residues (indicated by arrows). Accession numbers: Homo sapiens Lrp6 (human),NP_002327.2; Danio rerio Lrp6 (zebrafish), NP_001128156.1; Xenopus tropicalis Lrp6 (frog), NP_001079233.1; Mus musculus Lrp6 (mouse), NP_032540.2; Canis lupus familiaris Lrp6 (dog) , XP_534886.2; Pan troglodytes Lrp6 (chimpanzee), XP_001152103.1 ;Gallus gallus Lrp6 (chicken), XP_417286.3; Macaca mulatta Lrp6 (Rhesus monkey), NP_001244648.1.

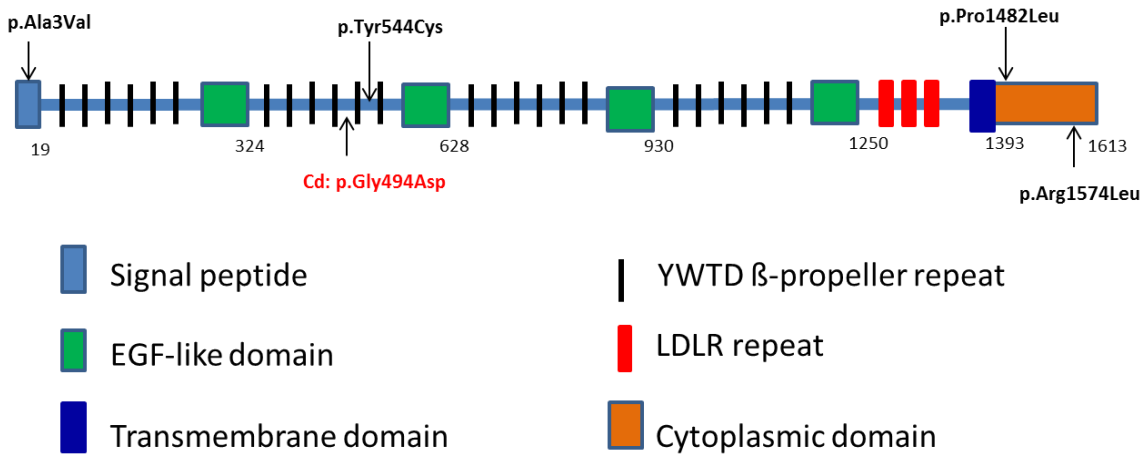

Figure 4.2 Rare Novel LRP6 Mutations Identified in Human Spina Bifida Patients

A schematic diagram of LRP6 showing the approximate locations of the 4 mutations, p.Ala3Val, p.Tyr544Cys, p.Pro1482Leu and p.Arg1574Leu, in relation to the general protein structure.

In addition to *in silico* predictions of damage, the functionality of these four novel mutations in the LRP6 protein was compared to the wildtype protein and a known mutation from the LRP6 Cd mouse. As a folate-responsive mouse model, the Cd point mutation is an interesting comparison when conducting human point mutation studies. Since the majority of human NTDs appear to be folate responsive, it is especially helpful to be able to use folate-responsive mouse models in efforts to learn more about the beneficial effects of folates on neural tube closure. It has been shown that the Cd mutation is a single amino acid change, glycine 494 to aspartate (G494D), in the second YWTD-EGF like repeat in the LRP6 protein, a very highly conserved tertiary structure throughout all of the LDL-receptor protein family (Carter et al, 2005). This Cd mutation has been shown to alter LRP6 localization based on its interrupted binding with the chaperone protein MESD (Gray et al, 2013). It is thought that mutations to the beta-propeller regions of the LDL-receptor protein family may disrupt some of their ability to bind ligands or other proteins (Cheng et al, 2011). In addition, using luciferase assays, it was shown that the Cd mutation abrogated canonical Wnt signaling and was not as responsive to stimuli to the PCP signaling pathway (Gray et al, 2013).

Luciferase assays are a simple method to determine the rate of transcription of various genes. The principle of a luciferase assay involves engineering various transcription factors to activate the luciferase protein from fireflies (Smale, 2010). In these engineered systems, instead of a transcription factor being activated by a

signaling cascade and transcribing the gene as it normally does, when the transcription factor is activated, the gene that codes for the luciferase protein is transcribed. When given the proper substrate, the production of this luciferase enzyme can easily be monitored by how much light is produced. The canonical Wnt signaling pathway luciferase plasmid (TOPFlash) has the TCF/LEF promoter, so every time that these genes would be activated by β-catenin, luciferase is produced. The non-canonical Wnt signaling pathway luciferase plasmid has an AP1 promoter, which is activated by the phosphorylation of JUN kinase. Therefore with a simple luminometer, one can measure the flux through a signaling pathway. Concurrent transfections with the plasmid that encodes for the Renilla protein (a light producing enzyme from the Sea Pansy) allows for standardization for transfection efficiency. For the PCP pathway studies performed here, Wnt5a conditioned media was used to stimulate an increased flux through this pathway. Wnt5a is one of the Wnt proteins that are associated with stimulating PCP signaling specifically (Niehrs, 2012). In addition, Vangl2 was also co-transfected with the cells to further facilitate PCP signaling. Vangl2 is a transmembrane protein that is involved in PCP signaling (Kibar et al, 2011) and thought to be a binding partner of disheveled (Lei et al, 2010).

Interestingly, the novel Y544C mutation is also located in the same second-beta-propeller region of the protein as the Cd mutation (Figure 4.2). This data, along with the "possibly damaging" prediction from PolyPhen, led to the hypothesis

that the Y544C mutation may be a damaging mutation by the same mechanism as the LRP6 Cd mutation. It was hypothesized that this Y544C mutation would also interrupt binding with the chaperon protein MESD, due to its proximity to the YWTD repeat and the extreme nature of the amino acid substitution. In both the Cd mutation and the Y544C mutation, a non-charged amino acid is being changed for a potentially charged amino acid. Therefore, the binding to the chaperone protein MESD, the subcellular localization, and the functionality of all the novel mutations described here were investigated. The studies here compare the novel mutations found in a cohort of spina bifida patients with the well-characterized NTD model of the Cd mutation.

4.2 MATERIALS AND METHODS

4.2.1 Plasmid DNA

Dr. ME Ross of Weill Cornell Medical School graciously provided wildtype and Cd Lrp6-GFP plasmid DNA in a pCMV vector. Mutations to DNA were made using the Stratagene Site Directed Mutagenesis Kit following the manufacturer's instructions. The mutations made were Alanine 3 to Valine, Tyrosine 544 to Cysteine, Proline 1482 to Lysine, and Arginine 1574 to Lysine. Mesdc2-Flag plasmid was kindly provided by Dr. Bernadette Holdener (Stony Brook University, New York, USA). Renilla and Vangl2 available from our laboratory having been previously obtained from Dr. Hongyan Wang (Fudan University, Shanghai, China). M50 Super 8x TOPFlash, human beta-catenin pcDNA3, and pcDNA3-S33Y Beta-catenin were purchased from Addgene (Kolligs et al, 1999; Veeman et al, 2003). Ap1 reporter plasmid was purchased from Agilent.

4.2.2 Bacterial Transformation and Plasmid Preparation

Plasmids were transformed into competent DH5 *E. coli* cells (Invitrogen). Transformed *E. coli* were grown on LB agar plates overnight with ampicillin selection. Positive colonies were selected for plasmid purification and grown in shaking culture overnight with ampicillin. HiSpeed Plasmid Maxi Kit (Qiagen) was used to collect the plasmid DNA from the *E. coli* per manufacturer's instructions. Concentrations were determined using NanoDrop 2000.

4.2.3 Co-Immunoprecipitation Assays

HEK293T cells were transiently transfected with the various LRP6 cDNA constructs and MESD-Flag. Lipofectamine 2000 (Invitrogen) transfection reagent was used per manufacturer's instructions at a ratio of 0.5 μL/1μg reagent to DNA. In short, cells were grown to around 80% confluence in 6-well plates (Corning) in DMEM with 10% bovine serum (Life Technologies). Growth media was removed and transfection mixture was added to the cells along with Opti-MEM low serum media (Gibco). Cells were allowed to incubate in the transfection media for 24 hours. Cells were then rinsed once with PBS. To collect whole cell lysate, TBS with 1% Triton X-100 and protease inhibitors (Roche) were added to the plates, which were rocked at 4^{o}C for 2 hours. Samples were spun at 2000xG to pellet cellular debris and the supernatant was collected as lysate. Total protein concentrations were determined using a Bradford Assay, as previously described. Lysate samples were normalized to total protein concentration and incubated with an anti-Flag antibody (1:500, Sigma) for 2 hours at room temperature. Protein A/G agarose beads (Pierce) were washed three times with TBS and then added to the samples. This mixture of beads, sample, and antibody, was allowed to rock overnight at 4^{o}C. Beads were washed 5 times with TBS with 0.5% Tween 20. The beads were boiled in SDS loading buffer and the supernatant was loaded onto a polyacrylamide gel for gel electrophoresis. The gel was transferred onto nitrocellulose membranes. Membranes were blocked with 5% milk solution for one hour at room temperature.

Beta Tubulin (Developmental Studies Hybridoma Bank, 1:500), LRP6 (Cell Signaling, 1:2000), and Flag (Sigma, 1:500) primary antibodies were used and all were incubated overnight at 4°C. LiCor secondary antibodies were used at 1:10000 and incubated for 45 minutes in the dark at room temperature. The LiCor Odyssey was used for imaging of blots.

4.2.4 Subcellular Localization

MDCK II cells were transiently transfected with Lipofectamine 2000 Reagent. MDCK II cells were plated in 12-well plates on cover slips (Corning) in MEM media with 10% bovine serum and grown to 70-90% confluence. MESD and LRP6 wildtype or mutant plasmids were co-transfected using Lipofectamine 2000 reagent in a 1:1 ratio of Lipofectamine 2000 to DNA, as previously described. Cells were incubated for 24 hours in transfection media. After 24 hours, cells were washed once with PBS then fixed with paraformaldehyde on the cover slips. Cover slips were rinsed with PBS and cell membranes were permeablized with 1% Triton X-100 in PBS. Cells were blocked with 5% BSA then incubated with anti-SCRIB antibody overnight (1:1000, Santa Cruz Biotechnology). Secondary anti-goat antibody was used (1:2000, Alexa Fluor 647). Cover slips were mounted on slides with Vectashield mounting media with 300ng/mL DAPI (Vector Biosciences) and sealed with clear nail polish. Images of slides were taken using a laser scanning confocal microscope (LSM710, Leica). Images for cell counting were taken with a 10X objective where around 100 GFP positive cells were visible in each field. These images were viewed

and overlaid in Image J. GFP was visually determined to be non-membrane bound or mostly membrane bound. Chi-squared analysis was performed in Microsoft Excel to compare the localization difference between wildtype and different LRP6 mutants. An oil immersion 100X objective was used for representative images.

4.2.5 Luciferase Assays

Canonical Wnt signaling was measured using a TOPFlash reporter plasmid. Non-canonical PCP signaling was measured using an AP1 reporter plasmid. In both cases, HEK293T cells were transfected with Lipofectamine 2000 (Invitrogen) as previously described. Renilla was used as an internal control. TOPFlash and AP1 transfection media was incubated with the cells overnight at 37^{o}C. After 24 hours, the TOPFlash media was removed and the cells were washed once with PBS. Cells were lysed and luciferase activity was determined using a Promega Dual Luciferase Assay per manufacturer's instructions. After 24 hours, the AP1 media was overlaid with Wnt5a conditioned media and allowed to incubate for 24 further hours. For the AP1 plasmid, after 48 hours, media was removed and cells were washed once with PBS. Again, cells were lysed and a Promega Dual Luciferase Assay kit was used. In both cases a BioTek-2 plate reader was used to measure luminescence and data was analyzed in Microsoft Excel. Significance was determined using a two-tailed t-test with a $p<0.05$ being the significance threshold.

4.2.5.1 Wnt5a Conditioned Media

Wnt5a secreting L Cells (ATCC) were grown to confluence in 75mm flasks (Corning) in DMEM/F12 media (Gibco) with 10% fetal bovine serum (FBS) and 0.6mg/mL G418 selection antibiotic (Invivogen). At the point of 100% confluence, the cells were trypsinized and split into 8 different 75mm flasks. These cells were then incubated for three days in DMEM/F12 with 10% FBS, with no selection antibiotic. After three days, the media was collected from the cells, sterile filtered (Millipore), and kept at 4^{o}C. New DMEM/F12 with 10% FBS was added to the cells and they were allowed to incubate for two more days. After two days, the media was harvested from the cells, sterile filtered, and added to the first round of collected media. This media was used as the Wnt5a conditioned media. The cells were discarded.

4.3 RESULTS

4.3.1 Novel LRP6 Mutations Affect Binding to Chaperone Protein MESD

A co-immunoprecipitation was used to probe the physical interactions between the various LRP6 mutations and the LRP6 chaperone protein MESD (Figure 4.3). The wildtype protein was used as a positive control and the Cd mutation was used as a negative control for binding. β-tubulin served as a loading control, and it is readily apparent that there is no difference in the amount of MESD-Flag in all the samples. When the membrane was probed with a GFP antibody, it was seen that the LRP6 Y544C mutation, like the Cd mutation, does not bind readily to the chaperone

protein, MESD. The other three novel mutations do not affect binding with MESD, and do not differ from the wildtype binding.

4.3.2 Novel Lrp6 Mutations Affect Sub-Cellular Localization

The disrupted binding between the LRP6 mutation Y544C and the chaperone protein MESD indicated that this mutation may not allow LRP6 to properly insert into the plasma membrane. The localization of the four novel mutations to the LRP6 gene was examined using immunocytochemistry in MDCK II cells. The LRP6 plasmids are fusion constructs with GFP (green), the plasma membranes are marked using SCRIB (red) (Lei, 2013) and the nuclei are seen with DAPI (blue). The Y544C mutation does not appropriately translocate to the cell membrane, similarly to the Cd mutation. This follows the prediction that MESD binding is essential for the proper localization of LRP6 to the plasma membrane. Figure 4.4 shows representative images of the immunocytochemistry of each construct, while Figure 4.5 shows the quantification of the subcellular localization of each of the LRP6 constructs. It is seen that the Cd and Y544C point mutations significantly alter the localization pattern in comparison to the wildtype protein.

4.3.3 Novel Lrp6 Mutations Abrogate Canonical Wnt Signaling

LRP6 is a known membrane-bound receptor in canonical beta-catenin dependent Wnt signaling. Previous studies have shown that the LRP6 Cd mutation does not properly conduct canonical Wnt signaling (Gray et al, 2013). It is

hypothesized that because LRP6 Cd cannot bind MESD and take a proper place in the plasma membrane, canonical Wnt signaling will be reduced. Figure 4.6 shows that similarly to the Cd mutant, the novel mutation Y544C, has a significantly lowered TOPFlash response. This indicates that both the Cd mutation and the Y544C mutation respond to their failure to translocate to the plasma membrane with a lowered amount of Wnt signaling. Additionally, Figure 4.6 shows that the p.Arg1574Leu mutant is a hyperactive canonical Wnt signaling mutation, with a significant increase over the wildtype plasmid.

4.3.4 Novel Lrp6 Mutations Enhance Non-Canonical Wnt Signaling

HEK293T cells were transfected with the various LRP6 constructs, Vangl2, the AP1 reporter gene, and Renilla served as an internal control. Wnt5a conditioned media was used as previously described (Allache et al, 2014) to stimulate transduction through the PCP pathway. Figure 4.7a shows that with increasing amounts of wildtype LRP6, a significant corresponding decrease in PCP signaling is seen. In Figure 4.7b, it was seen that in the presence of Vangl2, three of the novel mutations significantly increased PCP signaling when compared to the LRP6 wildtype plasmid. The P1482L mutation is seen to not increase the PCP signaling significantly over the wildtype protein. Panel C shows a representative western blot analysis showing that all of the transfected plasmids were expressed at comparable levels.

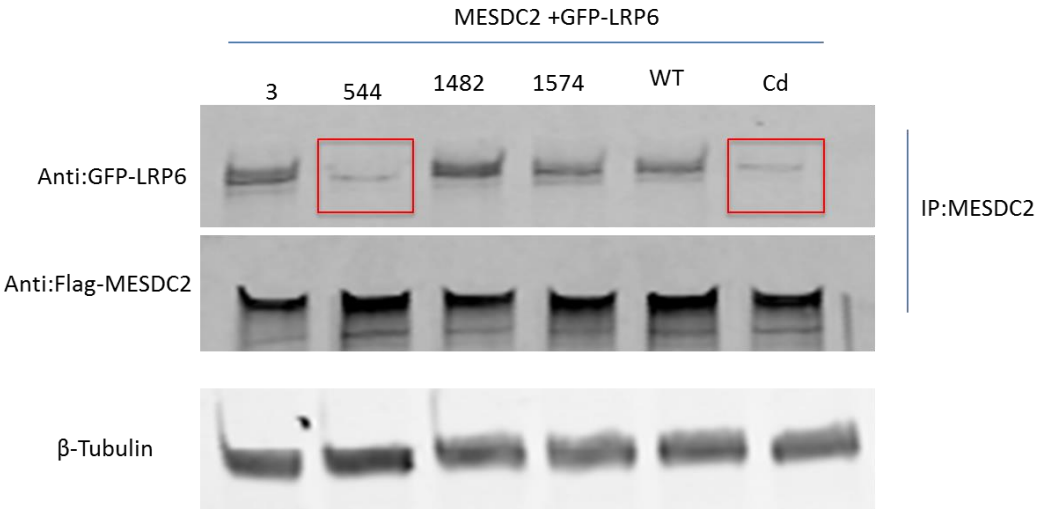

Figure 4.3 Co-Immunoprecipitation Between LRP6 Mutations and the Chaperone Protein MESD

Co-IP detected effect of mutations on LRP6 physical interaction with MESDC2 . Following Flag immunoprecipitation, blotting with anti-GFP confirmed physical interaction between wildtype LRP6 and MESDC2, while this interaction was affected in the variant Tyr544Cys as well as Cd mutant. β-Tubulin was taken as an internal control.

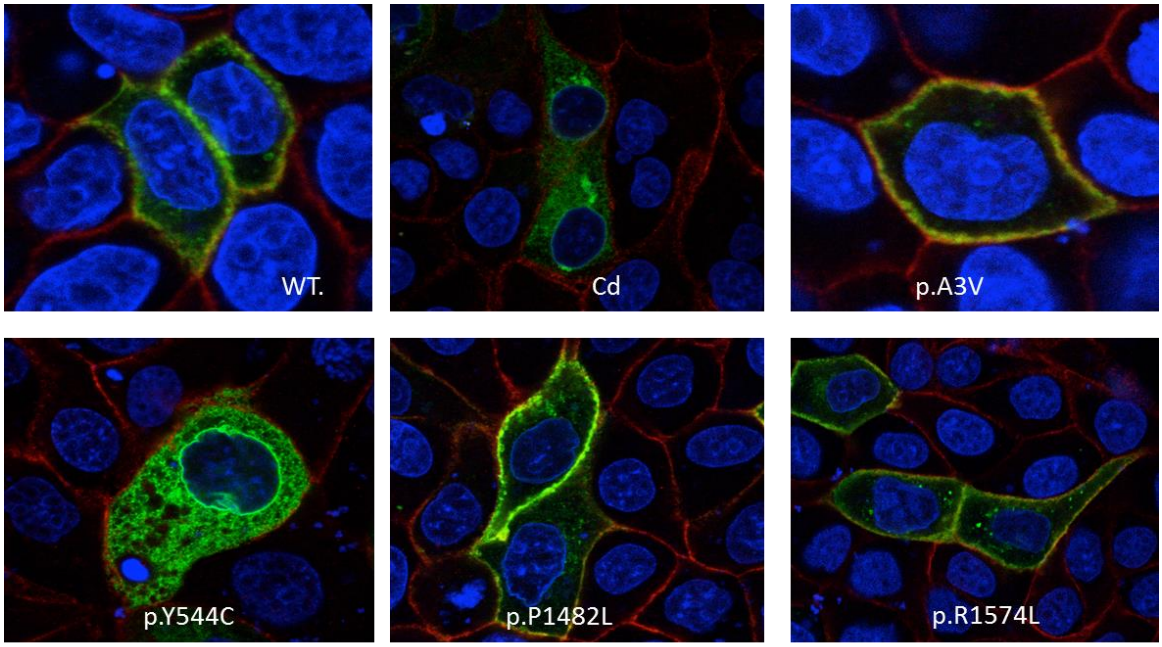

Figure 4.4 Representative Images of Subcellular Localization of LRP6 Mutants.

Protein subcellular localization in fixed MDCK II cells. Blue color indicates DAPI stain of nucleus. Red color indicates SCRIB stain for membrane marker. Green color indicates GFP for LRP6-fusion plasmid constructs.

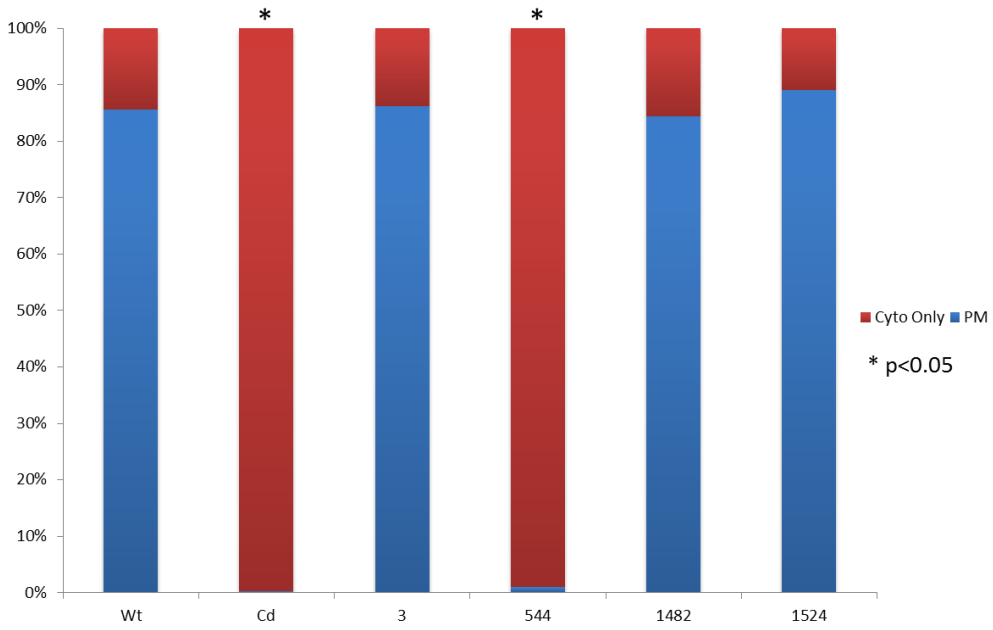

Figure 4.5 Quantitative Analysis of Subcellular Localization of LRP6 Mutants

Quantitative analysis of protein localization for GFP-LRP6 wildtype and its mutants. Fields of cells were imaged randomly and at least 100 GFP positive cells were counted per construct for each of the triplicates. Cells were classified as either GFP only in the cytoplasm or GFP predominantly in the plasma membrane. Asterisks represent a significant ($p<0.05$) departure from the wildtype construct using a chi-squared analysis.

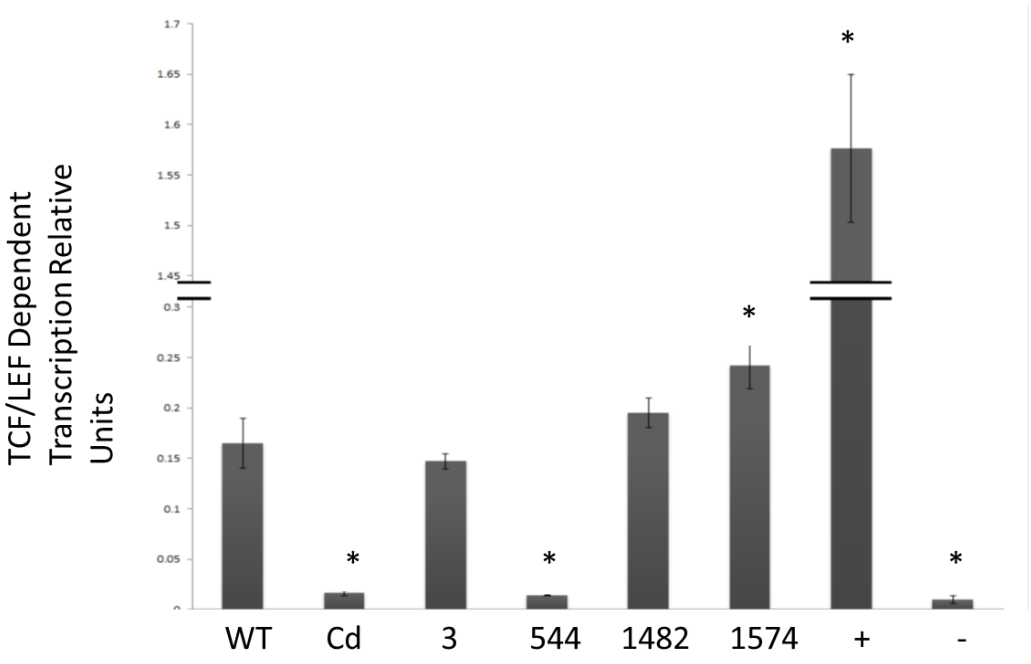

Figure 4.6 Novel Y544C LRP6 Mutation Decreases Canonical Wnt Signaling

LRP6 mutant effects on the canonical Wnt signaling pathway. TopFlash Reporter shows that both the Cd mutation and the Y544C mutation to the LRP6 gene decrease canonical Wnt/β Catenin signaling. Positive control was transfected with β-catenin. Negative control was a mutant TOPFlash with mutant β-catenin transfection. Asterisks indicate a significantly ($p<0.05$) down regulated Wnt signal (two-tailed t-test).

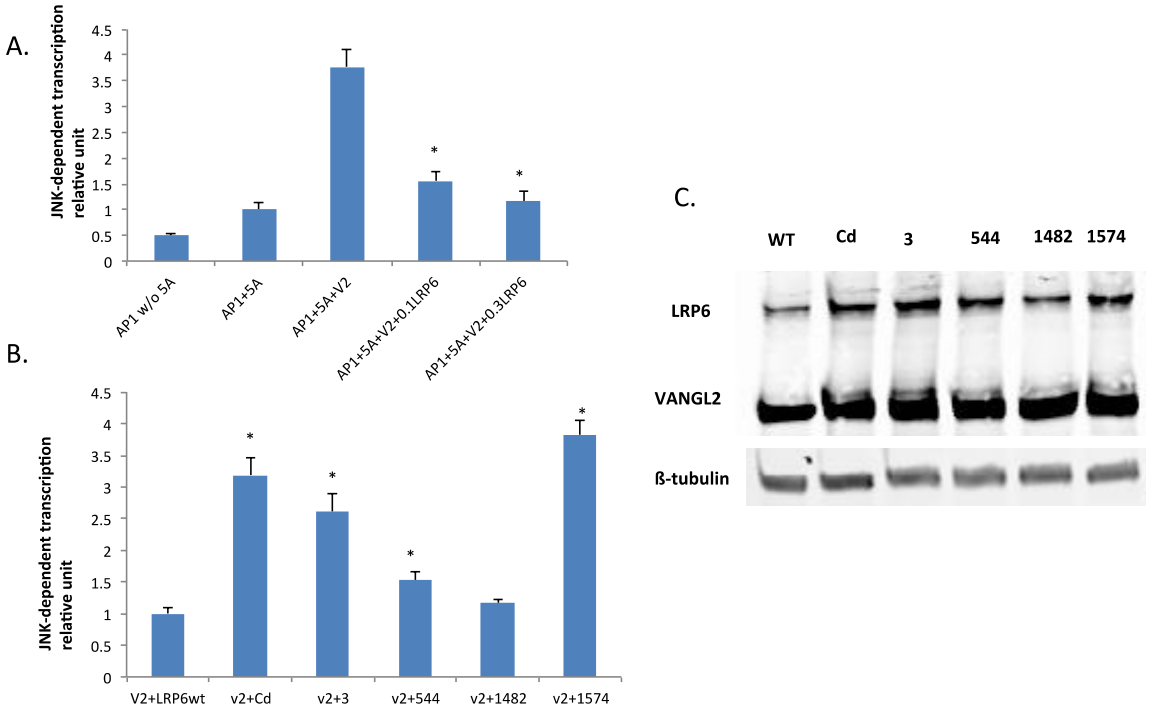

Figure 4.7 LRP6 Mutant Effects on Non-canonical Wnt Signaling Pathway

(A) JNK-AP1 activity was detected in the presence of Wnt5a. Increasing concentrations of LRP6 significantly inhibited AP1 activity in the presence of Wnt5a and VANGL2. (B) In the presence of VANGL2, LRP6 mutants (except P1482L) inhibited AP1 activity less when compared with the wildtype LRP6 construct. (C). A representative of western blot analysis showed that LRP6 and VANGL2 constructs expressed at a comparable level. (*$p<0.05$, two-tailed t-test)

4.4 DISCUSSION

Recent reports suggest that LRP6 functions not only in the canonical Wnt signaling pathway, but also in the PCP pathway (Allache et al, 2014; Gray et al, 2013), thus increasing interest in this gene with regards to its role during development and its potential relationship to developmental disorders. Links between PCP genes, cilia, and NTDs are currently a topic of considerable attention (Wallingford, 2006), making LRP6 an NTD candidate gene of interest, given its putative role in non-canonical Wnt signaling. The sequencing of the *LRP6* gene in a cohort of spina bifida patients and non-affected controls revealed 4 novel gene mutations in the patients that were not found in either the controls or in the public databases. The proximity of the Y544C mutation to the Cd mutation (Figure 4.2) in the second beta-propeller domain of the LRP6 protein indicated that Y544C may behave similarly to the already characterized Cd mutation. Indeed, it was seen that Y544C failed to bind the MESD chaperone protein, failed to properly translocate to the plasma membrane, and significantly altered Wnt signaling. The YWTD-EGF paired domains that are common to the low density lipoprotein receptor related protein family allows for the formation of the characteristic beta-propeller domains that provide this family of receptors with an extracellular binding surface for other ligands or proteins (Jeon et al, 2001). A mutation such as Y544C may alter the signature YWTD domain enough to compromise binding to other proteins. In fact, it has been previously hypothesized that this YWTD domain of LRP5/6 in the first and second β-propeller domains of the protein is necessary for the binding of MESD (Carter et al, 2005; Cheng et al, 2011). The data presented here support this hypothesis that correctly formed YWTD domains 1 and 2 of LRP6 are required for MESD binding and proper localization of LRP6 to the plasma membrane. The Y544C

mutation changes this signature YWTD domain by mutating the conserved amino acid tyrosine to cysteine. The failure to bind MESD did not allow the Cd mutation or the Y544C mutation to correctly insert into the plasma membrane or properly assist as a co-receptor in β-catenin signaling.

Not only is MESD required for the proper translocation of LRP6, it has been suggested that the protein may not even correctly fold without MESD binding (Cheng et al, 2011; Köhler et al, 2011). It has been observed using NMR spectroscopy that it is necessary for LRP6 to interface with the MESD protein for the correct formation of the beta-propellers (Köhler et al, 2011). Therefore, it would be expected that a mutation in the YWTD-EGF domain that may inhibit MESD binding can also have deleterious effects on the LRP6 protein function. The beta-propeller domains are the extracellular portions of the protein that interact with ligands and other proteins. An interruption of these crucial domains would also indicate that LRP6 would not properly function as a membrane-bound receptor in Wnt signaling. Indeed, it was observed that both the LRP6 Cd mutation and the novel Y544C mutation had a significant down-regulation in canonical Wnt signaling when compared to the wildtype protein. Interestingly, the R1574L mutant shows an increase in beta-catenin dependent signaling over the wildtype protein. This mutation changes a charged amino acid in the cytoplasmic portion of the protein to a hydrophobic amino acid. This dramatic change may increase the affinity of the intercellular binding partners of the LRP6 protein and increase the downstream effects. Additionally, the cytoplasmic tail of the LRP6 protein has been shown to be a crucial target for phosphorylation with repeats of PPPSPXS motifs (Piao et al, 2008). It is thought that these phosphorylation events govern the binding between LRP6 and its cytosolic binding partners GSK3 and Axin (Zeng et al, 2008). The

sequence surrounding the P1574L mutation is PPPTP-R-S. The similarity of the sequence surrounding this novel mutation and the canonical phosphorylation motifs may affect the phosphorylation of the LRP6 protein. The change from a charged amino acid to a small hydrophobic here may increase phosphorylation of the nearby threonine or serine residues, and then subsequently increase the Wnt/B-Catenin signaling by stabilizing complex formation.

Along with the traditional role of LRP6 in canonical Wnt signaling, the newly described role of LRP6 in PCP signaling was further explored in our experiments. Recently, LRP6 was seen to complex with disheveled-associated activator of morphogenesis 1 (DAAM1) (Gray et al, 2013). DAAM1 is a protein from the Formin family that complexes with Disheveled and activates RhoA (Gao & Chen, 2010). RhoA is a GTPase that is involved in PCP signaling and is responsible for the regulation of the actin cytoskeleton (Strutt et al, 1997). This interaction with DAAM1 gives LRP6 a potential role as part of the RhoA complex, a multi-protein interaction that takes place in the cytosol of the cell. In 2013, it was reported that the LRP6 Cd mutation actually activates PCP signaling (Gray et al, 2013). The proposed mechanism for this activation was through the cytosolic complex formed by DAAM1 and the LRP6 Cd mutation. It is logical that if this complex is formed in the cytosol and not the membrane, mutations that do not allow for LRP6 to properly locate to the membrane will also increase this complex formation and in turn, increase PCP signaling. Therefore, it was expected that the novel Y544C mutation would have an increased PCP signal, as was shown here. Unexpectedly, three of the mutations, not just the Y544C mutation, showed an increase in PCP signaling when compared to the wildtype protein. The reason for this is still unknown and needs to be further explored. It has been seen; however, that three other novel mutations in

the LRP6 gene that were found in NTD patients all expressed increased PCP signaling over the wildtype LRP6 protein (Allache et al, 2014). We further demonstrated that increasing amounts of the wildtype LRP6 protein decreased PCP signaling in a dose-dependent manner. The mutations to the LRP6 protein described here may increase the ability for the DAAM1/ Vangl2/LRP6 complex to form. It is also possible that they may make LRP6 less efficient at inhibiting Wnt5a stimulated PCP signaling. Interestingly, the mutation, P1482L, which was predicted to be tolerated by SIFT and benign by PolyPhen, mimics the response of the wildtype protein. This mutation, substituting a small hydrophobic amino acid for a different small hydrophobic amino acid falls in the cytoplasmic tail portion of the LRP6 protein. It is unsurprising that this mutation acts no differently than the wildtype LRP6 protein. The A3V mutation changed a conserved residue in the signal peptide region of LRP6. This novel mutation was seen to increase PCP signaling but, it did not change canonical Wnt signaling. It has previously been reported that the N-terminal of the LRP6 protein is not required for β-catenin dependent Wnt signaling to occur (Brennan et al, 2004; Tamai et al, 2004), therefore explaining that there is no significant change in canonical Wnt signaling for this mutation. The dysregulation that is seen in PCP signaling with this mutation however, underscores the putative participation of LRP6 in PCP signaling and neurulation as well. In any case, the fact that all of the LRP6 mutant proteins thus far examined in connection with NTD in mouse and man alter flux through the Wnt/PCP pathway while reducing (Y544C), leaving unchanged (A3V) or enhancing (R1547L) the canonical pathway, suggests that PCP signaling is the Wnt function most critical to successful neurulation.

Even with the existence of three different mouse models of the Lrp6 gene, and over 240 NTD mouse models (Harris & Juriloff, 2010), it has proven a challenge to relate these mouse models to those NTD cases found in the human population. Here, it was shown that the novel mutation to LRP6, Y544C, mimics the mouse Cd mutation by failing to properly bind to the chaperone protein MESD. The effects of this abrogated binding are similarly seen in both the Y544C mutant and also the Cd mutant; these mutant forms of the protein fail to insert into the plasma membrane and in turn decrease canonical Wnt signaling. This data highlights the translational importance of the folate-responsive LRP6 Cd mouse model by relating it to a relevant mutation found in the human population. Additionally, the three other novel mutations presented all properly bind the chaperone protein MESD and conduct proper canonical Wnt signaling, yet two of these mutations are seen to disregulate PCP signaling. This finding reiterates the yet unknown role of LRP6 in both canonical and non-canonical Wnt signaling, thereby reinforcing and expanding the essential role that LRP6 plays during development and neural tube closure. Both the novel genetic findings described here, along with their initial molecular characterization, being to open new avenues for the investigation into the complex etiology of NTDs and the role that the complexity of human genetics may play in this.

Chapter 5 Future Directions and Conclusions

5.1 Future Directions

The studies presented here are only fraction of the larger puzzle of the complex etiology of NTDs. The high-throughput assay along with its first application in presented in Chapter 2, provides a useful tool to approach many unanswered questions. The gene study presented in Chapter 4 further delved into the new idea that LRP6 could not only be associated with canonical Wnt signaling, but also PCP signaling. This newly explored role of the LRP6 protein emphasizes its importance during development, and also expands upon the already known LRP6 Cd mouse model as an NTD mouse model.

5.1.1 Adaptation Chemical N-Homocysteinylation Assay to Histological Marker

My work involved studying the chemistry of an aldehyde based aminothiol reaction as a marker of N-homocysteinylation events. The large availability of streptavidin tagged probes allows for an array of markers to further increase the versatility this assay. Slides with paraffin embedded tissue sections could easily withstand the pH of 3 that is required for this reaction. Because this is an irreversible reaction, a second stain could be used to identify a second marker, such as a specific protein antibody. Studies like this would be especially valuable for investigations of plaque formation, hard protein clusters that have been hypothesized to form secondary to N-homocysteinylation events. A simple hematoxylin and eosin stain could identify protein plaques and an N-

homocysteinylation stain could determine if these two were localized to the same area. This double staining could also identify if protein N-homocysteinylation was located in the same area as proteins of interest or even cell death through TUNEL staining.

5.1.2 Functional analysis of target N-homocysteinylated proteins

In addition to histological staining, key proteins of interest can be tested for modification and functionality in a cell culture modeling system. For example, the upregulation of folate receptors by folate starvation with an increased methionine media will target these key one-carbon metabolism proteins. Stimulation of the PCP pathway with a known Wnt ligand, while growth is occurring in an increased methionine media, will target proteins involved in the PCP pathway. These lysates can be enriched with an aldehyde solid state and modifications confirmed by mass spectrometry. In tandem, functional assays can be performed in cell culture to determine if the increased homocysteinylation will adversely affect protein function. Cell surface folate receptor binding assays and AP1 luciferase assays can be used to determine if N-homocysteinylation (confirmed by mass spectrometry) affects the function of these key proteins.

5.1.3 Increased Investigation into LRP6 and PCP signaling

The complexity of PCP signaling often leads to more questions than answers when a new observation is made. The recent studies that involve LRP6 in not only

canonical Wnt signaling, but also PCP signaling (Allache et al, 2014) (Gray et al, 2013) beg for further research to be conducted in order to determine the exact role that LRP6 may play. One of the first studies that would greatly help support the model proposed by Gray et al (Gray et al, 2013) that LRP6 can serve to help PCP signaling inside the cytosol through complexing with other proteins, would be to further explore this complex in relation to LRP6 mutants. The various point mutations found in the NTD patients presented here and in the paper by Allache et al (Allache et al, 2014) could be transfected into cells along with DAAM1, Dishevelled, and Vangl2. It would be hypothesized that the binding of these proteins to the various LRP6 constructs may increase in strength over the wildtype protein (measured by multiple co-immunoprecipitations). Various endpoints of the PCP pathway could also be probed, such as RhoA-GTP formation. In this study, only the AP1 reporter data was presented, but this is an endpoint reporter, and there are many unknowns concerning the role of LRP6 and AP1 based transcription.

5.2 Concluding Remarks

The studies presented in this document provide more tools and more information in the exploration of the multi-factorial origin of NTDs. NTDs are a global health problem affecting more than 300,000 babies each year worldwide. Many mysteries remain around the origin of these defects. In this document, only a small sampling of possible causes of NTDs were highlighted and explored. In Chapter 2, a new method of high throughput determination of N-homocysteinylation

was presented. This method was proved to be robust and accurate, will be useful not only in researching how hyperhomocysteinemia may be related to NTDs, but also its relationship to many other disease states. The first application of this method to a large set of biological samples was then presented in Chapter 3. The ease of which this assay was used for a large amount of samples has great potential to solve many of the mechanistic questions that remain regarding the link between high homocysteine levels and a number of disease states. Finally, a single gene of interest was explored and a novel human mutation was related to the LRP6 Cd mutant mouse that had been one of the subjects of earlier studies.

The data presented here represent both a broadening and a focusing of our knowledge. The availability of an easy and inexpensive way to determine N-homocysteinylation has the ability to solve many mysteries that remain in the field of one-carbon metabolism. The first application of this assay emphasized the importance of maternal diet and embryonic genetics on developmental outcomes. It also revealed the early age at which the inverse relationship between folate and homocysteine is established, once more underscoring the weight of properly regulated one carbon metabolism. Continued research using the assay presented here will allow for continued analysis of the suspected effects of protein N-homocysteinylation in maternal and embryonic samples. It is essential to determine if N-homocysteinylation plays a role in embryonic outcomes either based on maternal effects, embryonic effects, or both. The further exploration of one of the

genes used in the mouse study, LRP6, revealed four novel mutations in a human population of spina bifida patients. One of these human mutations was subsequently shown to mechanistically mimic the LRP6 Cd mouse mutation, expanding the possibilities for use of this mouse model. The human studies presented also highlight the newly discovered role for the LRP6 protein in PCP signaling, and the many questions that remain unanswered in how LRP6 functions in this second role. This body of work provided insight and tools for the further investigation into a group of congenital defects, the etiology of which has perplexed researchers for decades.

Appendix 1. Full Data Table from Chapter 3

Embryo Genotype	Diet	Embryo Folate	Embryo N-Hcy	somites	Dam Number	Dam Folate	Dam N-Hcy
1	1	32.95790816	0.008933673	22	651	9556	9.88
1	1	12.36922388	0.0040534	21	651	9556	9.88
1	1	8.814571195	0.00272849	19	651	9556	9.88
1	1	6.350255544	0.001428451	19	651	9556	9.88
1	1	2.471523862	0.001893011	18	651	9556	9.88
1	1	7.015552941	0.003349093	23	651	9556	9.88
1	1	8.459156281	0.003009324	21	651	9556	9.88
1	1	8.038015087	0.002299418	20	651	9556	9.88
1	1	3.957256077	0.002591581	24	651	9556	9.88
1	1	18.62747525	0.007532266	23	651	9556	9.88
1	1	10.32242748	0.002998185	24	480	6257	12.4
1	1	7.434664263	0.001644038	23	480	6257	12.4
1	1	12.08652822	0.00353538	22	480	6257	12.4
1	1	21.00422081	0.013700202	22	778	16261	11.46
1	1	42.481266	0.022151478	18	778	16261	11.46
1	1	103.0928762	0.032979487	19	778	16261	11.46
1	1	42.32934233	0.020049361	20	778	16261	11.46
1	1	13.57201083	0.007620205	21	778	16261	11.46
1	2	1.581535861	0.004112766	27	778	16261	11.46
1	2	5.294150754	0.004007794	25	778	16261	11.46
1	2	3.290319469	0.00389066	24	778	16261	11.46
1	2	2.796190222	0.003824769	25	778	16261	11.46
1	2	1.190373479	0.006712609	20	784	62239	6.02
1	2	0.658044898	0.004019368	19	784	62239	6.02
1	2	1.69826412	0.003750398	19	784	62239	6.02
1	2	0.548580907	0.004179589	30	784	62239	6.02
1	2	10.89022841	0.004815181	20	779	24297	13.61
1	2	15.32926829	0.017412602	20	779	24297	13.61
1	2	9.879272289	0.003449603	20	779	24297	13.61
1	2	9.415062838	0.003558307	20	779	24297	13.61
1	2	17.75640509	0.003868894	17	486	23909	14.15
1	2	12.78586266	0.003294814	15	486	23909	14.15
1	2	18.37802908	0.003700985	18	486	23909	14.15
1	2	6.610419864	0.002405245	20	486	23909	14.15
1	2	5.308520457	0.003915352	22	486	23909	14.15
1	2	10.57397541	0.011443989	20	486	23909	14.15
1	2	0.126078297	9.99806E-05	21	792	15585	12.7
1	2	261.1720996	0.082277176	18	792	15585	12.7
1	2	114.0596971	0.055647598	20	792	15585	12.7
1	2	56.80780586	0.022429236	20	792	15585	12.7
1	3	17.83397078	0.007579022	20	506	24297	13.61
1	3	27.45802886	0.004642217	20	506	24297	13.61
1	3	22.45391401	0.003142626	19	506	24297	13.61
1	3	32.37880193	0.005540608	21	506	24297	13.61

1	3	31.16174977	0.006046396	20	506	24297	13.61
1	3	21.69632353	0.00852451	21	506	24297	13.61
1	3	10.70112665	0.003675612	23	506	24297	13.61
1	3	5.121992715	0.004575003	24	506	24297	13.61
1	3	5.766869935	0.005394901	22	506	24297	13.61
1	3	5.447707182	0.005189234	21	506	24297	13.61
1	3	34.06359274	0.007056009	19	506	24297	13.61
1	3	41.59188456	0.005878315	20	506	24297	13.61
1	3	26.89033652	0.008166841	22	506	24297	13.61
1	3	8.231680869	0.003280575	21	776	75345	8.13
1	3	21.64395257	0.004810032	20	776	75345	8.13
1	3	5.727353709	0.003548798	17	776	75345	8.13
1	3	12.76315133	0.006863531	16	776	75345	8.13
1	3	22.47255736	0.005572576	20	776	75345	8.13
1	3	46.51328125	0.010107639	20	776	75345	8.13
1	3	3.785598385	0.003746165	20	776	75345	8.13
1	3	2.00632173	0.002407586	22	776	75345	8.13
1	3	41.86975	0.010538333	22	776	75345	8.13
1	3	84.1755505	0.028606102	21	840	5361	11.47
1	3	47.63977273	0.016535985	22	871	9556	12.25
1	3	43.72213542	0.012123264	21	871	9556	12.25
1	3	36.04877049	0.009506831	20	871	9556	12.25
1	3	2.139033451	0.007047561	24	871	9556	12.25
1	3	1.242486563	0.008994079	23	871	9556	12.25
1	3	2.853241229	0.009123898	22	871	9556	12.25
1	3	37.36527778	0.016368056	17	834	11904	8.5
1	3	1.549099988	0.006025508	22	834	11904	8.5
2	1	6.03580441	0.003287098	19	834	11904	8.5
2	1	4.213706869	0.003785448	23	834	11904	8.5
2	1	5.42052921	0.004311384	20	834	11904	8.5
2	1	9.369443756	0.003317015	21	834	11904	8.5
2	1	3.440453384	0.001416618	19	834	11904	8.5
2	1	7.11121856	0.001299563	18	834	11904	8.5
2	1	5.801816571	0.001742627	19	834	11904	8.5
2	1	4.537943803	0.002719282	24	834	11904	8.5
2	1	9.759541725	0.002860589	20	802	12376.7	13.57
2	1	7.257687924	0.002418746	22	802	12376.7	13.57
2	1	7.410007191	0.001939727	23	802	12376.7	13.57
2	1	6.73262844	0.002166875	22	802	12376.7	13.57
2	1	233.4961044	0.05885342	20	802	12376.7	13.57
2	1	24.03	0.007715873	20	802	12376.7	13.57
2	1	21.78349057	0.007907233	22	802	12376.7	13.57
2	1	37.71425439	0.011479532	21	860	11733	11.03
2	1	0.218761037	5.52251E-05	20	860	11733	11.03
2	1	65.20992647	0.022904412	23	860	11733	11.03

2	1	32.53071591	0.012686004	18	860	11733	11.03
2	2	2.230786839	0.004369027	27	861	25422	13.47
2	2	2.214763587	0.00629364	19	861	25422	13.47
2	2	1.867919521	0.005448284	22	861	25422	13.47
2	2	1.746508677	0.004750642	20	861	25422	13.47
2	2	2.50366452	0.003116591	29	861	25422	13.47
2	2	17.32678965	0.006734516	21	895	8970	9.41
2	2	8.415256685	0.00422356	20	895	8970	9.41
2	2	14.45204551	0.005603921	19	895	8970	9.41
2	2	87.02714286	0.011795238	18	895	8970	9.41
2	2	45.20176967	0.005921574	16	818	11882	10.25
2	2	13.53035434	0.003585949	19	818	11882	10.25
2	2	6.526875499	0.003618217	18	818	11882	10.25
2	2	9.440671346	0.002639961	18	880	11882	10.25
2	2	4.564827883	0.001823365	20	880	11882	10.25
2	2	0.133601295	6.87398E-05	20	880	11882	10.25
2	2	13.39824561	0.012276316	20	880	11882	10.25
2	2	0.084622624	9.06687E-05	22	880	11882	10.25
2	2	0.135119051	5.66026E-05	20	880	11882	10.25
2	3	38.04205052	0.008458003	22	880	11882	10.25
2	3	21.07394796	0.004261503	20	880	11882	10.25
2	3	6.560409032	0.00365063	20	875	12897	14.01
2	3	9.837807633	0.004491347	25	875	12897	14.01
2	3	5.258153726	0.005405118	22	875	12897	14.01
2	3	30.37733953	0.00504227	18	785	17517	14.57
2	3	10.12218407	0.002994855	20	785	17517	14.57
2	3	11.71162183	0.003180342	20	785	17517	14.57
2	3	57.15903614	0.012449799	20	785	17517	14.57
2	3	42.73910891	0.008783828	15	785	17517	14.57
2	3	62.48645833	0.013569444	21	785	17517	14.57
2	3	-5.457045219	-0.001606554	20	785	17517	14.57
2	3	38.60898058	0.01321521	20	785	17517	14.57
2	3	36.7697619	0.008942857	19	785	17517	14.57
2	3	22.94711049	0.010663458	21	785	17517	14.57
2	3	1.156708613	0.007659011	20	649	16021	15.34
3	1	6.280502467	0.003514177	17	649	16021	15.34
3	1	4.927958203	0.004739719	22	649	16021	15.34
3	1	6.898455692	0.004085878	18	649	16021	15.34
3	1	6.069358082	0.002157864	20	828	10614	9.74
3	1	9.355722473	0.001816182	19	828	10614	9.74
3	1	7.335639549	0.001750989	20	828	10614	9.74
3	1	5.819727892	0.001285732	19	828	10614	9.74
3	1	2.282474919	0.00166226	20	828	10614	9.74
3	1	4.840437077	0.003200307	21	828	10614	9.74
3	1	3.7841563	0.00313972	18	828	10614	9.74

3	1	3.54682593	0.002568615	20	828	10614	9.74
3	1	10.05165133	0.003429547	22	777	10993	13.52
3	1	5.242203321	0.001789603	22	777	10993	13.52
3	1	28.44811321	0.007693396	21	777	10993	13.52
3	1	0.826748901	0.000411445	16	777	10993	13.52
3	1	0.21596018	6.1535E-05	19	777	10993	13.52
3	1	0.157114013	4.07294E-05	20	777	10993	13.52
3	1	0.248302568	6.94249E-05	15	777	10993	13.52
3	1	22.80672309	0.0117178	22	777	10993	13.52
3	1	78.728125	0.022203125	20	777	10993	13.52
3	1	38.69636168	0.028416602	20	777	10993	13.52
3	1	5.438084261	0.00637068	19	805	12093	8.78
3	2	2.591772834	0.006021217	28	805	12093	8.78
3	2	2.03478688	0.003709399	21	805	12093	8.78
3	2	1.824659919	0.005875662	15	805	12093	8.78
3	2	1.287645142	0.005059464	17	805	12093	8.78
3	2	13.15286458	0.034984375	18	805	12093	8.78
3	2	2.001993666	0.003145375	28	805	12093	8.78
3	2	1.628888336	0.003259388	31	823	14556	10.1
3	2	2.621517862	0.00369575	26	823	14556	10.1
3	2	1.943106364	0.004061447	28	823	14556	10.1
3	2	17.06284887	0.005187972	14	823	14556	10.1
3	2	45.09140972	0.015542926	14	823	14556	10.1
3	2	17.55067532	0.004337582	10	823	14556	10.1
3	2	5.826102072	0.00195339	24	661	5961	12.68
3	2	5.964934316	0.002068938	20	661	5961	12.68
3	2	10.55162552	0.002484765	22	661	5961	12.68
3	2	0.178304407	8.81332E-05	18	661	5961	12.68
3	2	0.063500959	5.08537E-05	22	661	5961	12.68
3	2	0.092919175	6.69048E-05	22	781	11054	13.1
3	2	180.818	0.06218	20	781	11054	13.1
3	2	14.86206022	0.012775997	21	781	11054	13.1
3	3	5.126965456	0.00317183	15	781	11054	13.1
3	3	49.60243014	0.007993964	19	781	11054	13.1
3	3	17.49355845	0.004205645	19	781	11054	13.1
3	3	7.358479112	0.003943376	22	781	11054	13.1
3	3	4.730084858	0.005083482	18	833	31995	15.9
3	3	24.63253983	0.003446882	17	833	31995	15.9
3	3	15.61619735	0.003947379	21	758	11708	12.85
3	3	34.23960177	0.011786136	21	774	12861	12.8
3	3	11.8106089	0.003775856	20	774	12861	12.8
3	3	11.59589393	0.004117592	15	774	12861	12.8
3	3	7.933406892	0.002805065	20	774	12861	12.8
3	3	4.329588899	0.002066652	17	840	5361	11.47
3	3	3.310829077	0.002159759	20	840	5361	11.47

3	3	7.649152488	0.002781664	16	840	5361	11.47
3	3	20.42470288	0.003980463	10	840	5361	11.47
3	3	4.74331392	0.002983888	22	857	21029	13.21
3	3	61.16458333	0.012229167	16	857	21029	13.21
3	3	0.15911011	6.14633E-05	21	857	21029	13.21
3	3	33.47522124	0.013685841	22	857	21029	13.21
3	3	39.72916667	0.010008681	16	857	21029	13.21
3	3	23.58341584	0.01090264	20	857	21029	13.21
3	3	2.110279777	0.0082472	20	857	21029	13.21
4	1	17.64497795	0.004529728	27	857	21029	13.21
4	1	2.853801707	0.003460575	22	839	6598	8.44
4	1	8.61173003	0.003429343	20	839	6598	8.44
4	1	5.965279311	0.003820731	20	839	6598	8.44
4	1	8.396199352	0.003702015	21	839	6598	8.44
4	1	5.534048272	0.005252998	19	839	6598	8.44
4	1	4.781877435	0.001439257	18	839	6598	8.44
4	1	11.35649029	0.001512559	21	839	6598	8.44
4	1	90.93548387	0.012153226	22	832	76404	9.08
4	1	1.973931823	0.001454319	21	832	76404	9.08
4	1	9.792255059	0.005686637	22	832	76404	9.08
4	1	34.01881426	0.01087381	20	832	76404	9.08
4	1	4.690793298	0.00300235	18	832	76404	9.08
4	1	5.648597939	0.002261097	21	832	76404	9.08
4	1	10.26429446	0.003556106	20	832	76404	9.08
4	1	5.084989373	0.002060842	24	832	76404	9.08
4	1	2.829227038	0.001837561	22	832	76404	9.08
4	1	4.703687381	0.001882345	20	832	76404	9.08
4	1	9.23555163	0.003160457	20	832	76404	9.08
4	1	22.82124125	0.005136037	21	832	76404	9.08
4	1	32.66443856	0.011458156	19	801	6733	12.42
4	1	0.096493698	4.70594E-05	20	801	6733	12.42
4	1	1.153833795	0.000386999	20	801	6733	12.42
4	1	976.2018627	0.376729116	10	801	6733	12.42
4	1	23.28699053	0.024265322	20	801	6733	12.42
4	1	7.920544554	0.017876238	21	868	11733	11.6
4	2	2.172183066	0.004231628	27	868	11733	11.6
4	2	1.420053015	0.00448163	26	868	11733	11.6
4	2	50.33070652	0.006655797	20	868	11733	11.6
4	2	0.978838448	0.003329609	29	868	11733	11.6
4	2	0.736942881	0.002465576	30	868	11733	11.6
4	2	1.5940675	0.003168442	31	868	11733	11.6
4	2	10.87771017	0.004016114	20	868	11733	11.6
4	2	7.964168268	0.002600459	21	827	17169	12.3
4	2	7.041829058	0.00245808	23	827	17169	12.3
4	2	22.22883065	0.014020161	21	827	17169	12.3

4	2	10.43319565	0.004726453	17	827	17169	12.3
4	2	4.014365569	0.002373439	16	827	17169	12.3
4	2	7.849478818	0.002840935	20	827	17169	12.3
4	2	2.62598049	0.001036716	22	827	17169	12.3
4	2	0.082926904	5.84808E-05	23	827	17169	12.3
4	2	54.73559289	0.021995589	20	827	17169	12.3
4	2	53.32394737	0.012931579	18	827	17169	12.3
4	2	28.17330581	0.012993648	20	827	17169	12.3
4	2	22.47852142	0.019226921	21	827	17169	12.3
4	2	79.18956647	0.027166171	22	827	17169	12.3
4	2	43.74860646	0.017430916	15	827	17169	12.3
4	3	25.92590009	0.0064354	22	846	43775	13.82
4	3	7.163718441	0.004990472	17	846	43775	13.82
4	3	39.135	0.01196	20	846	43775	13.82
4	3	5.700376024	0.003648672	17	846	43775	13.82
4	3	31.84542477	0.007590968	18	846	43775	13.82
4	3	84.03998961	0.017035106	18	846	43775	13.82
4	3	16.71702611	0.003725829	18	846	43775	13.82
4	3	22.42281265	0.004849884	21	846	43775	13.82
4	3	30.23724949	0.005387463	19	846	43775	13.82
4	3	12.19664055	0.003767782	16	846	43775	13.82
4	3	16.68224224	0.00519212	18	846	43775	13.82
4	3	9.091683368	0.004166639	21	794	89080	12.6
4	3	133.4057664	0.028462208	22	794	89080	12.6
4	3	10.86507153	0.004999126	23	794	89080	12.6
4	3	7.507493917	0.00236318	18	794	89080	12.6
4	3	39.8255618	0.012325843	22	794	89080	12.6
4	3	0.05072992	5.04955E-05	20	794	89080	12.6
4	3	39.40324074	0.01320216	22	794	89080	12.6
4	3	619.125	0.238966667	23	794	89080	12.6
4	3	3.34163264	0.0100559	23	794	89080	12.6
4	3	3.363517373	0.007617838	25	794	89080	12.6
4	3	1.387796382	0.006024182	20	794	89080	12.6

Raw data tables from each of the embryos collected and analyzed for this project. The dam information for each embryo is next to the appropriate embryo. The diets are 1 (10ppm folic acid), 2 (2ppm folic acid), and 3 (1% methionine). The genotypes are 1(Folr1 +/+;Lrp6 Cd +/+), 2(Folr1 +/-; Lrp6 Cd +/+), 3(Folr1 /-;Lrp6 Cd +/-), and 4 (Folr1 +/+;Lrp6 +/-).

Appendix 2. List of Abbreviations

10-FTHF	10-formyltetrahydrofolate
5,10-MTHF	,10-methylenetetrahydrofolate
5-MTHF	5-methyltetrahydrofolate
AICART	Aminoimidazolecarboxamide Ribonucleotide Transferase
APC	Adenomatous Polyposis Coli
BLH	Bleomycin Hydrolase
BSA	Bovine Serum Albumin
CBS	Cystathionine Beta-Synthase
Cd	Crooked Tail (Lrp6 mouse point mutant)
CNS	Central Nervous System
CSE	Cystationine Gamma-Lyase
DAAM1	Disheveled-Associated Activator of Morphogenesis 1
DAG	1,2 Diacylglycerol
DAPI	4',6-diamidino-2-phenylindole
DHF	Dihydrofolate
DHFR	Dihydrofolate Reductase
DMEM	Dulbecco's Modified Eagle Medium
DMEM/F12	Dulbecco's Modified Eagle Medium : Nutrient Mix F12
dTMP	Deoxythymidine Monophosphate
dUMP	Deoxyuridine Monophosphate
ED	Embryonic Day
FA-HRP	Folic Acid-Horse Radish Peroxidase
FBP	Folate Bovine Protein
FBS	Fetal Bovine Serum
Folr1	Folate Receptor 1
FR	Folate Receptor
GART	Glycinamide Ribonucleotide Transformylase
GFP	Green Fluorescent Protein
GPI	Glycophosphatidylinositol
GSK3	Glycogen Synthase Kinase 3
HTl	Homocysteine Thiolactone
IP3	inositol 1,4,5-tri-phosphate
IRB	Institutional Review Board
JNK	c-JUN N-Terminal Kinase
LB	Luria Broth

Lrp6	Low-Density Lipoprotein like Receptor Protein 6
MANOVA	Multivariate Analysis of Varience
MAT	Methionine Adenyltransferase
MEM	Minimum Essential Media
MESD	Mesoderm Development Protein
MS	Methionine Synthase
MS/MS	Tandem Mass Spectrometry
MT	Methyltransferase
MTHFD	Methylenetetrahydrofolate Dehydrogenase
MTHFR	Methylene tetrahydrofolate reductase
MTX	Methotrexate
NaOH	Sodium Hydroxide
NTD	Neural Tube Defects
PBS	Phosphate Buffered Saline
PBS-T	Phosphate Buffered Saline with 0.1% Tween
PCFT	Proton Coupled Folate Carrier
PCP	Planar Cell Polarity
PCR	Polymerase Chain Reaction
PKC	Protein Kinase C
PLC	phospholipase C
PON1	Paroxonase 1
PTM	Post Translational Modification
RAC1	Ras-Related C3 Botulinum Toxin Substrate 1
RFC	Reduced Folate Carrier
RHO-A	Ras Homolog Gene Family, Member A
RIPA	Radio Immunoprecipitation Assay
ROR	Receptor Tyrosine Kinase-like Orphan Receptors
SAH	S-Adenosyl Homocysteine
SAHH	S-Adenosyl Homocysteine Hydrolase
SAM	S-Adenosyl Methionine
SNP	Single Nucleotide Polymorphism
TBS	Tris-Buffered Saline
TBS-T	Tris-Buffered Saline with 0.1% Tween
TCEP	tris (2-carboxyethyl)phosphine
THF	Tetrahydrofolate

TS	Thymidylate Synthase
VANGL	Van Gough Like
VPA	Valproic Acid
β-Cat	Beta Catenin

References

A.S. G, B.S. P (1996) *The Complement System*, 4 edn.

Aderem A, Ulevitch RJ (2000) Toll-like receptors in the induction of the innate immune response. *Nature* **406:** 782-787

Alexander RP, Fang G, Rozowsky J, Snyder M, Gerstein MB (2010) Annotating non-coding regions of the genome. *Nat Rev Genet* **11:** 559-571

Allache R, Lachance S, Guyot MC, De Marco P, Merello E, Justice MJ, Capra V, Kibar Z (2014) Novel mutations in Lrp6 orthologs in mouse and human neural tube defects affect a highly dosage-sensitive Wnt non-canonical planar cell polarity pathway. *Hum Mol Genet* **23:** 1687-1699

Amorim MR, Lima MA, Castilla EE, Orioli IM (2007) Non-Latin European descent could be a requirement for association of NTDs and MTHFR variant 677C > T: a meta-analysis. *Am J Med Genet A* **143A:** 1726-1732

Anderson OS, Sant KE, Dolinoy DC (2012) Nutrition and epigenetics: an interplay of dietary methyl donors, one-carbon metabolism and DNA methylation. *The Journal of nutritional biochemistry* **23:** 853-859

Ansari NA, Moinuddin, Ali R (2011) Glycated lysine residues: a marker for non-enzymatic protein glycation in age-related diseases. *Disease markers* **30:** 317-324

Antony AC (1996) Folate receptors. *Annu Rev Nutr* **16:** 501-521

Appling DR (1991) Compartmentation of folate-mediated one-carbon metabolism in eukaryotes. *FASEB J* **5:** 2645-2651

Au KS, Ashley-Koch A, Northrup H (2010) Epidemiologic and genetic aspects of spina bifida and other neural tube defects. *Dev Disabil Res Rev* **16:** 6-15

Bailey LB (1995) *Folate in Health and Disease*, New York, NY: Marcel Dekker, Inc.

Bard JL, Kaufman MH, Dubreuil C, Brune RM, Burger A, Baldock RA, Davidson DR (1998) An internet-accessible database of mouse developmental anatomy based on a systematic nomenclature. *Mech Dev* **74:** 111-120

Bejsovec A (2013) Wingless/Wnt signaling in Drosophila: the pattern and the pathway. *Mol Reprod Dev* **80:** 882-894

Beltowski J, Jamroz-Wiśniewska A, Borkowska E, Wójcicka G (2005) Differential effect of antioxidant treatment on plasma and tissue paraoxonase activity in hyperleptinemic rats. *Pharmacol Res* **51:** 523-532

Bennett GD, Mohl VK, Finnell RH (1990) Embryonic and maternal heat shock responses to a teratogenic hyperthermic insult. *Reprod Toxicol* **4:** 113-119

Bharathselvi M, Biswas J, Selvi R, Coral K, Narayanasamy A, Ramakrishnan S, Sulochana KN (2013) Increased homocysteine, homocysteine-thiolactone, protein homocysteinylation and oxidative stress in the circulation of patients with Eales' disease. *Ann Clin Biochem* **50:** 330-338

Boshnjaku V, Shim KW, Tsurubuchi T, Ichi S, Szany EV, Xi G, Mania-Farnell B, McLone DG, Tomita T, Mayanil CS (2012) Nuclear localization of folate receptor alpha: a new role as a transcription factor. *Sci Rep* **2:** 980

Bossenmeyer-Pourié C, Pourié G, Koziel V, Helle D, Jeannesson E, Guéant JL, Beck B (2013) Early methyl donor deficiency produces severe gastritis in mothers and offspring through N-homocysteinylation of cytoskeleton proteins, cellular stress, and inflammation. *FASEB J* **27:** 2185-2197

Botto LD, Moore CA, Khoury MJ, Erickson JD (1999) Neural-tube defects. *N Engl J Med* **341:** 1509-1519

Bozard BR, Ganapathy PS, Duplantier J, Mysona B, Ha Y, Roon P, Smith R, Goldman ID, Prasad P, Martin PM, Ganapathy V, Smith SB (2010) Molecular and biochemical characterization of folate transport proteins in retinal Müller cells. *Invest Ophthalmol Vis Sci* **51:** 3226-3235

Bradford MM (1976) A rapid and sensitive method for the quantitation of microgram quantities of protein utilizing the principle of protein-dye binding. *Anal Biochem* **72:** 248-254

Brender JD, Suarez L, Felkner M, Gilani Z, Stinchcomb D, Moody K, Henry J, Hendricks K (2006) Maternal exposure to arsenic, cadmium, lead, and mercury and neural tube defects in offspring. *Environ Res* **101:** 132-139

Brennan K, Gonzalez-Sancho JM, Castelo-Soccio LA, Howe LR, Brown AM (2004) Truncated mutants of the putative Wnt receptor LRP6/Arrow can stabilize beta-catenin independently of Frizzled proteins. *Oncogene* **23:** 4873-4884

Brown SD, Twells RC, Hey PJ, Cox RD, Levy ER, Soderman AR, Metzker ML, Caskey CT, Todd JA, Hess JF (1998) Isolation and characterization of LRP6, a novel member of the low density lipoprotein receptor gene family. *Biochem Biophys Res Commun* **248:** 879-888

Bruschi M, Santucci L, Candiano G, Ghiggeri GM (2013) Albumin heterogeneity in low-abundance fluids. The case of urine and cerebro-spinal fluid. *Biochimica et biophysica acta* **1830:** 5503-5508

Bryja V, Andersson ER, Schambony A, Esner M, Bryjová L, Biris KK, Hall AC, Kraft B, Cajanek L, Yamaguchi TP, Buckingham M, Arenas E (2009) The extracellular domain of Lrp5/6 inhibits noncanonical Wnt signaling in vivo. *Mol Biol Cell* **20:** 924-936

Burren KA, Mills K, Copp AJ, Greene ND (2006) Quantitative analysis of s-adenosylmethionine and s-adenosylhomocysteine in neurulation-stage mouse embryos by liquid chromatography tandem mass spectrometry. *Journal of chromatography B, Analytical technologies in the biomedical and life sciences* **844:** 112-118

Burren KA, Savery D, Massa V, Kok RM, Scott JM, Blom HJ, Copp AJ, Greene ND (2008) Gene-environment interactions in the causation of neural tube defects: folate deficiency increases susceptibility conferred by loss of Pax3 function. *Hum Mol Genet* **17:** 3675-3685

Cabaton NJ, Canlet C, Wadia PR, Tremblay-Franco M, Gautier R, Molina J, Sonnenschein C, Cravedi JP, Rubin BS, Soto AM, Zalko D (2013) Effects of low doses of bisphenol A on the metabolome of perinatally exposed CD-1 mice. *Environ Health Perspect* **121:** 586-593

Cabrera RM, Shaw GM, Ballard JL, Carmichael SL, Yang W, Lammer EJ, Finnell RH (2008) Autoantibodies to folate receptor during pregnancy and neural tube defect risk. *J Reprod Immunol* **79:** 85-92

Cadigan KM, Nusse R (1997) Wnt signaling: a common theme in animal development. *Genes Dev* **11:** 3286-3305

Carter M, Chen X, Slowinska B, Minnerath S, Glickstein S, Shi L, Campagne F, Weinstein H, Ross ME (2005) Crooked tail (Cd) model of human folate-responsive neural tube defects is mutated in Wnt coreceptor lipoprotein receptor-related protein 6. *Proc Natl Acad Sci U S A* **102:** 12843-12848

Carter M, Ulrich S, Oofuji Y, Williams DA, Ross ME (1999) Crooked tail (Cd) models human folate-responsive neural tube defects. *Hum Mol Genet* **8:** 2199-2204

Carter WG (2012) Detection and Quantification of Protein Post-Translational Modifications Using Novel Microchannel Plate Autoradiographic Imagers. *Med Chem* **11**

Challet E, Dumont S, Mehdi MK, Allemann C, Bousser T, Gourmelen S, Sage-Ciocca D, Hicks D, Pévet P, Claustrat B (2013) Aging-like circadian disturbances in folate-deficient mice. *Neurobiol Aging* **34:** 1589-1598

Chan J, Natekar A, Koren G (2014) Hot yoga and pregnancy: fitness and hyperthermia. *Can Fam Physician* **60:** 41-42

Chen WT, Mahmood U, Weissleder R, Tung CH (2005) Arthritis imaging using a near-infrared fluorescence folate-targeted probe. *Arthritis Res Ther* **7:** R310-317

Chen Z, Karaplis AC, Ackerman SL, Pogribny IP, Melnyk S, Lussier-Cacan S, Chen MF, Pai A, John SW, Smith RS, Bottiglieri T, Bagley P, Selhub J, Rudnicki MA, James SJ, Rozen R (2001) Mice deficient in methylenetetrahydrofolate reductase exhibit hyperhomocysteinemia and decreased methylation capacity, with neuropathology and aortic lipid deposition. *Hum Mol Genet* **10:** 433-443

Cheng Z, Biechele T, Wei Z, Morrone S, Moon RT, Wang L, Xu W (2011) Crystal structures of the extracellular domain of LRP6 and its complex with DKK1. *Nat Struct Mol Biol* **18:** 1204-1210

Chiao JH, Roy K, Tolner B, Yang CH, Sirotnak FM (1997) RFC-1 gene expression regulates folate absorption in mouse small intestine. *The Journal of biological chemistry* **272:** 11165-11170

Chwatko G, Jakubowski H (2005) The determination of homocysteine-thiolactone in human plasma. *Anal Biochem* **337:** 271-277

Copp AJ, Greene ND (2013) Neural tube defects--disorders of neurulation and related embryonic processes. *Wiley Interdiscip Rev Dev Biol* **2:** 213-227

Copp AJ, Greene ND, Murdoch JN (2003) The genetic basis of mammalian neurulation. *Nat Rev Genet* **4:** 784-793

Copp AJ, Stanier P, Greene ND (2013) Neural tube defects: recent advances, unsolved questions, and controversies. *Lancet Neurol* **12:** 799-810

Correa A, Gilboa SM, Besser LM, Botto LD, Moore CA, Hobbs CA, Cleves MA, Riehle-Colarusso TJ, Waller DK, Reece EA (2008) Diabetes mellitus and birth defects. *Am J Obstet Gynecol* **199:** 237.e231-239

Crider KS, Yang TP, Berry RJ, Bailey LB (2012) Folate and DNA methylation: a review of molecular mechanisms and the evidence for folate's role. *Adv Nutr* **3:** 21-38

Cronstein BN (1997) The mechanism of action of methotrexate. *Rheum Dis Clin North Am* **23:** 739-755

Culi J, Mann RS (2003) Boca, an endoplasmic reticulum protein required for wingless signaling and trafficking of LDL receptor family members in Drosophila. *Cell* **112:** 343-354

Damaraju VL, Hamilton KF, Seth-Smith ML, Cass CE, Sawyer MB (2005) Characterization of binding of folates and antifolates to brush-border membrane vesicles isolated from human kidney. *Mol Pharmacol* **67:** 453-459

Das P, Mandal AK, Chandar NB, Baidya M, Bhatt HB, Ganguly B, Ghosh SK, Das A (2012) New chemodosimetric reagents as ratiometric probes for cysteine and homocysteine and possible detection in living cells and in blood plasma. *Chemistry* **18:** 15382-15393

Das UN (2004) Metabolic syndrome X: an inflammatory condition? *Curr Hypertens Rep* **6:** 66-73

De A (2011) Wnt/Ca2+ signaling pathway: a brief overview. *Acta biochimica et biophysica Sinica* **43:** 745-756

Delves PJ, Roitt IM (2000) The immune system. Second of two parts. *N Engl J Med* **343:** 108-117

Denny KJ, Coulthard LG, Jeanes A, Lisgo S, Simmons DG, Callaway LK, Wlodarczyk B, Finnell RH, Woodruff TM, Taylor SM (2013a) C5a receptor signaling prevents folate deficiency-induced neural tube defects in mice. *J Immunol* **190:** 3493-3499

Denny KJ, Jeanes A, Fathe K, Finnell RH, Taylor SM, Woodruff TM (2013b) Neural tube defects, folate, and immune modulation. *Birth Defects Res A Clin Mol Teratol* **97:** 602-609

Deplancke B, Gaskins HR (2002) Redox control of the transsulfuration and glutathione biosynthesis pathways. *Curr Opin Clin Nutr Metab Care* **5:** 85-92

Detrait ER, George TM, Etchevers HC, Gilbert JR, Vekemans M, Speer MC (2005) Human neural tube defects: developmental biology, epidemiology, and genetics. *Neurotoxicol Teratol* **27:** 515-524

Devi S, Kennedy RH, Joseph L, Shekhawat NS, Melchert RB, Joseph J (2006) Effect of long-term hyperhomocysteinemia on myocardial structure and function in hypertensive rats. *Cardiovascular pathology : the official journal of the Society for Cardiovascular Pathology* **15:** 75-82

DiLiberti JH, Farndon PA, Dennis NR, Curry CJ (1984) The fetal valproate syndrome. *Am J Med Genet* **19:** 473-481

Downs KM, Davies T (1993) Staging of gastrulating mouse embryos by morphological landmarks in the dissecting microscope. *Development* **118:** 1255-1266

Dunlevy LP, Burren KA, Mills K, Chitty LS, Copp AJ, Greene ND (2006) Integrity of the methylation cycle is essential for mammalian neural tube closure. *Birth Defects Res A Clin Mol Teratol* **76:** 544-552

Eichholzer M, Tönz O, Zimmermann R (2006) Folic acid: a public-health challenge. *Lancet* **367:** 1352-1361

Endresen GK, Husby G (2001) Folate supplementation during methotrexate treatment of patients with rheumatoid arthritis. An update and proposals for guidelines. *Scand J Rheumatol* **30:** 129-134

Eom DS, Amarnath S, Agarwala S (2013) Apicobasal polarity and neural tube closure. *Dev Growth Differ* **55:** 164-172

Etheredge AJ, Finnell RH, Carmichael SL, Lammer EJ, Zhu H, Mitchell LE, Shaw GM (2012) Maternal and infant gene-folate interactions and the risk of neural tube defects. *Am J Med Genet A* **158A:** 2439-2446

Feuk L, Carson AR, Scherer SW (2006) Structural variation in the human genome. *Nat Rev Genet* **7:** 85-97

Finnell RH, Moon SP, Abbott LC, Golden JA, Chernoff GF (1986) Strain differences in heat-induced neural tube defects in mice. *Teratology* **33:** 247-252

Fleming A, Copp AJ (1998) Embryonic folate metabolism and mouse neural tube defects. *Science* **280:** 2107-2109

Frosst P, Blom HJ, Milos R, Goyette P, Sheppard CA, Matthews RG, Boers GJ, den Heijer M, Kluijtmans LA, van den Heuvel LP (1995) A candidate genetic risk factor for vascular disease: a common mutation in methylenetetrahydrofolate reductase. *Nat Genet* **10:** 111-113

Ganapathy V, Smith SB, Prasad PD (2004) SLC19: the folate/thiamine transporter family. *Pflugers Arch* **447:** 641-646

Gao C, Chen YG (2010) Dishevelled: The hub of Wnt signaling. *Cell Signal* **22:** 717-727

Garel J, Tawfik DS (2006) Mechanism of hydrolysis and aminolysis of homocysteine thiolactone. *Chemistry* **12:** 4144-4152

Gelineau-van Waes J, Maddox JR, Smith LM, van Waes M, Wilberding J, Eudy JD, Bauer LK, Finnell RH (2008) Microarray analysis of E9.5 reduced folate carrier (RFC1; Slc19a1) knockout embryos reveals altered expression of genes in the cubilin-megalin multiligand endocytic receptor complex. *BMC Genomics* **9:** 156

Gelineau-van Waes J, Starr L, Maddox J, Aleman F, Voss KA, Wilberding J, Riley RT (2005) Maternal fumonisin exposure and risk for neural tube defects: mechanisms in an in vivo mouse model. *Birth Defects Res A Clin Mol Teratol* **73:** 487-497

Geller J, Kronn D, Jayabose S, Sandoval C (2002) Hereditary folate malabsorption: family report and review of the literature. *Medicine (Baltimore)* **81:** 51-68

Getz GS, Reardon CA (2004) Paraoxonase, a cardioprotective enzyme: continuing issues. *Curr Opin Lipidol* **15:** 261-267

Gilfix BM, Blank DW, Rosenblatt DS (1997) Novel reductant for determination of total plasma homocysteine. *Clin Chem* **43:** 687-688

Giron P, Dayon L, Mihala N, Sanchez JC, Rose K (2009) Cysteine-reactive covalent capture tags for enrichment of cysteine-containing peptides. *Rapid Commun Mass Spectrom* **23:** 3377-3386

Glowacki R, Jakubowski H (2004) Cross-talk between Cys34 and lysine residues in human serum albumin revealed by N-homocysteinylation. *The Journal of biological chemistry* **279:** 10864-10871

Golden JA, Chernoff GF (1995) Multiple sites of anterior neural tube closure in humans: evidence from anterior neural tube defects (anencephaly). *Pediatrics* **95:** 506-510

Gordon JW, Ruddle FH (1981) Integration and stable germ line transmission of genes injected into mouse pronuclei. *Science* **214:** 1244-1246

Gray J, Ross ME (2011) Neural tube closure in mouse whole embryo culture. *J Vis Exp*

Gray JD, Kholmanskikh S, Castaldo BS, Hansler A, Chung H, Klotz B, Singh S, Brown AM, Ross ME (2013) LRP6 exerts non-canonical effects on Wnt signaling during neural tube closure. *Hum Mol Genet* **22:** 4267-4281

Gray JD, Nakouzi G, Slowinska-Castaldo B, Dazard JE, Rao JS, Nadeau JH, Ross ME (2010) Functional interactions between the LRP6 WNT co-receptor and folate supplementation. *Hum Mol Genet* **19:** 4560-4572

Greene ND, Stanier P, Copp AJ (2009) Genetics of human neural tube defects. *Hum Mol Genet* **18:** R113-129

Greene ND, Stanier P, Moore GE (2011) The emerging role of epigenetic mechanisms in the etiology of neural tube defects. *Epigenetics : official journal of the DNA Methylation Society* **6:** 875-883

Groenen PM, van Rooij IA, Peer PG, Ocké MC, Zielhuis GA, Steegers-Theunissen RP (2004) Low maternal dietary intakes of iron, magnesium, and niacin are associated with spina bifida in the offspring. *The Journal of nutrition* **134:** 1516-1522

Gundry RL, White MY, Nogee J, Tchernyshyov I, Van Eyk JE (2009) Assessment of albumin removal from an immunoaffinity spin column: critical implications for proteomic examination of the albuminome and albumin-depleted samples. *Proteomics* **9:** 2021-2028

Habas R, Dawid IB (2005) Dishevelled and Wnt signaling: is the nucleus the final frontier? *J Biol* **4:** 2

Hague WM (2003) Homocysteine and pregnancy. *Best practice & research Clinical obstetrics & gynaecology* **17:** 459-469

Hamid A, Wani NA, Kaur J (2009) New perspectives on folate transport in relation to alcoholism-induced folate malabsorption--association with epigenome stability and cancer development. *FEBS J* **276:** 2175-2191

Han ZJ, Song G, Cui Y, Xia HF, Ma X (2011) Oxidative stress is implicated in arsenic-induced neural tube defects in chick embryos. *Int J Dev Neurosci* **29:** 673-680

Hannon-Fletcher MP, Armstrong NC, Scott JM, Pentieva K, Bradbury I, Ward M, Strain JJ, Dunn AA, Molloy AM, Kerr MA, McNulty H (2004) Determining bioavailability of food folates in a controlled intervention study. *Am J Clin Nutr* **80:** 911-918

Harris MJ, Juriloff DM (2007) Mouse mutants with neural tube closure defects and their role in understanding human neural tube defects. *Birth Defects Res A Clin Mol Teratol* **79:** 187-210

Harris MJ, Juriloff DM (2010) An update to the list of mouse mutants with neural tube closure defects and advances toward a complete genetic perspective of neural tube closure. *Birth Defects Res A Clin Mol Teratol* **88:** 653-669

Heimann M, Roth DR, Ledieu D, Pfister R, Classen W (2010) Sublingual and submandibular blood collection in mice: a comparison of effects on body weight, food consumption and tissue damage. *Lab Anim* **44:** 352-358

Hendricks KA, Simpson JS, Larsen RD (1999) Neural tube defects along the Texas-Mexico border, 1993-1995. *Am J Epidemiol* **149:** 1119-1127

Herz J, Marschang P (2003) Coaxing the LDL receptor family into the fold. *Cell* **112:** 289-292

Hill DS, Wlodarczyk BJ, Palacios AM, Finnell RH (2010) Teratogenic effects of antiepileptic drugs. *Expert Rev Neurother* **10:** 943-959

Hill RD, Huang S, Stasolla C (2013) Hemoglobins, programmed cell death and somatic embryogenesis. *Plant Sci* **211:** 35-41

Hodge R (2010) *Developmental Biology: From a Cell to an Organism*, New York, NY: Facts on File, Inc.

Hofmann MA, Lalla E, Lu Y, Gleason MR, Wolf BM, Tanji N, Ferran LJ, Kohl B, Rao V, Kisiel W, Stern DM, Schmidt AM (2001) Hyperhomocysteinemia enhances vascular inflammation and accelerates atherosclerosis in a murine model. *J Clin Invest* **107:** 675-683

Honein MA, Paulozzi LJ, Mathews TJ, Erickson JD, Wong LY (2001) Impact of folic acid fortification of the US food supply on the occurrence of neural tube defects. *JAMA* **285:** 2981-2986

Hortin GL, Seam N, Hoehn GT (2006) Bound homocysteine, cysteine, and cysteinylglycine distribution between albumin and globulins. *Clin Chem* **52:** 2258-2264

Hsieh CL, Wang HE, Tsai WJ, Peng CC, Peng RY (2012) Multiple point action mechanism of valproic acid-teratogenicity alleviated by folic acid, vitamin C, and N-acetylcysteine in chicken embryo model. *Toxicology* **291:** 32-42

Hsieh JC, Lee L, Zhang L, Wefer S, Brown K, DeRossi C, Wines ME, Rosenquist T, Holdener BC (2003) Mesd encodes an LRP5/6 chaperone essential for specification of mouse embryonic polarity. *Cell* **112:** 355-367

Huh JY, Park YJ, Ham M, Kim JB (2014) Crosstalk between Adipocytes and Immune Cells in Adipose Tissue Inflammation and Metabolic Dysregulation in Obesity. *Mol Cells*

Hwang CS, Shemorry A, Varshavsky A (2010) N-terminal acetylation of cellular proteins creates specific degradation signals. *Science* **327:** 973-977

Ichi S, Nakazaki H, Boshnjaku V, Singh RM, Mania-Farnell B, Xi G, McLone DG, Tomita T, Mayanil CS (2012) Fetal neural tube stem cells from Pax3 mutant mice proliferate, differentiate, and form synaptic connections when stimulated with folic acid. *Stem Cells Dev* **21:** 321-330

Ifergan I, Jansen G, Assaraf YG (2008) The reduced folate carrier (RFC) is cytotoxic to cells under conditions of severe folate deprivation. RFC as a double edged sword in folate homeostasis. *The Journal of biological chemistry* **283:** 20687-20695

Jaenisch R, Mintz B (1974) Simian virus 40 DNA sequences in DNA of healthy adult mice derived from preimplantation blastocysts injected with viral DNA. *Proc Natl Acad Sci U S A* **71:** 1250-1254

Jakubowski H (1991) Proofreading in vivo: editing of homocysteine by methionyl-tRNA synthetase in the yeast Saccharomyces cerevisiae. *EMBO J* **10:** 593-598

Jakubowski H (1999) Protein homocysteinylation: possible mechanism underlying pathological consequences of elevated homocysteine levels. *FASEB J* **13:** 2277-2283

Jakubowski H (2000) Homocysteine thiolactone: metabolic origin and protein homocysteinylation in humans. *The Journal of nutrition* **130:** 377S-381S

Jakubowski H (2001) Protein N-homocysteinylation: implications for atherosclerosis. *Biomed Pharmacother* **55:** 443-447

Jakubowski H (2004) Molecular basis of homocysteine toxicity in humans. *Cell Mol Life Sci* **61:** 470-487

Jakubowski H (2005) Anti-N-homocysteinylated protein autoantibodies and cardiovascular disease. *Clin Chem Lab Med* **43:** 1011-1014

Jakubowski H (2006) Mechanism of the condensation of homocysteine thiolactone with aldehydes. *Chemistry* **12:** 8039-8043

Jakubowski H (2008) New method for the determination of protein N-linked homocysteine. *Anal Biochem* **380:** 257-261

Jakubowski H, Perla-Kaján J, Finnell RH, Cabrera RM, Wang H, Gupta S, Kruger WD, Kraus JP, Shih DM (2009) Genetic or nutritional disorders in homocysteine or folate metabolism increase protein N-homocysteinylation in mice. *FASEB J* **23:** 1721-1727

Janeway CA, Medzhitov R (2002) Innate immune recognition. *Annu Rev Immunol* **20:** 197-216

Jentink J, Dolk H, Loane MA, Morris JK, Wellesley D, Garne E, de Jong-van den Berg L, Group EASW (2010) Intrauterine exposure to carbamazepine and specific congenital malformations: systematic review and case-control study. *Bmj* **341:** c6581

Jeon H, Meng W, Takagi J, Eck MJ, Springer TA, Blacklow SC (2001) Implications for familial hypercholesterolemia from the structure of the LDL receptor YWTD-EGF domain pair. *Nat Struct Biol* **8:** 499-504

Jin L, Liu J, Ye B, Ren A (2014) Concentrations of selected heavy metals in maternal blood and associated factors in rural areas in Shanxi Province, China. *Environ Int* **66:** 157-164

Johnson MH (2009) From mouse egg to mouse embryo: polarities, axes, and tissues. *Annu Rev Cell Dev Biol* **25:** 483-512

Johnson MP, Gerdes M, Rintoul N, Pasquariello P, Melchionni J, Sutton LN, Adzick NS (2006) Maternal-fetal surgery for myelomeningocele: neurodevelopmental outcomes at 2 years of age. *Am J Obstet Gynecol* **194:** 1145-1150; discussion 1150-1142

Joiner DM, Ke J, Zhong Z, Xu HE, Williams BO (2013) LRP5 and LRP6 in development and disease. *Trends Endocrinol Metab* **24:** 31-39

Jones C, Chen P (2007) Planar cell polarity signaling in vertebrates. *Bioessays* **29:** 120-132

Kamen BA, Smith AK (2004) A review of folate receptor alpha cycling and 5-methyltetrahydrofolate accumulation with an emphasis on cell models in vitro. *Adv Drug Deliv Rev* **56:** 1085-1097

Kelly OG, Pinson KI, Skarnes WC (2004) The Wnt co-receptors Lrp5 and Lrp6 are essential for gastrulation in mice. *Development* **131:** 2803-2815

Khodadadi S, Riazi GH, Ahmadian S, Hoveizi E, Karima O, Aryapour H (2012) Effect of N-homocysteinylation on physicochemical and cytotoxic properties of amyloid β-peptide. *FEBS Lett* **586:** 127-131

Kibar Z, Salem S, Bosoi CM, Pauwels E, De Marco P, Merello E, Bassuk AG, Capra V, Gros P (2011) Contribution of VANGL2 mutations to isolated neural tube defects. *Clin Genet* **80:** 76-82

Kim NG, Xu C, Gumbiner BM (2009) Identification of targets of the Wnt pathway destruction complex in addition to beta-catenin. *Proc Natl Acad Sci U S A* **106:** 5165-5170

Kim YI (2007) Folate and colorectal cancer: an evidence-based critical review. *Mol Nutr Food Res* **51:** 267-292

Kimelman D, Xu W (2006) beta-catenin destruction complex: insights and questions from a structural perspective. *Oncogene* **25:** 7482-7491

King JC (2006) Maternal obesity, metabolism, and pregnancy outcomes. *Annu Rev Nutr* **26:** 271-291

Klaus A, Birchmeier W (2008) Wnt signalling and its impact on development and cancer. *Nat Rev Cancer* **8:** 387-398

Köhler C, Lighthouse JK, Werther T, Andersen OM, Diehl A, Schmieder P, Du J, Holdener BC, Oschkinat H (2011) The structure of MESD45-184 brings light into the mechanism of LDLR family folding. *Structure* **19:** 337-348

Kokubu C, Heinzmann U, Kokubu T, Sakai N, Kubota T, Kawai M, Wahl MB, Galceran J, Grosschedl R, Ozono K, Imai K (2004) Skeletal defects in ringelschwanz mutant mice reveal that Lrp6 is required for proper somitogenesis and osteogenesis. *Development* **131:** 5469-5480

Kolligs FT, Hu G, Dang CV, Fearon ER (1999) Neoplastic transformation of RK3E by mutant beta-catenin requires deregulation of Tcf/Lef transcription but not activation of c-myc expression. *Mol Cell Biol* **19:** 5696-5706

Komiya Y, Habas R (2008) Wnt signal transduction pathways. *Organogenesis* **4:** 68-75

Kondo A, Kamihira O, Ozawa H (2009) Neural tube defects: prevalence, etiology and prevention. *Int J Urol* **16:** 49-57

Koslowski MJ, Teltschik Z, Beisner J, Schaeffeler E, Wang G, Kübler I, Gersemann M, Cooney R, Jewell D, Reinisch W, Vermeire S, Rutgeerts P, Schwab M, Stange EF, Wehkamp J (2012) Association of a functional variant in the Wnt co-receptor LRP6 with early onset ileal Crohn's disease. *PLoS Genet* **8:** e1002523

Kubota T, Michigami T, Sakaguchi N, Kokubu C, Suzuki A, Namba N, Sakai N, Nakajima S, Imai K, Ozono K (2008) Lrp6 hypomorphic mutation affects bone mass through bone resorption in mice and impairs interaction with Mesd. *J Bone Miner Res* **23:** 1661-1671

Kurahara H, Takao S, Kuwahata T, Nagai T, Ding Q, Maeda K, Shinchi H, Mataki Y, Maemura K, Matsuyama T, Natsugoe S (2012) Clinical significance of folate receptor β-expressing tumor-associated macrophages in pancreatic cancer. *Ann Surg Oncol* **19:** 2264-2271

Lammer EJ, Sever LE, Oakley GP (1987) Teratogen update: valproic acid. *Teratology* **35:** 465-473

Larsen MR, Trelle MB, Thingholm TE, Jensen ON (2006) Analysis of posttranslational modifications of proteins by tandem mass spectrometry. *Biotechniques* **40:** 790-798

Lei Y, Zhu H, Duhon C, Yang W, Ross ME, Shaw GM, Finnell RH (2013) Mutations in planar cell polarity gene SCRIB are associated with spina bifida. *PloS one* **8:** e69262

Lei Y, Zhu H, Yang W, Ross ME, Shaw GM, Finnell RH (2014) Identification of novel CELSR1 mutations in spina bifida. *PloS one* **9:** e92207

Lei YP, Zhang T, Li H, Wu BL, Jin L, Wang HY (2010) VANGL2 mutations in human cranial neural-tube defects. *N Engl J Med* **362:** 2232-2235

Li Z, Ren A, Zhang L, Ye R, Li S, Zheng J, Hong S, Wang T (2006) Extremely high prevalence of neural tube defects in a 4-county area in Shanxi Province, China. *Birth Defects Res A Clin Mol Teratol* **76:** 237-240

Li Z, Zhang L, Ye R, Pei L, Liu J, Zheng X, Ren A (2011) Indoor air pollution from coal combustion and the risk of neural tube defects in a rural population in Shanxi Province, China. *Am J Epidemiol* **174:** 451-458

Linask KK, Huhta J (2010) Folate protection from congenital heart defects linked with canonical Wnt signaling and epigenetics. *Curr Opin Pediatr* **22:** 561-566

Ling C, Del Guerra S, Lupi R, Rönn T, Granhall C, Luthman H, Masiello P, Marchetti P, Groop L, Del Prato S (2008) Epigenetic regulation of PPARGC1A in human type 2 diabetic islets and effect on insulin secretion. *Diabetologia* **51:** 615-622

Locksmith GJ, Duff P (1998) Preventing neural tube defects: the importance of periconceptional folic acid supplements. *Obstet Gynecol* **91:** 1027-1034

Logan CY, Nusse R (2004) The Wnt signaling pathway in development and disease. *Annu Rev Cell Dev Biol* **20:** 781-810

Lu Y, Sega E, Leamon CP, Low PS (2004) Folate receptor-targeted immunotherapy of cancer: mechanism and therapeutic potential. *Adv Drug Deliv Rev* **56:** 1161-1176

Lu Z, Cheng Z, Zhao Y, Volchenboum SL (2011) Bioinformatic analysis and post-translational modification crosstalk prediction of lysine acetylation. *PloS one* **6:** e28228

Lucock M, Yates Z (2009) Folic acid fortification: a double-edged sword. *Curr Opin Clin Nutr Metab Care* **12:** 555-564

MacDonald BT, Tamai K, He X (2009) Wnt/beta-catenin signaling: components, mechanisms, and diseases. *Dev Cell* **17:** 9-26

MacDougald OA, Burant CF (2007) The rapidly expanding family of adipokines. *Cell Metab* **6:** 159-161

Macfarlane AJ, Behan NA, Matias FM, Green J, Caldwell D, Brooks SP (2012) Dietary folate does not significantly affect the intestinal microbiome, inflammation or tumorigenesis in azoxymethane-dextran sodium sulphate-treated mice. *The British journal of nutrition***:** 1-9

Madden S, Maggs JL, Park BK (1996) Bioactivation of carbamazepine in the rat in vivo. Evidence for the formation of reactive arene oxide(s). *Drug Metab Dispos* **24:** 469-479

Maldonado G, Delzell E, Tyl RW, Sever LE (2003) Occupational exposure to glycol ethers and human congenital malformations. *Int Arch Occup Environ Health* **76:** 405-423

Marczak L, Sikora M, Stobiecki M, Jakubowski H (2011) Analysis of site-specific N-homocysteinylation of human serum albumin in vitro and in vivo using MALDI-ToF and LC-MS/MS mass spectrometry. *J Proteomics* **74:** 967-974

Matherly LH, Hou Z, Deng Y (2007) Human reduced folate carrier: translation of basic biology to cancer etiology and therapy. *Cancer Metastasis Rev* **26:** 111-128

McCully KS (2007) Homocysteine, vitamins, and vascular disease prevention. *Am J Clin Nutr* **86:** 1563S-1568S

McLin VA, Hu CH, Shah R, Jamrich M (2008) Expression of complement components coincides with early patterning and organogenesis in Xenopus laevis. *Int J Dev Biol* **52:** 1123-1133

Medzhitov R, Janeway CA (2002) Decoding the patterns of self and nonself by the innate immune system. *Science* **296:** 298-300

MEUNIER H, CARRAZ G, NEUNIER Y, EYMARD P, AIMARD M (1963) [Pharmacodynamic properties of N-dipropylacetic acid]. *Therapie* **18:** 435-438

Millar DS, Horan M, Chuzhanova NA, Cooper DN (2010) Characterisation of a functional intronic polymorphism in the human growth hormone (GH1) gene. *Hum Genomics* **4:** 289-301

Miller JW, Nadeau MR, Smith D, Selhub J (1994) Vitamin B-6 deficiency vs folate deficiency: comparison of responses to methionine loading in rats. *Am J Clin Nutr* **59:** 1033-1039

Mills JL, McPartlin JM, Kirke PN, Lee YJ, Conley MR, Weir DG, Scott JM (1995) Homocysteine metabolism in pregnancies complicated by neural-tube defects. *Lancet* **345:** 149-151

Missmer SA, Suarez L, Felkner M, Wang E, Merrill AH, Rothman KJ, Hendricks KA (2006) Exposure to fumonisins and the occurrence of neural tube defects along the Texas-Mexico border. *Environ Health Perspect* **114:** 237-241

Mitchell LE (2005) Epidemiology of neural tube defects. *Am J Med Genet C Semin Med Genet* **135C:** 88-94

Molloy AM, Quadros EV, Sequeira JM, Troendle JF, Scott JM, Kirke PN, Mills JL (2009) Lack of association between folate-receptor autoantibodies and neural-tube defects. *N Engl J Med* **361:** 152-160

Moretti ME, Bar-Oz B, Fried S, Koren G (2005) Maternal hyperthermia and the risk for neural tube defects in offspring: systematic review and meta-analysis. *Epidemiology* **16:** 216-219

Morgan WC (1954) A new crooked tail mutation involving distinctive pleiotropism. *Journal of Genetics* **52:** 354-373

Murphy MM, Fernandez-Ballart JD (2011) Homocysteine in pregnancy. *Adv Clin Chem* **53:** 105-137

Narisawa A, Komatsuzaki S, Kikuchi A, Niihori T, Aoki Y, Fujiwara K, Tanemura M, Hata A, Suzuki Y, Relton CL, Grinham J, Leung KY, Partridge D, Robinson A, Stone V, Gustavsson P, Stanier P, Copp AJ, Greene ND, Tominaga T, Matsubara Y, Kure S (2012) Mutations in genes encoding the glycine cleavage system predispose to neural tube defects in mice and humans. *Hum Mol Genet* **21:** 1496-1503

Nazki FH, Sameer AS, Ganaie BA (2014) Folate: metabolism, genes, polymorphisms and the associated diseases. *Gene* **533:** 11-20

Nekrassova O, Lawrence NS, Compton RG (2003) Analytical determination of homocysteine: a review. *Talanta* **60:** 1085-1095

Nicholson JK, Lindon JC (2008) Systems biology: Metabonomics. *Nature* **455:** 1054-1056

Niehrs C (2012) The complex world of WNT receptor signalling. *Nat Rev Mol Cell Biol* **13:** 767-779

Nusse R, Varmus H (2012) Three decades of Wnts: a personal perspective on how a scientific field developed. *EMBO J* **31:** 2670-2684

Nygren-Babol L, Jägerstad M (2012) Folate-binding protein in milk: a review of biochemistry, physiology, and analytical methods. *Crit Rev Food Sci Nutr* **52:** 410-425

Nykjaer A, Willnow TE (2002) The low-density lipoprotein receptor gene family: a cellular Swiss army knife? *Trends Cell Biol* **12:** 273-280

Ohrvik VE, Witthoft CM (2011) Human folate bioavailability. *Nutrients* **3:** 475-490

Padmanabhan R (1987) Abnormalities of the ear associated with exencephaly in mouse fetuses induced by maternal exposure to cadmium. *Teratology* **35:** 9-18

Paoli P, Sbrana F, Tiribilli B, Caselli A, Pantera B, Cirri P, De Donatis A, Formigli L, Nosi D, Manao G, Camici G, Ramponi G (2010) Protein N-homocysteinylation induces the formation of toxic amyloid-like protofibrils. *J Mol Biol* **400:** 889-907

Paul BD, Snyder SH (2012) H_2S signalling through protein sulfhydration and beyond. *Nat Rev Mol Cell Biol* **13:** 499-507

Perla-Kajan J, Stanger O, Luczak M, Ziolkowska A, Malendowicz LK, Twardowski T, Lhotak S, Austin RC, Jakubowski H (2008) Immunohistochemical detection of N-homocysteinylated proteins in humans and mice. *Biomed Pharmacother* **62:** 473-479

Phiel CJ, Zhang F, Huang EY, Guenther MG, Lazar MA, Klein PS (2001) Histone deacetylase is a direct target of valproic acid, a potent anticonvulsant, mood stabilizer, and teratogen. *The Journal of biological chemistry* **276:** 36734-36741

Piao S, Lee SH, Kim H, Yum S, Stamos JL, Xu Y, Lee SJ, Lee J, Oh S, Han JK, Park BJ, Weis WI, Ha NC (2008) Direct inhibition of GSK3beta by the phosphorylated cytoplasmic domain of LRP6 in Wnt/beta-catenin signaling. *PloS one* **3:** e4046

Piedrahita JA, Oetama B, Bennett GD, van Waes J, Kamen BA, Richardson J, Lacey SW, Anderson RG, Finnell RH (1999) Mice lacking the folic acid-binding protein Folbp1 are defective in early embryonic development. *Nat Genet* **23:** 228-232

Pinson KI, Brennan J, Monkley S, Avery BJ, Skarnes WC (2000) An LDL-receptor-related protein mediates Wnt signalling in mice. *Nature* **407:** 535-538

Preedy VR, Adamolekun B, Armitage JM. (2013) B Vitamins and Folate: Food and Nutritional Components in Focus. Royal Society of Chemistry Publishing, Cambridge, UK.

Qiu A, Jansen M, Sakaris A, Min SH, Chattopadhyay S, Tsai E, Sandoval C, Zhao R, Akabas MH, Goldman ID (2006) Identification of an intestinal folate transporter and the molecular basis for hereditary folate malabsorption. *Cell* **127:** 917-928

Ramaekers VT, Rothenberg SP, Sequeira JM, Opladen T, Blau N, Quadros EV, Selhub J (2005) Autoantibodies to folate receptors in the cerebral folate deficiency syndrome. *N Engl J Med* **352:** 1985-1991

Ramensky V, Bork P, Sunyaev S (2002) Human non-synonymous SNPs: server and survey. *Nucleic Acids Res* **30:** 3894-3900

Rao TP, Kühl M (2010) An updated overview on Wnt signaling pathways: a prelude for more. *Circulation research* **106:** 1798-1806

Ravnskov U, McCully KS (2009) Review and Hypothesis: Vulnerable plaque formation from obstruction of Vasa vasorum by homocysteinylated and oxidized lipoprotein aggregates complexed with microbial remnants and LDL autoantibodies. *Ann Clin Lab Sci* **39:** 3-16

Redon R, Ishikawa S, Fitch KR, Feuk L, Perry GH, Andrews TD, Fiegler H, Shapero MH, Carson AR, Chen W, Cho EK, Dallaire S, Freeman JL, González JR, Gratacòs M, Huang J, Kalaitzopoulos D, Komura D, MacDonald JR, Marshall CR, Mei R, Montgomery L, Nishimura K, Okamura K, Shen F, Somerville MJ, Tchinda J, Valsesia A, Woodwark C, Yang F, Zhang J, Zerjal T, Armengol L, Conrad DF, Estivill X, Tyler-Smith C, Carter NP, Aburatani H, Lee C, Jones KW, Scherer SW, Hurles ME (2006) Global variation in copy number in the human genome. *Nature* **444:** 444-454

Reece EA (2012) Diabetes-induced birth defects: what do we know? What can we do? *Curr Diab Rep* **12:** 24-32

Ren A, Qiu X, Jin L, Ma J, Li Z, Zhang L, Zhu H, Finnell RH, Zhu T (2011) Association of selected persistent organic pollutants in the placenta with the risk of neural tube defects. *Proc Natl Acad Sci U S A* **108:** 12770-12775

Rijnboutt S, Jansen G, Posthuma G, Hynes JB, Schornagel JH, Strous GJ (1996) Endocytosis of GPI-linked membrane folate receptor-alpha. *J Cell Biol* **132:** 35-47

Robert E, Guibaud P (1982) Maternal valproic acid and congenital neural tube defects. *Lancet* **2:** 937

Rosenberg G (2007) The mechanisms of action of valproate in neuropsychiatric disorders: can we see the forest for the trees? *Cell Mol Life Sci* **64:** 2090-2103

Rosenquist TH, Ratashak SA, Selhub J (1996) Homocysteine induces congenital defects of the heart and neural tube: effect of folic acid. *Proc Natl Acad Sci U S A* **93:** 15227-15232

Ross JF, Chaudhuri PK, Ratnam M (1994) Differential regulation of folate receptor isoforms in normal and malignant tissues in vivo and in established cell lines. Physiologic and clinical implications. *Cancer* **73:** 2432-2443

Ross JF, Wang H, Behm FG, Mathew P, Wu M, Booth R, Ratnam M (1999) Folate receptor type beta is a neutrophilic lineage marker and is differentially expressed in myeloid leukemia. *Cancer* **85:** 348-357

Ross ME (2010) Gene-environment interactions, folate metabolism and the embryonic nervous system. *Wiley Interdiscip Rev Syst Biol Med* **2:** 471-480

Rothenberg SP, da Costa MP, Sequeira JM, Cracco J, Roberts JL, Weedon J, Quadros EV (2004) Autoantibodies against folate receptors in women with a pregnancy complicated by a neural-tube defect. *N Engl J Med* **350:** 134-142

Saadeldien HM, Mohamed AA, Hussein MR (2012) Iron-induced damage in corpus striatal cells of neonatal rats: attenuation by folic acid. *Ultrastruct Pathol* **36:** 89-101

Sabharanjak S, Mayor S (2004) Folate receptor endocytosis and trafficking. *Adv Drug Deliv Rev* **56:** 1099-1109

Sadler TW, Merrill AH, Stevens VL, Sullards MC, Wang E, Wang P (2002) Prevention of fumonisin B1-induced neural tube defects by folic acid. *Teratology* **66:** 169-176

Salazar MD, Ratnam M (2007) The folate receptor: what does it promise in tissue-targeted therapeutics? *Cancer Metastasis Rev* **26:** 141-152

Salojin KV, Cabrera RM, Sun W, Chang WC, Lin C, Duncan L, Platt KA, Read R, Vogel P, Liu Q, Finnell RH, Oravecz T (2011) A mouse model of hereditary folate malabsorption: deletion of the PCFT gene leads to systemic folate deficiency. *Blood* **117:** 4895-4904

Schorah C (2009) Dick Smithells, folic acid, and the prevention of neural tube defects. *Birth Defects Res A Clin Mol Teratol* **85:** 254-259

Schwaninger M (1999) Elevated plasma concentrations of homocysteine in antiepileptic drug treatment. *Epilepsia* **40:** 345-350

Selhub J (1999) Homocysteine metabolism. *Annu Rev Nutr* **19:** 217-246

Selhub J, Jacques PF, Bostom AG, Wilson PW, Rosenberg IH (2000) Relationship between plasma homocysteine and vitamin status in the Framingham study population. Impact of folic acid fortification. *Public Health Rev* **28:** 117-145

Sen S, Manzoor A, Deviasumathy M, Newton C (2001) Maternal knowledge, attitude and practice regarding folic acid intake during the periconceptional period. *Public Health Nutr* **4:** 909-912

Seo J, Lee KJ (2004) Post-translational modifications and their biological functions: proteomic analysis and systematic approaches. *J Biochem Mol Biol* **37:** 35-44

Sever LE (1995) Looking for causes of neural tube defects: where does the environment fit in? *Environ Health Perspect* **103 Suppl 6:** 165-171

Shane B (2003) Folate fortification: enough already? *Am J Clin Nutr* **77:** 8-9

Shaw GM, Velie EM, Schaffer D (1996) Risk of neural tube defect-affected pregnancies among obese women. *JAMA* **275:** 1093-1096

Shayeghi M, Latunde-Dada GO, Oakhill JS, Laftah AH, Takeuchi K, Halliday N, Khan Y, Warley A, McCann FE, Hider RC, Frazer DM, Anderson GJ, Vulpe CD, Simpson RJ, McKie AT (2005) Identification of an intestinal heme transporter. *Cell* **122:** 789-801

Shen F, Ross JF, Wang X, Ratnam M (1994) Identification of a novel folate receptor, a truncated receptor, and receptor type beta in hematopoietic cells: cDNA cloning, expression, immunoreactivity, and tissue specificity. *Biochemistry* **33:** 1209-1215

Shen F, Wu M, Ross JF, Miller D, Ratnam M (1995) Folate receptor type gamma is primarily a secretory protein due to lack of an efficient signal for glycosylphosphatidylinositol modification: protein characterization and cell type specificity. *Biochemistry* **34:** 5660-5665

Shin DS, Mahadeo K, Min SH, Diop-Bove N, Clayton P, Zhao R, Goldman ID (2011) Identification of novel mutations in the proton-coupled folate transporter (PCFT-SLC46A1) associated with hereditary folate malabsorption. *Molecular genetics and metabolism* **103:** 33-37

Simmons D (2008) **The use of animal models in studying genetic disease: transgenesis and induced mutation**. *Nature Education* **1**

Slack JMW (2013) *Essential Developmental Biology*, 3 edn. Oxford, UK: Blackwell Publishing, Inc.

Smale ST (2010) Luciferase assay. *Cold Spring Harb Protoc* **2010:** pdb.prot5421

Smithells RW, Nevin NC, Seller MJ, Sheppard S, Harris R, Read AP, Fielding DW, Walker S, Schorah CJ, Wild J (1983) Further experience of vitamin supplementation for prevention of neural tube defect recurrences. *Lancet* **1:** 1027-1031

Smithells RW, Sheppard S, Wild J, Schorah CJ (1989) Prevention of neural tube defect recurrences in Yorkshire: final report. *Lancet* **2:** 498-499

Spiegelstein O, Merriweather MY, Wicker NJ, Finnell RH (2003) Valproate-induced neural tube defects in folate-binding protein-2 (Folbp2) knockout mice. *Birth Defects Res A Clin Mol Teratol* **67:** 974-978

Starheim KK, Gevaert K, Arnesen T (2012) Protein N-terminal acetyltransferases: when the start matters. *Trends Biochem Sci* **37:** 152-161

Stroylova YY, Chobert JM, Muronetz VI, Jakubowski H, Haertlé T (2012) N-homocysteinylation of ovine prion protein induces amyloid-like transformation. *Arch Biochem Biophys* **526:** 29-37

Strutt DI, Weber U, Mlodzik M (1997) The role of RhoA in tissue polarity and Frizzled signalling. *Nature* **387:** 292-295

Suarez L, Felkner M, Brender JD, Canfield M, Zhu H, Hendricks KA (2012) Neural tube defects on the Texas-Mexico border: what we've learned in the 20 years since the Brownsville cluster. *Birth Defects Res A Clin Mol Teratol* **94:** 882-892

Sugiyama A, Awaji H, Horie K, Kim M, Nakata R (2012) The beneficial effect of folate-enriched egg on the folate and homocysteine levels in rats fed a folate- and choline-deficient diet. *Journal of food science* **77:** H268-272

Sukanya S, Bay BH, Tay SS, Dheen ST (2012) Frontiers in research on maternal diabetes-induced neural tube defects: Past, present and future. *World J Diabetes* **3:** 196-200

Takata K, Reh S, Tomida J, Person MD, Wood RD (2013) Human DNA helicase HELQ participates in DNA interstrand crosslink tolerance with ATR and RAD51 paralogs. *Nature communications* **4:** 2338

Tam PP, Behringer RR (1997) Mouse gastrulation: the formation of a mammalian body plan. *Mech Dev* **68:** 3-25

Tamai K, Zeng X, Liu C, Zhang X, Harada Y, Chang Z, He X (2004) A mechanism for Wnt coreceptor activation. *Mol Cell* **13:** 149-156

Tang LS, Finnell RH (2003) Neural and orofacial defects in Folp1 knockout mice [corrected]. *Birth Defects Res A Clin Mol Teratol* **67:** 209-218

Troen AM, Shea-Budgell M, Shukitt-Hale B, Smith DE, Selhub J, Rosenberg IH (2008) B-vitamin deficiency causes hyperhomocysteinemia and vascular cognitive impairment in mice. *Proc Natl Acad Sci U S A* **105:** 12474-12479

Tyagi N, Kandel M, Munjal C, Qipshidze N, Vacek JC, Pushpakumar SB, Metreveli N, Tyagi SC (2011) Homocysteine mediated decrease in bone blood flow and remodeling: role of folic acid. *J Orthop Res* **29:** 1511-1516

Tyagi N, Qipshidze N, Munjal C, Vacek JC, Metreveli N, Givvimani S, Tyagi SC (2012) Tetrahydrocurcumin ameliorates homocysteinylated cytochrome-c mediated autophagy in

hyperhomocysteinemia mice after cerebral ischemia. *Journal of molecular neuroscience : MN* **47:** 128-138

Ueland PM, Mansoor MA, Guttormsen AB, Müller F, Aukrust P, Refsum H, Svardal AM (1996) Reduced, oxidized and protein-bound forms of homocysteine and other aminothiols in plasma comprise the redox thiol status--a possible element of the extracellular antioxidant defense system. *The Journal of nutrition* **126:** 1281S-1284S

Ueland PM, Refsum H, Stabler SP, Malinow MR, Andersson A, Allen RH (1993) Total homocysteine in plasma or serum: methods and clinical applications. *Clin Chem* **39:** 1764-1779

Undas A, Perła J, Lacinski M, Trzeciak W, Kaźmierski R, Jakubowski H (2004) Autoantibodies against N-homocysteinylated proteins in humans: implications for atherosclerosis. *Stroke* **35:** 1299-1304

Undas A, Stepień E, Glowacki R, Tisończyk J, Tracz W, Jakubowski H (2006) Folic acid administration and antibodies against homocysteinylated proteins in subjects with hyperhomocysteinemia. *Thromb Haemost* **96:** 342-347

van Beynum IM, den Heijer M, Thomas CM, Afman L, Oppenraay-van Emmerzaal D, Blom HJ (2005) Total homocysteine and its predictors in Dutch children. *Am J Clin Nutr* **81:** 1110-1116

van der Put NM, Steegers-Theunissen RP, Frosst P, Trijbels FJ, Eskes TK, van den Heuvel LP, Mariman EC, den Heyer M, Rozen R, Blom HJ (1995) Mutated methylenetetrahydrofolate reductase as a risk factor for spina bifida. *Lancet* **346:** 1070-1071

van Mil NH, Oosterbaan AM, Steegers-Theunissen RP (2010) Teratogenicity and underlying mechanisms of homocysteine in animal models: a review. *Reprod Toxicol* **30:** 520-531

Vanaerts LA, Blom HJ, Deabreu RA, Trijbels FJ, Eskes TK, Copius Peereboom-Stegeman JH, Noordhoek J (1994) Prevention of neural tube defects by and toxicity of L-homocysteine in cultured postimplantation rat embryos. *Teratology* **50:** 348-360

Varga EA, Sturm AC, Misita CP, Moll S (2005) Cardiology patient pages. Homocysteine and MTHFR mutations: relation to thrombosis and coronary artery disease. *Circulation* **111:** e289-293

Veeman MT, Slusarski DC, Kaykas A, Louie SH, Moon RT (2003) Zebrafish prickle, a modulator of noncanonical Wnt/Fz signaling, regulates gastrulation movements. *Curr Biol* **13:** 680-685

Villeneuve LM, Natarajan R (2010) Epigenetics of diabetic complications. *Expert Rev Endocrinol Metab* **5:** 137-148

Wallingford JB (2005) Neural tube closure and neural tube defects: studies in animal models reveal known knowns and known unknowns. *Am J Med Genet C Semin Med Genet* **135C:** 59-68

Wallingford JB (2006) Planar cell polarity, ciliogenesis and neural tube defects. *Hum Mol Genet* **15 Spec No 2:** R227-234

Wallingford JB, Niswander LA, Shaw GM, Finnell RH (2013) The continuing challenge of understanding, preventing, and treating neural tube defects. *Science* **339:** 1222002

Wang H, Ross JF, Ratnam M (1998) Structure and regulation of a polymorphic gene encoding folate receptor type gamma/gamma'. *Nucleic Acids Res* **26:** 2132-2142

Wang W, Escobedo JO, Lawrence CM, Strongin RM (2004) Direct detection of homocysteine. *J Am Chem Soc* **126:** 3400-3401

Webster WS, Messerle K (1980) Changes in the mouse neuroepithelium associated with cadmium-induced neural tube defects. *Teratology* **21:** 79-88

Wilkins MR, Sanchez JC, Williams KL, Hochstrasser DF (1996) Current challenges and future applications for protein maps and post-translational vector maps in proteome projects. *Electrophoresis* **17:** 830-838

Williams BO, Insogna KL (2009) Where Wnts went: the exploding field of Lrp5 and Lrp6 signaling in bone. *J Bone Miner Res* **24:** 171-178

Witze ES, Old WM, Resing KA, Ahn NG (2007) Mapping protein post-translational modifications with mass spectrometry. *Nat Methods* **4:** 798-806

Wlodarczyk B, Spiegelstein O, Gelineau-van Waes J, Vorce RL, Lu X, Le CX, Finnell RH (2001) Arsenic-induced congenital malformations in genetically susceptible folate binding protein-2 knockout mice. *Toxicology and applied pharmacology* **177:** 238-246

Wodarz A, Nusse R (1998) Mechanisms of Wnt signaling in development. *Annu Rev Cell Dev Biol* **14:** 59-88

Woodruff TM, Pollitt S, Proctor LM, Stocks SZ, Manthey HD, Williams HM, Mahadevan IB, Shiels IA, Taylor SM (2005) Increased potency of a novel complement factor 5a receptor antagonist in a rat model of inflammatory bowel disease. *J Pharmacol Exp Ther* **314:** 811-817

WRISTON JC, MACKENZIE CG (1957) Synthesis and metabolism of 1, 3-thiazane-4-carboxylic acid derived from formaldehyde and homocysteine. *The Journal of biological chemistry* **225:** 607-613

Wu M, Fan J, Gunning W, Ratnam M (1997) Clustering of GPI-anchored folate receptor independent of both cross-linking and association with caveolin. *J Membr Biol* **159:** 137-147

Wu M, Gunning W, Ratnam M (1999) Expression of folate receptor type alpha in relation to cell type, malignancy, and differentiation in ovary, uterus, and cervix. *Cancer Epidemiol Biomarkers Prev* **8:** 775-782

Xu Y, Gong W, Peng J, Wang H, Huang J, Ding H, Wang DW (2014) Functional analysis LRP6 novel mutations in patients with coronary artery disease. *PloS one* **9:** e84345

Yang J, Hu X, Zhang Q, Cao H, Wang J, Liu B (2012) Homocysteine level and risk of fracture: A meta-analysis and systematic review. *Bone* **51:** 376-382

Zang T, Dai S, Chen D, Lee BW, Liu S, Karger BL, Zhou ZS (2009) Chemical methods for the detection of protein N-homocysteinylation via selective reactions with aldehydes. *Analytical chemistry* **81:** 9065-9071

Zeng X, Huang H, Tamai K, Zhang X, Harada Y, Yokota C, Almeida K, Wang J, Doble B, Woodgett J, Wynshaw-Boris A, Hsieh JC, He X (2008) Initiation of Wnt signaling: control of Wnt coreceptor Lrp6 phosphorylation/activation via frizzled, dishevelled and axin functions. *Development* **135:** 367-375

Zhao J, Zhu W, Liu T, Yang J, Li G (2010) Electrochemical probing into cytochrome c modification with homocysteine-thiolactone. *Anal Bioanal Chem* **397:** 695-701

Zhao R, Gao F, Goldman ID (2002) Reduced folate carrier transports thiamine monophosphate: an alternative route for thiamine delivery into mammalian cells. *Am J Physiol Cell Physiol* **282:** C1512-1517

Zhao R, Matherly LH, Goldman ID (2009a) Membrane transporters and folate homeostasis: intestinal absorption and transport into systemic compartments and tissues. *Expert Rev Mol Med* **11:** e4

Zhao R, Min SH, Wang Y, Campanella E, Low PS, Goldman ID (2009b) A role for the proton-coupled folate transporter (PCFT-SLC46A1) in folate receptor-mediated endocytosis. *The Journal of biological chemistry* **284:** 4267-4274

Zhao R, Russell RG, Wang Y, Liu L, Gao F, Kneitz B, Edelmann W, Goldman ID (2001) Rescue of embryonic lethality in reduced folate carrier-deficient mice by maternal folic acid supplementation reveals early neonatal failure of hematopoietic organs. *The Journal of biological chemistry* **276:** 10224-10228

Zimny J (2008) [Mechanisms that protect against homocysteine toxicity]. *Postepy Biochem* **54:** 91-98

Vita

Kristin Fathe was born in Phoenix, AZ. Kristin was raised in Phoenix, AZ and attended Trinity University from 2004-2008, where she received a BS in Biochemistry. Kristin worked as a Clinical Coordinator at SAM Clinical Research when she graduated and enrolled at University of Texas Austin for her graduate work in Biochemistry in 2009.

Permanent Address: kfathe@alum.trinity.edu

This dissertation was typed by Kristin Fathe.